

THE METAMORPHISM AND THE RELATIONSHIP BETWEEN INFRA AND SUPRASTRUCTURES OF THE BİTLİS MASSIF - TURKEY

Metin ŞENGÜN*

ABSTRACT.- The infrastructure of the massife consists essentially of amphibolites, gneisses and micaschists intruded by a biotite granite and the successive hololeucocratic phase. The mantling rocks of the suprastructure comprise metapelitic rocks unconformably underlying metacarbonates dated as Middle Devonian- Mesozoic. The infra-suprastructure boundary is interpreted as a surface of transgressive overlap. The rocks of infra and suprastructure are involved in isoclinal folds with ductile deformation along most of the boundary conclusively suggesting in situ position of the suprastructure during the Alpine deformation. The shear planes are discontinuous, en echelon and run independent of the infra-suprastructure boundary. A uniform sequence of Palaeozoic rocks, which is not intruded by the granites of the infra-structure, together with the infra-suprastructure boundary being a sedimentary contact, are conclusive evidence for the existence of a Precambrian event. Eradication of Precambrian paragenesis occurs in the flanks of major folds where a complete Alpine zoning exists from very low grade to anatectic conditions as exemplified by the Kesandere section in contrast to the preservation of Precambrian parageneses in the unshered competent rocks of the infrastructure of the hinge areas. There is no gap in physical conditions with regard to a single episode of deformation. The gap occurring between the infra and the suprastructure is due to different physical conditions of Precambrian and Alpine deformations. Retrograde effects are presumably due to an Alpine imprint on the Precambrian parageneses, whereas they are attributed to a continuous process of deformation with contemporaneous uplift and progressive diminution of physical conditions in the case of imprint on early Alpine parageneses. The interpretation herein presented in relation to nature of infra and suprastructure boundary and metamorphism of Bitlis massive is consistent, for all aspects, with the regional geologic data showing that it is the deformed Alpine passive margin of the Arabian plate.

INTRODUCTION

This paper aims to discuss and interpret some of the topics of debate with emphasis on the nature of the infra-suprastructure boundary and the history of deformation of Bitlis massif, southeastern Turkey. The presented argument is part of a doctorate thesis (Şengün, 1984) carried out in the Hacettepe University, Ankara. The area of investigation (Fig.1) was selected on the north-western hinge of a major structure following a preliminary investigation.

The earliest work related to the topics discussed in this paper was by Yılmaz (1971) who, on the basis of Rb-Sr isotopic data obtained from amphibolites (920 ± 224 m.y.), paragneisses (596 ± 89 m.y.) and granites (325 ± 3 m.y. with re-interpretation (Yılmaz et. al., 1981) to 570 m.y.), suggested that the infrastructure was the Pan-African basement unconformably overlain by a low grade metasedimentary cover. Hall (1976) suggested that an oceanic domain to the south of Bitlis massif was consumed by Miocene through northward subduction. Existence of such an ocean known as the, southern branch of Neotethys (Şengör and Yılmaz,

1981) resulted in a sceptical look on the sedimentary nature of the infra-suprastructure boundary (Yılmaz, 1971). It is unavoidable that the suprastructure, Paleozoic-Mesozoic in age, is allochthonous if the infrastructure of Bitlis is the active margin of the suggested ocean. This will help to explain why the low grade Alpine metamorphism do not eradicate the earlier deformations. However, investigations by Erdoğan and Dora (1983), Yurtsever et. al. (1983), Çağlayan et. al. (1984) and Genç (1987) brought in explicit information about the sedimentary nature of the primary boundary between the infra and the suprastructure, conforming with the earliest suggestion of Yılmaz (1971). The fact that granites of the infrastructure is unconformably capped by Permian sedimentation (Göncüoğlu and Turhan, 1985) and radiometric dating of Yılmaz (1971) and of Helvacı (1983) are further evidence supporting this interpretation. This paper defends that the infra-suprastructure boundary is a sedimentary contact corresponding to an angular unconformity of Precambrian age with transgressive onlaps during Early Paleozoic.

Polymetamorphic nature of Bitlis is generally accepted (Boray, 1973; Mason, 1975, Hall, 1976).

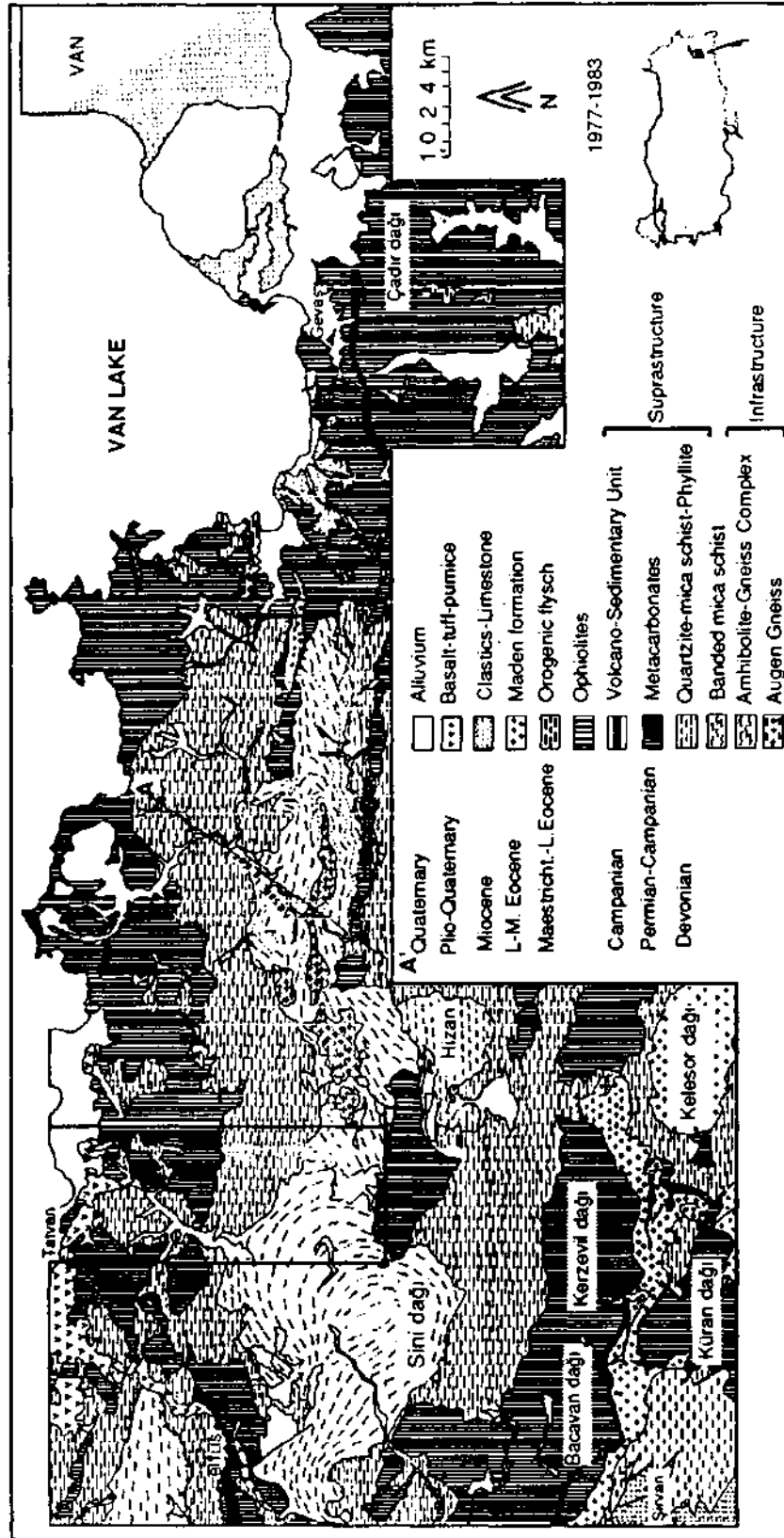


Fig. 1- Location map showing locations of the investigated area and the Kesandere section shown of the map compiled by Çağlayan et. al. 1984.

STRATIGRAPHY

The rock sequence consists of a basement complex (Yolcular fm.) unconformably overlain by a sedimentary mantle (Kotum group). The basement complex consists essentially of amphibolites, micro-

cline gneiss, biotite gneiss/schist and muscovite gneiss/schist intruded by a biotite granite succeeded by a hololeucocratic aplitic-pegmatitic phase. The suprastructure is subdivided into Kuytu, Arpik and Nasurdağı formations (Fig. 2).

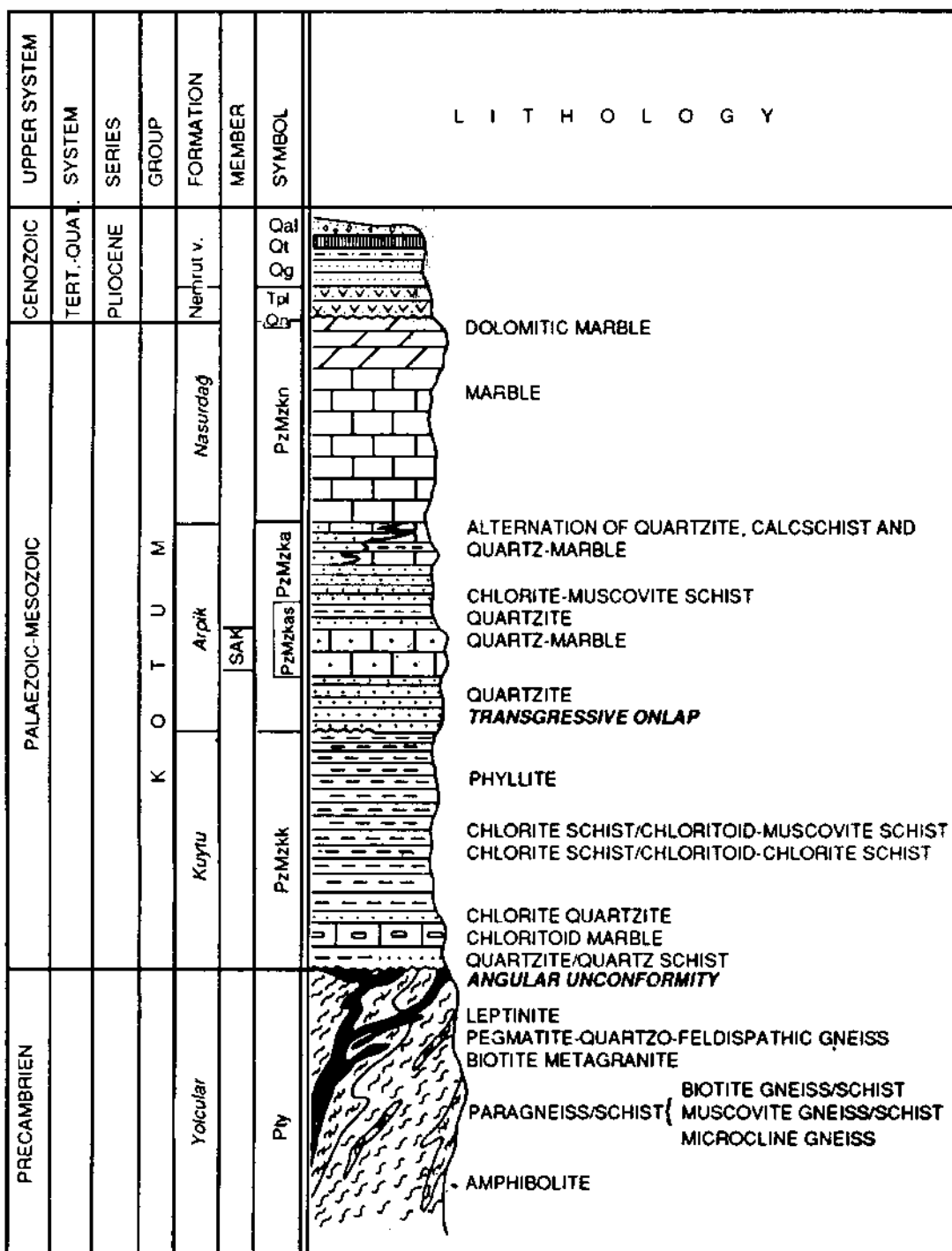


Fig. 2- Generalised columnar section of the investigated area.

Yolcular formation

It consists of the rock types briefly described below.

Amphibolite— It occurs as massive bodies of various shapes dissected by granitic and pegmatitic dykes showing isoclinal folding. Lenticular masses, up to a few meters in diameter, are commonly seen. The hand specimen is generally massive showing occasional incipient foliation. Actinolitization and chloritization are common along shear planes. The generalised paragenesis is:

Hornblend+Quartz+Oligoclase+Alkali feldspar+Garnet±Rutile±Biotite±Magnetite±Apatite

Hornblend is nomenclated as "Ferroan Pargasite - Ferroan Pargasitic Hornblend" according to Leake (1978). The massive amphibolite has been converted, along Alpine shear zones, into well-foliated rocks with a strong b-lineation with the generalised paragenesis of

Actinolite+Quartz+Albite+Epidote+Mg-Chlorite ±Sphene±Biotite±Magnetite

Paragneiss/schist The rock types included comprise microcline gneiss, muscovite gneiss/schist and biotite gneiss/schist showing compositional banding that form an alternating series showing sharp boundaries with respect to rock fabric, texture and colour. A rough generalization of respective parageneses of these rock types are as follows

Quartz + Albite (or Oligoclase) + Microcline + Garnet + Biotite ±Epidote± Zircon ± Sphene

Quartz + Albite (or Oligoclase) + Alkali feldspar + Muscovite ± Biotite ± Zircon ± Sphene

Quartz + Albite (or Oligoclase) + Alkali Feldspar + Biotite + Muscovite + Garnet + Mg-Chlorite ± Zircon ± Sphene

These rock types show appropriate variations in mineral assemblages with respect to metamorphic grade. Kyanite and incipient growths of sillimanite (Fig. 3) are observed in



Fig. 3- Kyanite sillimanite association in biotite gneiss. (1.2x1.8 mm), plane light.

several localities where anatectic conditions prevailed (Fig. 4). Staurolite porphyroblasts (Fig. 5) are also observed in biotite gneisses of favourable bulk compositions in the Kesandere section (Fig. 12).

Granitic Rocks of the Infrastructure- The amphibolites, paragneisses and micaschists of the basement complex are intruded by a biotite meta-granite followed by its hololeucocratic phase. The



Fig. 4- Pyritmatic veins in biotite gneiss.

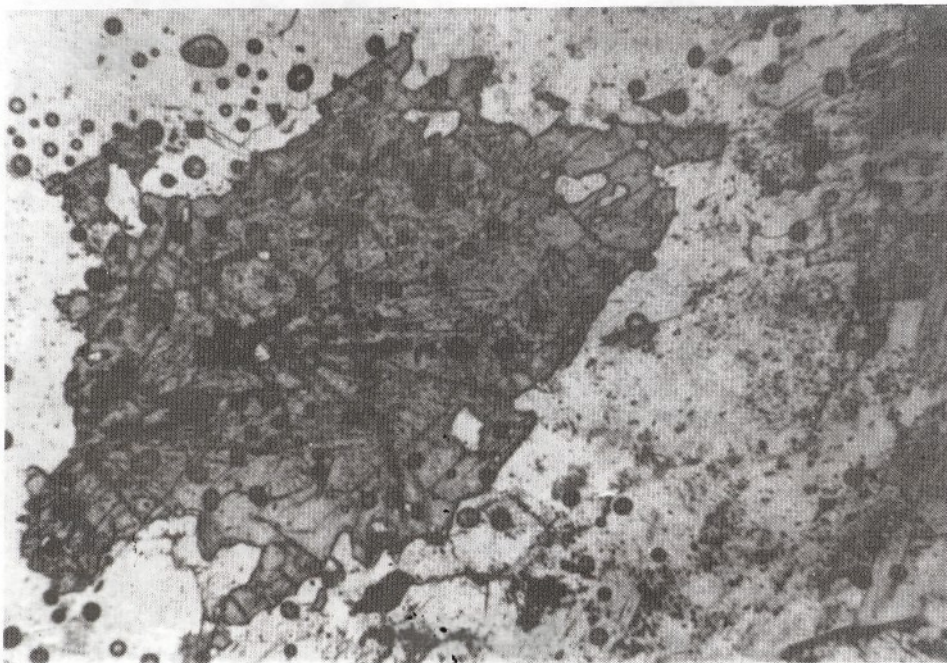


Fig. 5- Staurolite megacrystal in garnetiferous micaschists (3.2x4.8 mm.), plane light.

biotite metagranite, correlated with the augen gneiss of the northern flank of the major anticlinorium, is dissected by dyke swarms of quartzofeldspathic gneiss and metapegmatites. Leptinites, locally preserving their original texture, constitute the uppermost unit of the basement complex and are interpreted as the extrusive equivalents of the granite that is post-tectonic with respect to the Pan-African event.

Biotite granite is a coarse grained, holocrystalline rock of hypautomorphic texture, generally having a quartz monzonitic composition. A break cleavage, mutually dissecting amphibolite lenses, biotite granite and the leucocratic dykes, shows a progressive change to flow cleavage of the augen gneiss through an intermediate stage of shear cleavage. Granitic origin of the augen gneiss is also supported by the petrochemical analyses of Genç (1987). The dykes of the leucocratic phase show isoclinal folding resulting in boudinage of amphibolites (Fig. 6) and other associated basement rocks. The metapegmatites consist essentially of quartz

Kotum Group

The suprastructure, nomenclated as the Kotum group, is subdivided into Kuytu, Arpik and Nasurdağı formations.

Kuytu formation is composed essentially of phyllites and chlorite schists with the generalised parageneses of:

Quartz + Chloritoid + Muscovite + Chlorite + Pyrite+Fe-rich carbonate (Fig.8).

Quartz + Chlorite + Muscovite + Albite + Pyrite

Calcite + Dolomite + Chloritoid ± Quartz ± Muscovite + Chlorite

Quartz + Albite + Muscovite ± Chlorite ± Tourmaline,

Arpik formation consists essentially of inter-fingering quartz schists and quartzites showing occasional wave ripples and cross bedding. Sak member consists essentially of medium to thick bedded quartz marbles with occasional intercala-



Fig. 6- The relation between amphibolite and quartzofeldspathic gneiss.

with minor kyanite, dumortierite, tourmaline and topaz suggesting the effectiveness of a volatile phase (Fig. 7).

tions of shale. The generalised parageneses of the Arpik formation and of the Sak member are respectively given below.

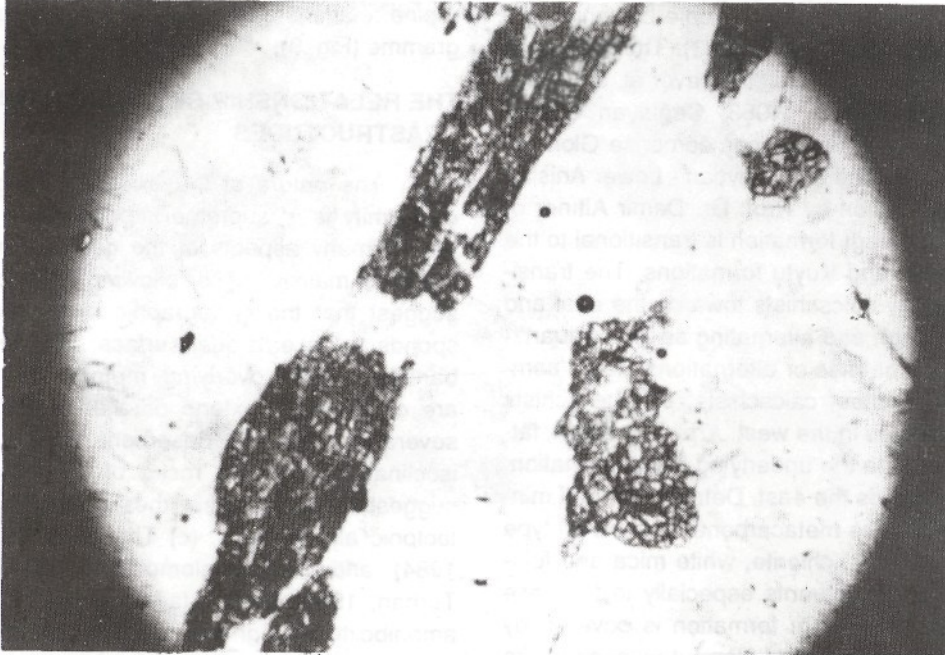


Fig. 7- A dumortierite megacrystal in metapegmatites. (3.2x4.8 mm.), plane light.

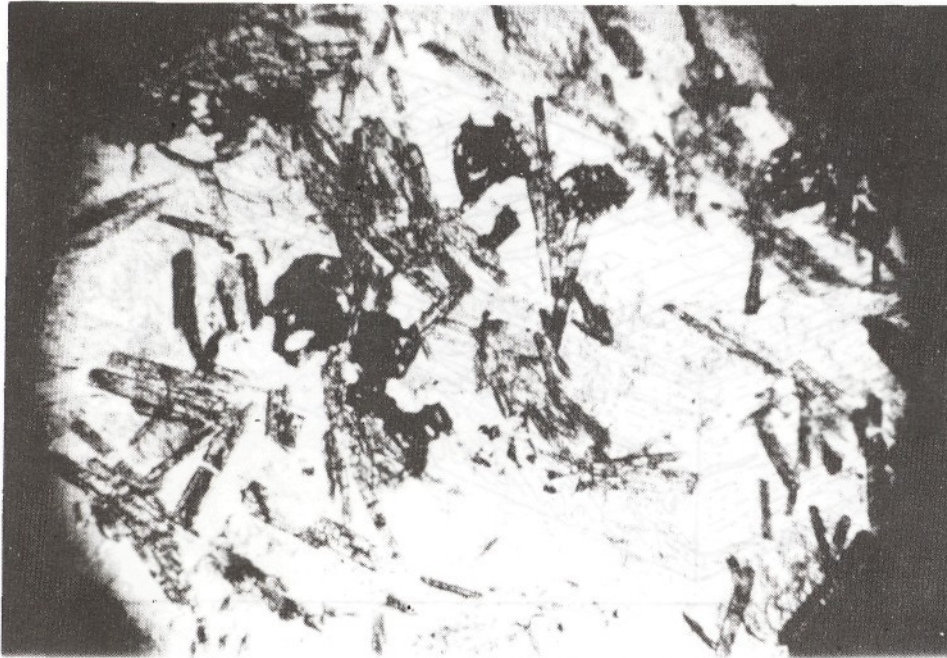


Fig. 8- Chloritoid micaschist. (3.2x4.8 mm.), plane light.

Quartz + Albite + Microcline + Muscovite +
Biotite ± Zircon ± Apatite ± Tourmaline

Calcite ± Dolomite ± Muscovite ± Chlorite ±
Quartz ± Feldspar

Nasurdağı formation, a metacarbonate sequence thickened due to isoclinal folding, constitutes the uppermost section of the suprastructure. It is dated as Middle Devonian - Mesozoic(?). The

base of the sequence yielded Middle Devonian corals (Göncüoğlu and Turhan, 1983). The sequence comprises fusulinid species (Yurtsever et. al., 1983; Göncüoğlu and Turhan, 1983; Çağlayan et. al., 1984). The dolomitic limestones comprise *Glomospirella Facilis* Ho., and are Schythian - Lower Anisian in age (determination by Prof. Dr. Demir Altınar of M.E.T.U.). Nasurdağı formation is transitional to the underlying Arpik and Kuytu formations. The transition is fulfilled by calcschists towards the east and is realised through an alternating series of quartzites and quartz marbles or alternations of any combination of quartzites, calcschists, chlorite schists and quartz marbles in the west. Arpik formation, laterally transitional to the underlying Kuytu formation, wedges out towards the east. Detrital rock and mineral fragments in the metacarbonates show all type of variations. Quartz, chlorite, white mica and feldspar are major constituents especially in the case of calcschists. Nasurdağı formation is covered by the volcanic products of the Nemrut volcano in the investigated area.

Alpine relations of the Kotum group on a block diagramme (Fig. 9).

THE RELATIONSHIP BETWEEN INFRA AND SUPERSTRUCTURES

The nature of the existing cartographic unconformity is of supreme importance in interpretation of many aspects of the geologic evolution of the Bitlis massive. The following field observations suggest that the cartographic unconformity corresponds to an erosional surface, (a) Compositional banding of the overlying metasedimentary rocks are observed to extend parallel to the contact at several localities, (b) Basement rocks show mutual isoclinal folding with rocks of the suprastructure suggesting conclusively the impossibility of post-tectonic allochthoneity. (c) The quartzites (Şengün, 1984) and metaconglomerates (Göncüoğlu and Turhan, 1985) contain fairly rounded fragments of amphibolite and gneiss, (d) The sequence of the suprastructure is extremely uniform and represents a complete and undissected sedimentary wedge

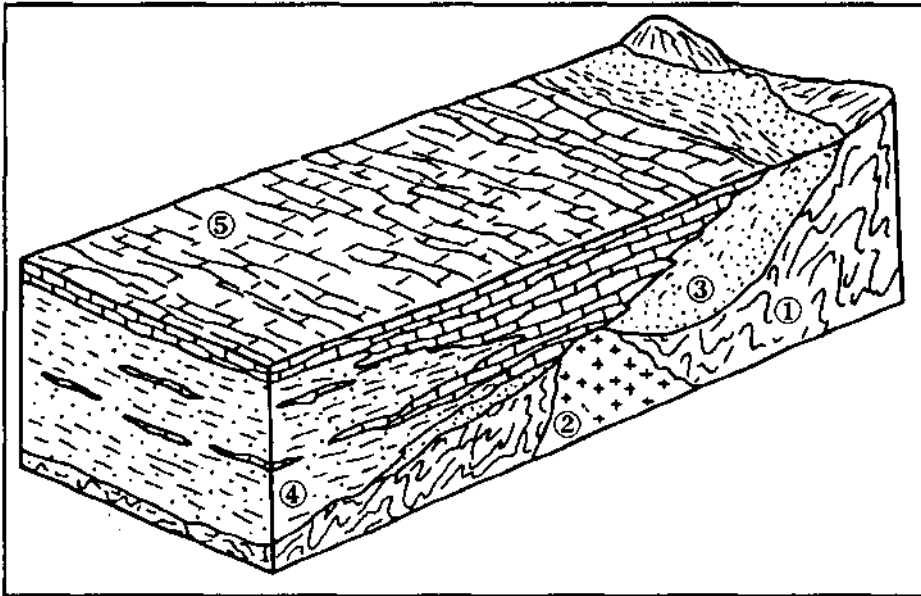


Fig. 9- Block diagramme showing the pre-Alpine relations of the Kotum group. 1. Precambrian basement 2. Granite 3. Kuytu formation 4. Arpik formation 5. Nasurdağı fm.

The Kotum group is dissected by aplite and diabase dykes that are implicitly considered to be feeders of the Eocene volcanism (Çağlayan et. al., 1984). A tentative attempt is made to show the pre-

(Fig. 9). (e) The shear planes dissect mutually rocks of the basement and of the suprastructure implying syntectonic movements are independent of the primary sedimentary contact.

The extreme resemblance of the suprastructure to the Arabian platform (Çağlayan et. al., 1984) implies an erosional surface of Precambrian age with transgressive overlaps during the Early Palaeozoic. The uniformity of the sedimentary wedge implies that pre-tectonic allochtony is also unlikely.

THE METAMORPHISM

There has been no dispute, so far, on the polymetamorphic nature of the Bitlis massive. However, timing of deformational episodes is either vague or controversial.

mentary to the deductions presented above, (a) There is a large gap of physical conditions between the Pan-African granites and those of the amphibolites and the biotite gneisses. The metamorphism of the former can be correlated with that of the suprastructure. The incipient gneissic foliation of the granitic rocks is penetrative into other basement rocks with crystallisation of chlorite and white mica along the mutual cleavage planes which show a complete gradation from a break cleavage in the investigated area to the flow cleavage of Kesandere region through an intermediate stage of shear cleavage. (It is not possible to confuse the Precambrian granitic



Fig. 10- Alpine aplite dyke. Note the discordant relation to the regional grain.

If the infra-suprastructure boundary is assumed to be primarily a sedimentary contact, there is one single path of deductive reasoning. (1) The granitic dykes showing isoclinal folding are pre-Devonian, in fact Precambrian in age on consideration of regional geologic data. (2) The associated country rocks display a medium to high grade metamorphism suggesting that they were deformed prior to the granitic intrusions. (3) There have been at least two episodes of metamorphism, one, predating the Precambrian intrusions and the other postdating Palaeozoic-Mesozoic sedimentation.

The field evidence cited below is comple-

dykes with the seldom occurring post-Alpine granitic rocks that are distinguishable by their discordant relations to the country rock and their undeformed nature (Fig. 10). (b) The low grade parageneses seen in the peripheral shear planes of the amphibolite boudins correlate well with those of the hosting phyllites and chlorite schists with regard to the grade of metamorphism as well as the penetrative cleavage.

The physical conditions of the Precambrian event is deduced from the following observations in the anatectic areas outside of the investigated area. The quartzo-feldspathic gneiss shows incipient foli-

ation penetrating to the S2 planes of the biotite gneiss and the amphibolite. The following parageneses belong to the microlithons enclosed between the referred cleavage planes of amphibolites and biotite gneisses.

Hornblend + Oligoclase + Quartz + Garnet ± Rutile

Biotite + Quartz + Muscovite + Garnet + Oligoclase + Orthoclase + Kyanite ± Sillimanite ± Zircon

The physical conditions, attributed to the Precambrian event necessarily following the discussion given above, must be a little higher than the value suggested by the triple junction of the Al_2SiO_5 polymorphs. The temperature and the hydrostatic pressure at this locality was read from the intersection of kyanite-sillimanite boundary (Winkler, 1976) with curves A (Storre and Karrotke, 1971) and B (Tuttle and Bowen, 1958) giving the respective values of

650 C at hydrostatic pressures of 6.5 kbars, and 630 C at hydrostatic pressures of 6.2 kbars (Fig. 11).

Other parageneses of the amphibolites and of the biotite gneisses suggest physical conditions of the medium grade and the minimum physical conditions correspond, probably to that of the epidote amphibolite facies as suggested by the paragenesis:

Quartz + Biotite + Muscovite + Mg-Chlorite + Garnet + Albite

The physical conditions of the Alpine metamorphism varies from very low grade to probably "biotite in" isograd in the investigated area. However, in the northern flank of the major structure, a complete Alpine zoning occurs with total eradication of the Precambrian parageneses. This interpretation is deduced from the stratigraphic and structural characteristics of the Kesandere section (Fig. 12). The core of the section consists essentially of an augen gneiss, correlated to the biotite granite in its lateral extension, with minor boudins of garnetiferous amphibolite. Kyanite bearing biotite gneiss is also encountered in the core of the section. This assemblage is overlain by quartzites that laterally grades into the Sallica marble (Yurtsever et al., 1983) and micaschists. The sequence continues with phyllites and the Palaeozoic-Mesozoic carbonates. Sallica marble repeats itself in all of the met-

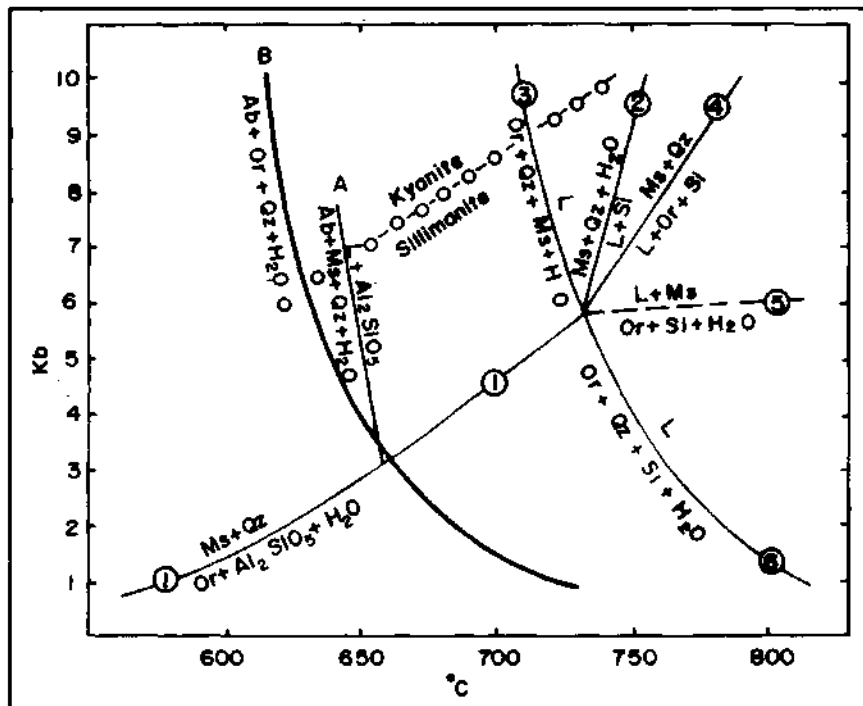


Fig. 11- Reactions between quartz, muscovite and feldspar (after Winkler, 1976).

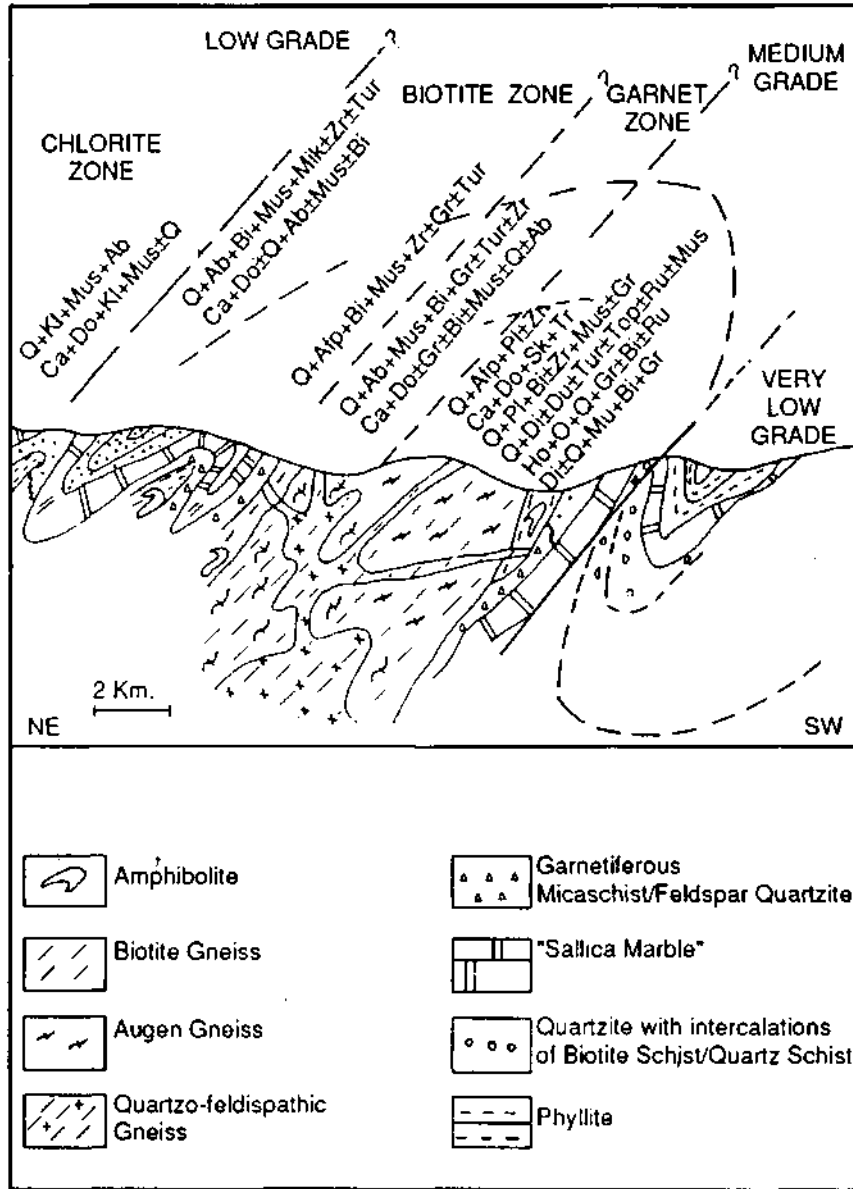


Fig. 12. Structural and metamorphic characteristics of the Kesandere section.

amorphic zones through isoclinal folding. The continuity of the Sallica marble is accepted as conclusive evidence for progressive variation of physical conditions. The metamorphism has to be Alpine in age as the section comprises Mesozoic rocks in its uppermost part.

The Alpine deformation is progressive in time and space. The isograds dip north in Kesandere, are independent of the lithology and are par-

allel to the axial planes of isoclinal folds. The early foliation planes were subject to multistage shear resulting in multidirectional cleavage. The cross-sectional shortening, strikingly well-defined in the medial parts of the major structure compared to the western hinge (Fig. 1), is a clear illustration that the intensity of deformation is also controlled by the geometry of the major structure. In other words, flanks of folds are extremely sheared in comparison to the hinges.

DISCUSSION AND CONCLUSION

The presence of a Mesozoic sequence correlating well with that of the Arabian platform (Çağlayan et.al., 1983), and the Eocene sediments mutually covering the Bitlis massif and the ophiolites (Çağlayan et.al., 1984), may be regarded as conclusive evidence for in situ position of the Bitlis massif, implying that it is the northern extension of the Arabian platform (Özkaya, 1982; Yazgan, 1984) during the Mesozoic, also implying non-existence of an oceanic domain south of Bitlis. Undeformed nature of Mesozoic-Tertiary sedimentary units of the northern margin of border folds and the progressive diminution of intensity of Alpine deformation are complementary evidence for non-existence of an ocean south of Bitlis. On the other hand, the presence of an undeformed Cretaceous-Tertiary sequence to the north of Lake Van and its incorrelatable nature with medial Eocene syndeformational sedimentation (Maden formation) of northern Bitlis complemented by the presence of undeformed units in East Anatolia, shows that Neotethys lied in immediate north of Bitlis. There has been an extensional regime in southern parts of Bitlis coeval with Alpine deformation of the northern segments. This is ascribed to block rotations to close up the relicts of Neotethyan domains. However, northward movement of the Arabian plate (McKenzie, 1972) put a brake on rifting of the Maden-Çüngüş foredeep before break-up of the continental crust. Planes of movement were subject to Alpine deformation (post-Eocene) while medium grade (Winkler, 1976) metamorphism of the lithons were mostly preserved.

It may, thus, be said in conclusion:

1- The cartographic unconformity between infra and suprastructures is an angular unconformity of Precambrian age, showing transgressive overlaps during Early Palaeozoic.

2- An Alpine metamorphism, eradicating all pre-Alpine deformations, with physical conditions varying from very low grade to anatexis conditions, is exemplified (Fig. 12) and it is suggested that the Alpine deformation loses its intensity towards the south, in fact, there is a co-existing distensional regime in the southern segments. The effectiveness of Alpine deformation has been controlled by structural elements such that the rock cleavage is pene-

trative into the basement in crestal areas, representing mutually the retrograde metamorphism of the basement and the very low grade metamorphism of the suprastructure. The Alpine metamorphism is restricted to the shear planes while Precambrian parageneses are preserved in the lithons.

3- The infrastructure of Bitlis massive is not an active Alpine margin. In case it is transported (Şengör and Yılmaz, 1981) prior to Alpine deformations, the suprastructure has to be transported after the Alpine deformation so that the granites can be Alpine in age. In other words, magmatism of the continental margin should dissect the infra and suprastructure mutually. Radiometric data (Yılmaz, 1971; Helvacı, 1983) also supports the fact that granites belong to the Pan-African basement. The following basic evidence is conclusive to show non-existence of a south-lying oceanic domain that was consumed with northward polarity, between Cretaceous and Miocene (Hall, 1976).

a- The Mesozoic-Tertiary units of the northern segments of the border folds are entirely undeformed.

b- The Mesozoic units reported from south of Bitlis province show a perfect match with those of the Arabian platform implying Bitlis and the border folds were on the same north facing Mesozoic platform.

c- Alpine deformations show a progressive diminution of intensity towards the south.

d- The sedimentary sequence north of Lake Van is a clear indication of an ocean lying in immediate north of Bitlis. In other words, southern branch of Neotethys (Şengör and Yılmaz, 1981) lies in immediate north of the Bitlis/Pütürge massifs.

ACKNOWLEDGEMENTS

I gratefully acknowledge the kind supervision of Prof. Dr. Yavuz Erkan of the Hacettepe University and thank him for constructive criticism throughout the theses work. I also thank the academic and administrative staff of the Hacettepe University for various contributions to this work. I am grateful to Mr.

Atilla MTA for his Çağlayan operation throughout the fulfillment of the Bitlis project.

REFERENCES

- Boray, A., 1973, The structure and metamorphism of the Bitlis area, southeast Turkey: University of London, Doctorate thesis, 233p, (unpublished).
- Çağlayan, M.A.; Dağ, Z.; Erkanol, D.; İnal, R.N.; Sevin, M. and Şengün, M., 1983, Bitlis masifinde Mesozoyik yaşlı kaya birimleri ve GD Anadolu otoktonu He deneştirilmesi: TJK, 37. Bilimsel ve Teknik Kongresi Bildiri Özetleri, 65.
- ; İnal, R.N.; Şengün, M. and Yurtsever, A., 1984, Structural setting of Bitlis massive: International symposium of the geology of the Taurus belt, MTA special publication, p. 245-254.
- Erdoğan, B. and Dora, Ö., 1983, Bitlis masifi apatitli demir yataklarının jeolojisi ve oluşumu: TJK Bull., 26, 133-144.
- Genç, S., 1987, Petrogenesis of metamorphics in the Çökekyazı-Gökay (Hizan-Bitlis) area of the Bitlis massive: Geological Congress of Turkey, Abstracts, p.33.
- Göncüoğlu, C.M. and Turhan, N., 1983, Bitlis masifinde yeni yaş, bulguları: MTA Bull., 95/96, 44-48.
- and ———, 1985, Bitlis metamorfik kuşağı orta bölümünün temel jeolojisi: MTA Rep., 7707 (unpublished), Ankara.
- Hall, R., 1976, Ophiolite emplacement and the evolution of the Taurus suture zone, Southeastern Turkey: Geol. Soc. American Bull., 87, 1078-1088.
- Helvacı, C., 1983, Bitlis masifi Avnik (Bingöl) bölgesi metamorfik kayaçlarının petrojenezi: TJK Bull., 26, 117-132.
- Leake, B.E., 1978, Nomenclature of amphiboles: Amer. Min., 63, 1023-1050.
- Mason, R., 1975, Bitlis masifinin tektonik durumu: Cumhuriyetin 50. Yılı Yerbilimleri Kongresi, 31-41, Ankara, Turkey.
- McKenzie, D.P., 1972, Active tectonics of the Mediterranean region: Geophys. J.R. astr. Soc. 30, 109-185.
- Özkaya, I., 1982, Marginal basin ophiolites at Oramar and Karadağ, SE Turkey: J. Geol. Soc. London, 139, 203-210.
- Storre, B. and Karrotke, E., 1971, Glimmerschiefern in Modellsystemmen: Fortschr. Mineral., 49, 56-58.
- Şengör, A.M.C. and Yılmaz, Y., 1981, Tethyan evolution of Turkey :a plate tectonic approach, Tectonophysics, 75,181-241.
- Şengün, M., 1984, Tatvan güneyinin (Bitlis masifi) jeolojik/ petrografik incelenmesi: Doktora tezi, 157p. (unpublished).
- Tuttle, O.F. and Bowen, N.L., 1958, Origin of granite in the light of experimental studies in the system: Geol. Soc. Am. Mem., 74, 1-153.
- Winkler, H.G.F., 1976, Petrogenesis of metamorphic rocks: Springer Verlag, New York, 320p.
- Yazgan, E., 1984, Geodynamic evolution of Eastern Taurus: TJUS, Int. Symp., Proceeding, 199-208.
- Yılmaz, O., 1971, Etude petrographique et geochronologique de la region de Cacas: Univ. Grenoble, Doctorate theses (unpublished), 230p.
- ; Michel, R.; Vialette, Y. and Bonhomme, M.G., 1981, Reinterpretation des donnees isotopiques Rb-Sr obtenues sur les metamorphites de la partie meridionale du massif de Bitlis (Turquie): Sci. Geol. Bull., 34/1, 59-73.
- Yurtsever, A.; Aksoy, Ö.; Boztepe, Y.; Dağ, Z.; Konuk, O.; Şengün, M. and Yurtsever, G., 1983, Gevaş (Van) dolayının jeolojisi: MTA Rep., (unpublished), Ankara, Turkey.

ORIGIN AND PETROLOGY OF EKECİKDAĞ GRANITOID IN WESTERN CENTRAL ANATOLIAN CRYSTALLINE MASSIF

T. Kemal TÜRELİ*; M. Cemal GÖNCÜOĞLU" and Orhan AKIMAN"

ABSTRACT— A belt formed by a number of granitoid intrusions is situated at the western part of the Central Anatolian Crystalline Massif. One of the granitoid intrusion at the southwest of the belt crops out between Aksaray and Ortaköy and is called Ekecikdağ. Ekecikdağ granitoid, which is composed of monzogranites and granodiorites, intruded both the metamorphic and ophiolitic host rocks. Ekecikdağ granitoid is differentiated into following subunits with respect to their petrographical and chemical composition: Borucu granodiorite-monzogranite, Sinandı mikrogranite, Hisarkaya porphyritic granite, Kalebalta teucogranite and aplite granite. All these subunits are genetically related to each other. Borucu granodiorite-monzogranite represents the main magmatic phase whereas aplite granite the latest. Ekecikdağ granitoid has a calcalkaline character and show aluminofemic trend. It has features which favour both I and S types of granite. Enclaves observed in granitoid is thought to be xenoliths derived from pre-existing gabbroic rocks during the emplacement of the granitic magma. The geochemical data suggest a post collisional tectonic setting and a continental crustal source for Ekecikdağ granitoid. In regard to regional data, during Upper Cretaceous, the existence of an ensimatic arc to the north of the Central Anatolian Crystalline Massif is suggested. It is also proposed that collision and obduction of this ensimatic arc on to the Central Anatolian continental crust caused crustal thickening and increase in the geothermal gradient in the region. This gave rise to the partial melting of the continental crust and to the formation of a granitic magma.

TWO NEW SPECIES OF CAPRINIDAE FROM THE BAYBURT AREA (EASTERN BLACK SEA, TURKEY)

Sacit ÖZER* and Mükerrerrem FENERCİ**

ABSTRACT.- Two new species of Caprinidae *Sabinia ornata* n. sp. and *Mitrocaprina madeniana* n. sp. have been described from the Maastrichtian sandy limestones of Maden (Bayburt) area.

INTRODUCTION

The aim of this study is mainly to describe the new species of Caprinidae collected from the Sırataşlar ridge, SW Maden-Bayburt area (Fig. 1).

In the eastern Black sea, the Upper Cretaceous rudistid formations show sparse distributions (Fig. 1). The rudists occur in the volcano-sedimenter sequence around Ordu, Giresun, and Trabzon (Özsayar et al., 1981; Özer, 1988, 1991),

but, they are present in turbiditic sequence not including volcanic interbedding in the Bayburt and Erzurum area (Bektaş. et al., 1984). Among these localities only the rudist fauna of Maden (Bayburt) area recently determined by Fenerci (1992).

The Caprinidae specimens are collected by present authors at the different times from Maden area. The holotypes and paratypes of the new species are preserved at Geological Engineering Department of Dokuz Eylül University, İzmir.

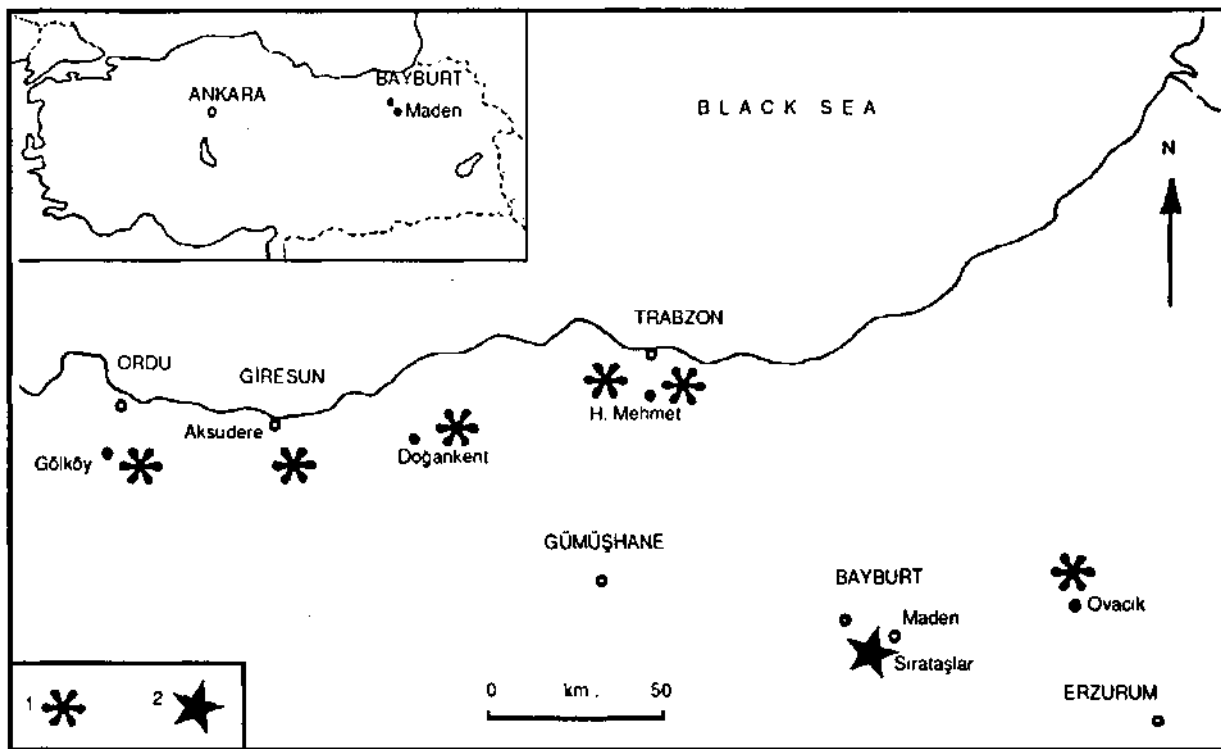


Fig. 1- Map showing distribution of rudistid outcrops (1) in the Eastern Pontids and location (2) of the new species.

STRATIGRAPHIC SETTING

The geology of Maden (Bayburt) area has been studied by Ketin (1951), Gattinger et al. (1962), Özsayar et al. (1981) and Bektaş et al. (1984).

The rudists are found in the reefal limestones overlying the ophiolitic serie. The rudist formation is made up sandy limestones consisting abundant rudists, gastropods, and hermatypic corals. The rudist fauna is poor and consists of *Hippurites sulcatoides* Douville, *Hippurites* sp., *Vaccinites ultimus* Milovanovic, *Joufia cappadociensis* (Cox), and *Sabinia* sp. (Pl. IV, fig. 5; Pl. V, fig. 3,4).

Vaccinites ultimus and *Joufia cappadociensis* are characteristic for the Maastrichtian of Turkey (Özer, 1988, 1992). These species are well known and determined with rudists and benthonic foraminifers indicated a Maastrichtian age in the Eastern Anatolia (Karacabey, 1972) and Central Anatolia (Özer, 1983, 1985). *Vaccinites ultimus* and *Joufia cappadociensis* are also found in the Maastrichtian of Kocaeli Peninsula (Kaya et al., 1986; Özer et al., 1990), and Western Pontids (Kaya et al., 1986a). *Vaccinites ultimus* is widespread in the Maastrichtian of Eastern Als (Sladic, 1957; Sladic-Trifunovic, 1978), Yugoslavia (Sladic-Trifunovic, 1977), Bulgaria (Pamouktchiev, 1961, 1981). and Sicily (Camoin, 1983). *Joufia capadociensis* is known from the Maastrichtian of Romania (Lupu, 1976).

According to the stratigraphic and geographic distribution of *Vaccinites ultimus* and *Joufia capadociensis* in Turkey and also in the Eastern Mediterranean sub-province, a Maastrichtian age has been proposed to the rudists of Maden (Bayburt) area by Fenerci (1992). So, the Maastrichtian age is also accepted here for the new species.

In the studied area, the rudistid reefal limestones are unconformably overlain by the flysch-type sediments of Eocene age.

PALEONTOLOGY

Classis: Bivalvia Linne, 1758

Ordo: Hippuritoida Newell, 1965

Super Familia: Hippuntacea Gray, 1848

Familia: Caprinidae d'Orbigny, 1850

Genus; *Mitrocaprina* Boehm, 1895

Mitrocaprina madeniana n.sp.

(Pl. I, fig. 1-5; Pl. II, fig. 1-5; Text-fig. 2, 3)

Derivation of Name: From Maden where the specimens have been found.

Material: Three specimens with both of the lower and upper valves and upper valve of one specimen.

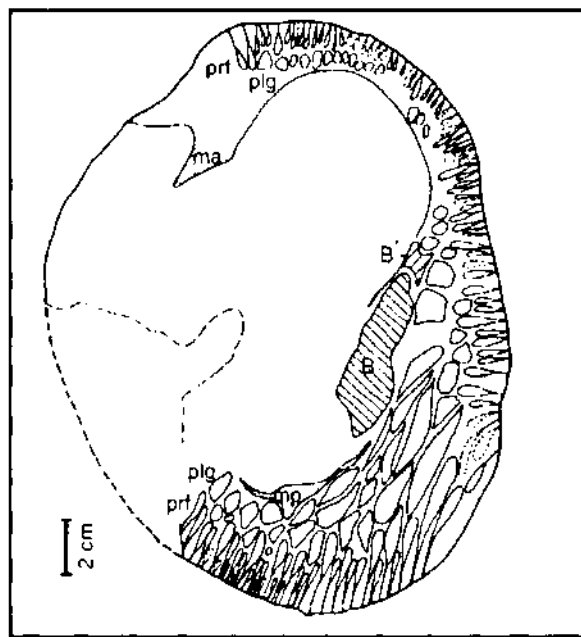


Fig. 2- *Mitrocaprina madeniana* n.sp.

Transverse section of the upper valve passing 12 mm above the commissure, holotype, No. Pm 27. The canal layer consists of two types canals such as pyriform (prf) in the outer part and polygonal (plg) in the inner part. In the posterior side, the canal layer comprise three rows of pyriform canals and also two rows of polygonal canals. Note the second row of polygonal canals which are elongated towards the cardinal area. The teeth (B, B') and myophores (mp, ma) are well preserved. Compare with the Fig. 3 in the Pl. II.

Holotype: Holotype is given in the Pl. I, fig. 1; Pl. II, fig. 1,2,3,4, and Text-fig. 2.

Type locality: In the southwest of Maden (Bayburt) the Sırataşlar ridge, map reference; Trabzon H44-c3; coordinate; 18.350:46.425 and 18.750:46750.

Type level: Maastrichtian.

Diagnosis: Lower valve short and conical. Upper valve capuloid towards the anterior side. Transverse section of the upper valve oval or sub-circular. Teeth robust. Posterior myophore (mp) thin and plate, anterior myophore (ma) grand. Canal layer of the upper valve occupies almost a whole periphery and consists of three outer rows of pyriform canals and two inner rows of polygonal canals. Canal layer thick in the posterior side.

Description: The lower valve is short (50-80 mm) and conical in shape. On the surface of the valve, only thin lamellae can be observed (Pl. I, fig. 1). The transverse section of the valve is ovaloid. The diameter is 60x100 mm in the holotype and 50x80 mm or 60x100 mm in the paratypes (Pl. I, fig. 3-5). The shell wall is thin (4-10 mm) and dark colored in the inner part. The teeth and myophores are clearly preserved in the paratypes. The anterior myophore (ma) is more developed than the posterior myophore (mp) (Pl. I, fig. 3-5).

The upper valve is capuloid in shape and inclined towards the anterior side overlapping the commissure about 10-12 mm (Pl. I, fig. 1; Pl. II, fig. 1). The height of the valve ranges from 50 mm to 70 mm. The transverse section is oval or sub-circular in shape and the diameter varies from 90x110 mm to 140x155 mm. The teeth are very robust and clearly observed. In the holotype the posterior tooth (B) is generally bigger than the anterior tooth (B) and it cover the grand part of the cardinal area. The anterior tooth is located above the posterior tooth (Pl. II, fig. 3, 2). The myophores are well preserved in all of the specimens. The anterior myophore (ma) is better developed than the posterior myophore (mp). The posterior myophore (mp) begins near the posterior tooth (B) being thin plate in shape. The canal layer is well preserved around the periphery of the valve. But, it is better devel-

ped in the posterior side of the valve (Pl. II, fig. 3-5; Fig. 2,3). The thickness of the canal layer is 40 mm in the posterior side, whereas it is diminished towards the anterior side, about 7-10 mm. The canal layer consists of two types of canals such as pyriforms and polygonals. The outer part of the canal layer comprises three rows of pyriform canals like *Plagiptychus* Matheron and they are elongated about 20-30 mm towards the inner part of the canal layer, especially around the posterior side. The inner part of the canal layer consists of two rows of polygonal canals which are located around the posterior side and near the cardinal area. The second row of polygonal canals are generally elongated

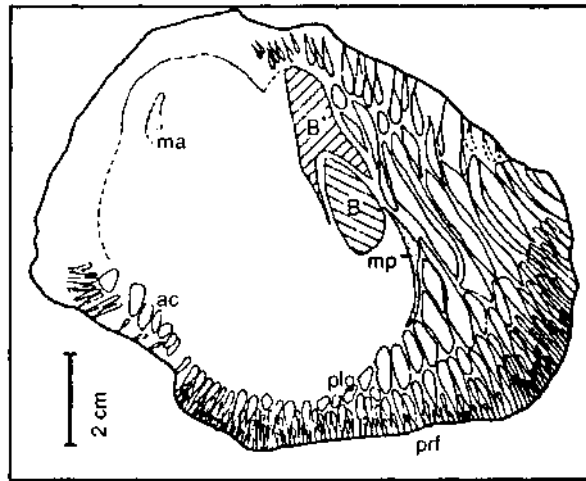


Fig. 3- *Mitrocaprina madeniana* n.sp.
Transverse section of the upper valve passing 10 mm above the commissure, paratype, No. Pm29.

The teeth are very robust and clearly observed. Towards the anterior side, some sections (ac) showing resemblances with the accessory cavities of caprinids, could be seen. Compare with the Fig. 4 in the Pl. II.

(20-37 mm) towards the cardinal area. In the anterior part, one row of little polygonal canals are also present. In the anterior side of some specimens, some sections showing similarities with the accessory cavities of caprinids could be seen (Pl. II, fig. 4,5; Fig. 3).

Discussion: The canal layer of the specimens shows principal features of the genus *Mitrocaprina* Boehm. The specimens present some similarities to *Mitrocaprina vidali* Douville and *Mitrocaprina bulgarica* Tzankov, by the organization of the canal layer of the upper valve. But, they differ from these species by the presence of many pyriform canals, and by the inclination of the upper valve towards the anterior side, while *Mitrocaprina vidali* Douville and *Mitrocaprina bulgarica* Tzankov have a beak inclined to the cardinal area (Douville, 1904; Tzankov, 1965). *Mitrocaprina madeniana* n. sp. distinguish from the all known species of the genus *Mitrocaprina* Boehm by the oval or subcircular transverse section of the upper valve, by the canal layer which are almost observed around the periphery and by the position and well preservation of the cardinal area of the upper valve.

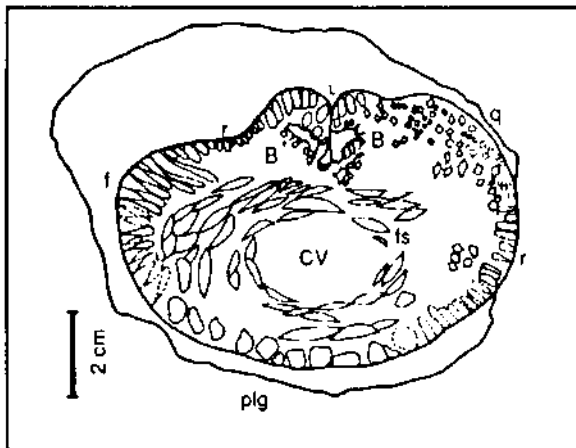


Fig. 4- *Sabinia ornata* n. sp.
Transverse section of the lower valve passing 15 mm below the commissure, holotype, No. Pm25.

The canal layer consists of fusiform (f), rectangular (r), quadrangular (q), and polygonal (plg) canals. Around the central cavity (CV), the fusiform sections (fs) showing some resemblances with the canals of caprinids, are also present. Compare with the Fig.1 in the Pl. IV.

Genus: *Sabinia* Parona, 1909.

Sabinia ornata n.sp.

(Pl. III, fig. 1-5; P. IIV, fig. 1-4; Pl. V, fig. 1,2; Text-fig. 4-6)

Derivation of Name: Because of the ornamentation of the siphonal region of the lower valve.

Material: One sample with two valves, three lower valves with partly preserved upper valve and five lower valves.

Holotype: Holotype is given Pl. III, fig. 1, 2; Pl. IV, fig. 1,4, and Text-Fig. 4, 5.

Type locality: In the southwest of Maden (Balyurt) the Sırataşlar ridge, map reference; Trabzon H44-c3; coordinate; 18.350:46.425 and 18.750:46.750.-

Type Level: Maastrichtian.

Diagnosis: Siphonal region of the lower valve ornamented with longitudinal costae and grooves. Posterior band (S) longitudinal costae, whereas the anterior- band (E) a smooth groove. Interband (I) very wide than the other bands and it represented by the longitudinal costae. Lamellae densely imbricate in the cardinal area. Ligamental ridge (L) long and truncated at the top. Canal layer of lower valve consists of four type canals such as fusiform, rectangular, quadrangular and polygonal. Canal layer of the upper valve thin and compose with fusiform and polygonal canals in small-size.

Description: The lower valve vary from conical to cylindroconical shape (Pl. III, fig. 1, 3-5; Pl. V, fig. 1, 2). The holotype is conical in shape and 60 mm in length, whereas the paratypes are cylindroconical in shape and 80 mm to 120 mm length. The external characters of the valve are not clearly preserved in the holotype, whereas, some lamellae which are characteristic of the new species, could be observed near the cardinal area. The surface of the paratypes is ornamented with 2-3 mm thick costae and grooves 2-3 mm wide (Pl. III, fig. 3, 4, 5; Pl. V, fig. 1, 2). The costae and grooves are located around the siphonal region where the growth lamellae cut the costae a strong zigzag pattern. In the cardinal area of the paratypes, the lamellae are densely imbricated (Pl. V, fig. 1). The ligamental ridge (L) can be seen at the surface as a 0.5 mm wide groove. The posterior band (S) is characterized by a 10 mm wide longitudinal costae (Pl. III, fig. 3-5; Pl. V, fig. 2). The anterior band (E) is marked

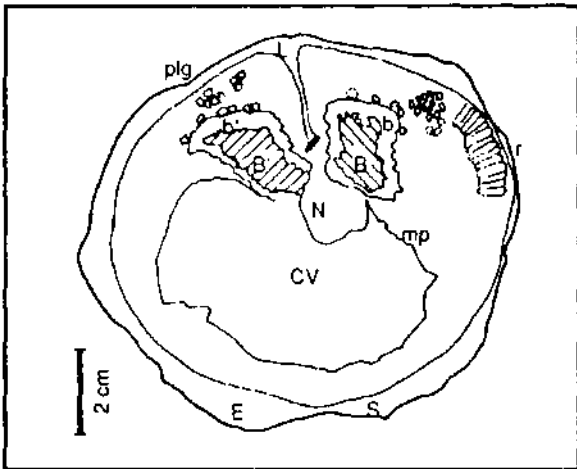


Fig. 5- *Sabinia omata* n. sp.
Transverse section of the lower valve passing 8 mm below the commissure, paratype, No. Pm26.

The teeth (B, B') and sockets (b, b') are well preserved. Only some canals such as rectangular (r) and polygonal (plg) are observed. Compare with the Fig. 2 in the Pl. IV.

with a 11 mm wide groove along the lower valve. This groove is very smooth but not deep. Interband (I) is typically very wide (35-40 mm) than the other bands, and it consists of 6-7 costae which are the same size with those of the posterior and anterior parts (Pl. III, fig. 3, 4, 5). The shape of the transverse section is subcircular to circular. The thickness of the shell wall of the holotype is not the same everywhere; it is 15 mm thick in the siphonal region, whereas 10-20 mm thick between the anterior and cardinal area. The holotype and some paratypes have an inward inflexion in the anterior side of the lower valve, near the ligamental ridge (Pl. IV, fig. 1, 3). The shell wall consists of regular polygonal cells about 0.5 mm in size, and sometimes they are elongated. In some transverse section, the siphonal bands show a slight curve the inner side of the shell wall and cause to undulate the prismatic cells. The ligamental ridge (L) is thin (1-1.5 mm), long (9-22 mm), and it is truncated at the top and widens towards the anterior side. At the top of ligamental ridge (L) black calcite filling is generally observed. The teeth (B, B') are well preserved and

they show zigzag contours (Pl. IV, fig. 2; fig. 4, 5). The anterior tooth (B') are generally bigger than the posterior tooth (B). The tooth of the lower valve (N) is partly preserved. The myophores are not preserved, because of the recrystallization. Only, in one sample, the posterior myophore (mp) can be partly observed (Pl. IV, fig. 2). The central cavity (CV) is oval in shape and more nearer to the siphonal area.

The canal layer of the lower valve is 10-20 mm thick and it comprises of four canal types. These are fusiform, rectangular, quadrangular, and polygonal. These canal types are typically observed in the holotype (Pl. IV, fig. 1; Fig. 4), whereas the paratypes have some canals such as rectangular and quadrangular. The polygonal canals are observed both of sides of the ligamental ridge and at the contours of the upper valve's teeth. Around the ligamental ridge, the polygonal canals are generally of the same size, but some of them are elongated towards the shell wall. In the siphonal area a single row of 11 polygonal canals are also observed. These canals are very large, about 3-7 mm in size, than the other polygonal canals. Many quadrangular canals are located between the ligamental ridge and posterior side of the lower valve. A row of rectangular canals are observed between the quadrangular and polygonal canals in the posterior side, and also between the fusiform and polygonal canals in the anterior side of the valve. In the anterior side, 10-15 mm length, 9 fusiform canals are observed. Some fusiform canals are elongated near the rectangular canals. There are also some fusiform sections around the central cavity (CV), showing resemblances with the canal structures.

The upper valve is strongly inclined towards the cardinal area and the beak overlapping the commissure line descending about 10 mm below (Pl. III, fig. 1). The height of the valve is 90 mm in the holotype. A lot and thin radial canals are seen, because the outer layer is partly eroded (Pl. III, fig. 2). The transversal section, passing 10 mm above the commissure, is circular in shape and the diameter is about 100 mm (Pl. IV, fig. 4). The ligamental ridge (L) is thin, long (14-15 mm), truncated and enlarged at the top towards the posterior side. The

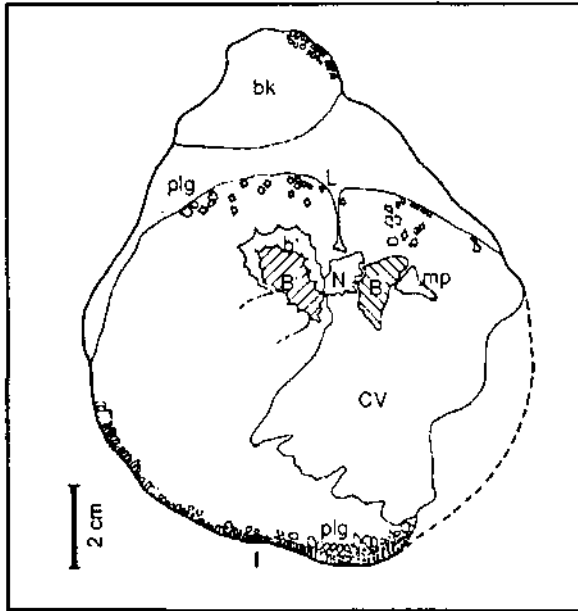


Fig. 6- *Sabinia ornata* n. sp.
Transverse section of the upper valve passing 10 mm above the commissure, holotype, No. Pm25.
The cardinal area is well preserved. The canal layer consists of fusiform (f) and polygonal (plg) canals. The section of the beak (bk) containing canals is also seen in the upper part of the figure. Compare with the Fig. 4 in the Pl. IV.

teeth of the valve are clearly preserved. The anterior tooth (B') is bigger than the other. The edge of the teeth are mostly zigzag in shape. The tooth of the lower valve is well developed. The posterior myophore (mp) is partly preserved.

The canal layer of the upper valve is not wide, about 3-5 mm, and it consists of fusiform and polygonal canals (Pl. IV, fig. 4; Fig. 6). The fusiform canals are 1-5 mm in length, and made generally of one row. However, in the siphonal region two row of the fusiform canals are observed. In the inner part of the canal layer, very little (1 mm) one row of numerous polygonal canal are arranged. In the both side of the ligamental ridge, many polygonal canals are also observed.

Discussion: *Sabinia ornata* n. sp. shows some resemblances to *Sabinia klinghardtii* Bohm

with the shape of the upper valve (Bohm, 1927), to *Sabinia aniensis* Parona and *Sabinia serbica* Kuhn and Pejovic with the shape of the canal of the upper valve (Parona, 1908; Kuhn and Pejovic, 1959). But, it differs from these species by the disposition of the canals of the upper and lower valve.

New species distinguish from all known species of *Sabinia* Parona by the characteristic structure of the siphonal region.

Manuscript received February 19, 1993

REFERENCES

- Bektaş, O.; Pelin, S. and Korkmaz, S., 1984, Mantle uprising and polygenetic ophiolites in the Eastern Pontid (Turkey) back-arc basin: TCK Ketin Simp. 175-188, Ankara, Turkey.
- Bohm, J., 1927, Beitrag zur Kenntnis der Senon der bithynischen Halbinsel: *Paleontographica*, V.LXIX, 187-222, Stuttgart.
- Camoin, G., 1983, Plats-formes carbonates et récifs à Rudistes du Crétacé de Sicile: *Trav. Lab. Geol. Hist. Paleont. Uni. Provence., Marseille.,* 13, 244
- Douville, H., 1904, Sur quelques rudistes à canaux: *Bul. Soc. Geol. France., Ser. 4, V. IV,* 536-538, Paris.
- Fenerci, M., 1992, The rudist fauna of Maden (Bayburt) Area: *Inst. Sci. Eng. Dokuz Eylül Univ. İzmir, Master thesis,* 68 p.
- Gattinger, T.E., Erentöz, C. and Ketin, İ., 1962, Explanatory text of the geological map of MTA Bull. Ankara, Turkey., 1-73.
- Karacabey, N., 1972, Quelques Rudistes provenant de la région de Divriği (Turquie Orientale): *MTA Bull.,* 78, 46-54, Ankara, Turkey.
- Kaya, O., Dizer, A., Tansel, I. and Özer, S., 1986a, Stratigraphy of the Upper Cretaceous and Paleogene in Yiğilca-Bolu (NE Turkey): *MTA Bull.,* 107, 1-21, Ankara, Turkey.
- ; Wiedmann, J., Kozur, H., Özdemir, Ü., Özer, S. and Beauvais, L., 1986b, A new discovery of the Lower Cretaceous in İstanbul, Turkey: *MTA Bull.,* 107, 106-112, Ankara, Turkey.

- Ketin, İ., 1951, Über die geologie der gegend von Bayburt in Nordost Anatolian: Rev. Fac. Sci. Univ. İstanbul., Ser. B, 16, 2, 113-127.
- Kuhn, O. and Pejovic, D., 1959, Zwei neue Rudisten aus Westserbien: Osterreichische Akademie der Wissenschaften Mathematisch-Naturwissenschaftliche Klasse, Sitzungsberichte, Abt. I., V., 158 (1-10), 980-989.
- Lupu, D., 1976, Contribution a l'etude des Rudistes Senonien des Monts Apuseni: Mem. Inst. Geol. Geof., 24, 83-152.
- Özer, S., 1983, Les formations a Rudistes du Senonien superieur d'Anatolie Centrale: Trav. Lab. Stra. Paleoco. Univ. Province., Marseille, nouvelle Serie 1, 32 p.
- , 1985, İç Anadolu bölgesi rudist paleontolojisi ve paleobiyoğrafyası. Doktora tezi, Dokuz Eylül Üniv., 183 p.
- , 1988, Distribution stratigraphiques et geographiques des rudistes du Cretace Superieur en Turquie: First Inter. Conf. Rudists.. Belgrade, Abstracts, p. 16.
- , 1991, Upper Cretaceous rudist provinces in Turkey: Suat Erk Geol. Sym. Ankara, Abstract p. 111.
- , 1992, Relationships between the Anatolian and Arabian Plates during the Maastrichtian related to the Rudist fauna: 9th Petroleum Congress and Exhibition of Türkiye, Abstracts, p. 154, Ankara.
- Özer, S., Tansel, I. and Meriç, E., 1990, Biostratigraphy (Rudist, Foraminifer) of Upper Cretaceous-Paleocene sequences of Hereke-Kocaeli: J. Fac. Eng. Arch. Selçuk Konya, 1-2, 41-50.
- Özsayar, T., Pelin, S. and Gedikoğlu, A., 1981, Cretaceous in the Eastern Pontides: Black Sea Tec. Univ. Eart. Sci. Bul., 1, 2, 65-114.
- Pamouktchiev, A., 1961, Fauna Rudiste du Cretace superieur en Bulgarie I. Sur certains Hippurites de l'arrondissement de Breznik, Bulgarie de l'ouest: Ann. Univ. Sofia Geologie, 2, 56, 102-106.
- , 1981, Les fossils de Bulgarie: Accad. Bulgare Sci., 5, 152-206.
- Parona, C.I., 1908, Fauna a Rudiste della Pietra di Subiaco Nella Valle Dell-Aniene: Bul. Soc. Geol. Italie, 27, 299 p.
- Sladic, M., 1957, *Hippurites (Vaccinites) ultimus* Milovanovic iz sugulgan Potoka u Istocnoj Srbiji: Bul. Serv. Geol. Geophys. R.P. Serbie, 13, 273-282.
- Sladic-Trifunovic, M., 1977, Hippurites from the Maestrichtien sediments of Eastern Serbia: Ann. Geol. Pen. Balka., 41, 257-268.
- , 1978, *Hippurites hentschi* and the Maestrichtien rudist horizon in the Senonian sediments at St. Bartholoma (Kamachbecken, Austria): Ann. Geol. Pen. Balka., 42, 429-445.
- Tzankov, V., 1965, Sur la presence de *Plagioptychus belunensis* Mennessier dans le Turonien pres du village Ljalentzi-Env. de ville Tran-Bulgarie du Sud-Quest: Ann. Univ. Sofia Fac. Geol. Geog., 1, 58, 21-24.

PLATES

PLATE-I

Fig. 1 -5- *Mitrocaprina* madeniana n. sp.
Maastrichtian, Sırataşlar ridge, Maden, Bay-
burt.

Fig. 1- Upper and lower valves, posterior side, holo-
type, No. Pm 27, X0.6 Note thin lamellae (ar-
row) on the surface of the lower valve.

Fig. 2- Upper valve, view of the radial canals, para-
type, No. Pm 28, X0.5.

Fig. 3- Lower valve, transverse section near the com-
missure, paratype, No. Pm 31, X0.8. Some ca-
nals (arrow) of the upper valve are also ob-
served in the posterior side.

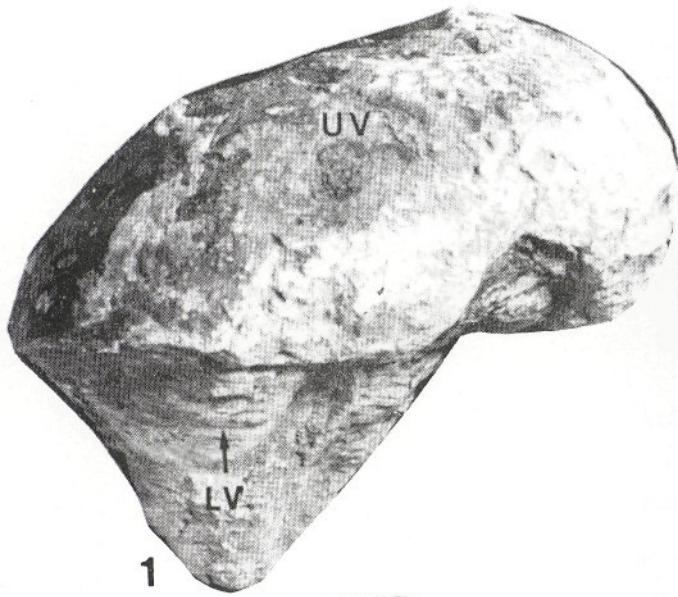
Fig. 4- Lower valve, transverse section near the com-
missure, paratype, No. Pm 31, X0.7. Note the
canals (arrow) of the upper valve.

Fig. 5- Lower valve, transverse section below 10 mm
of the commissure, paratype, No. Pm 29 X0.7.

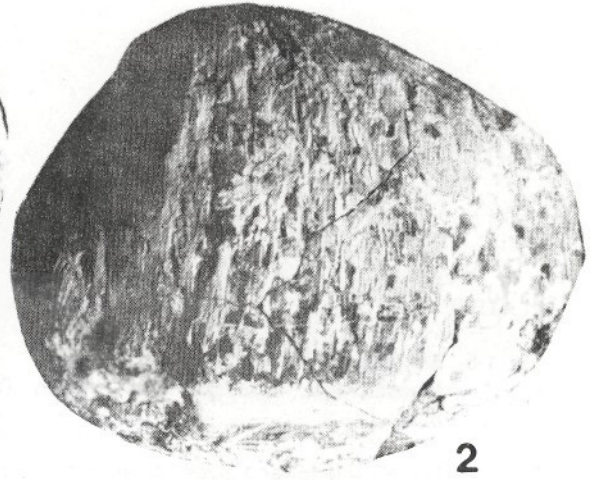
UV, LV Upper and lower valves.

B , B ' Posterior and anterior teeth.

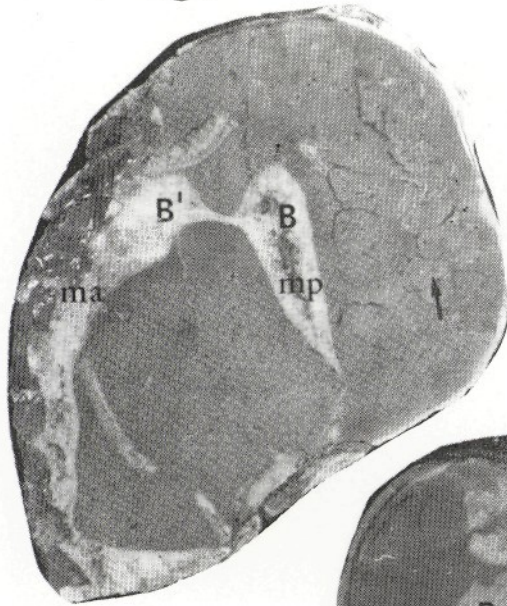
mp, ma Posterior and anterior myophores.



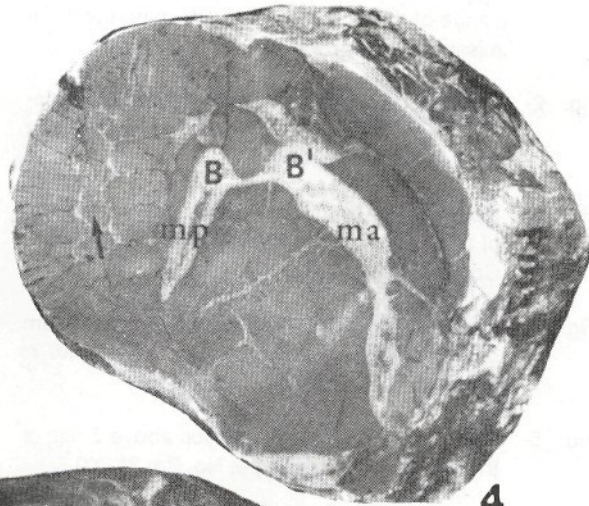
1



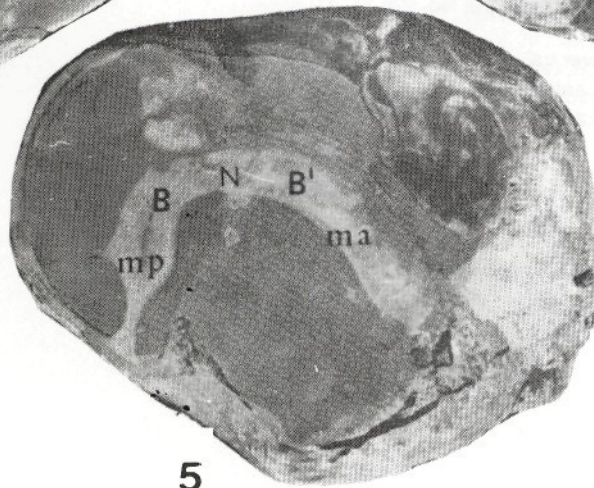
2



3



4



5

PLATE-II

Fig. 1 -5- *Mitrocaprina madeniana* n. sp.
Maastrichtian, Sırataşlar ridge, Maden, Bay-
burt.

Fig. 1- Upper and lower valves, anterior side, holo-
type, No. Pm 27, X0.6. Note the capuloid
shape of the upper valve overlapping the com-
missure line (arrows).

Fig. 2- Upper and lower valves, external surface, holo-
type, No. Pm 27, X 0.5. Note the radial canals
(arrows) of the upper valve.

Fig. 3- Upper valve, transverse section above 12 mm
of the commissure, holotype, No. Pm 27, X0.6.
Compare with the Text-Fig. 2

Fig. 4- Upper valve, transverse section above 10 mm
of the commissure, paratype, No. Pm 29, X0.7.
Compare with Text-fig. 3.

Fig. 5- Upper valve, transverse section above 7 mm of
the commissure, paratype, No. Pm 31, X0.7.

UV, LV Upper and lower valves.

B, B' Posterior and anterior teeth.

mp, ma Posterior and anterior myophores.

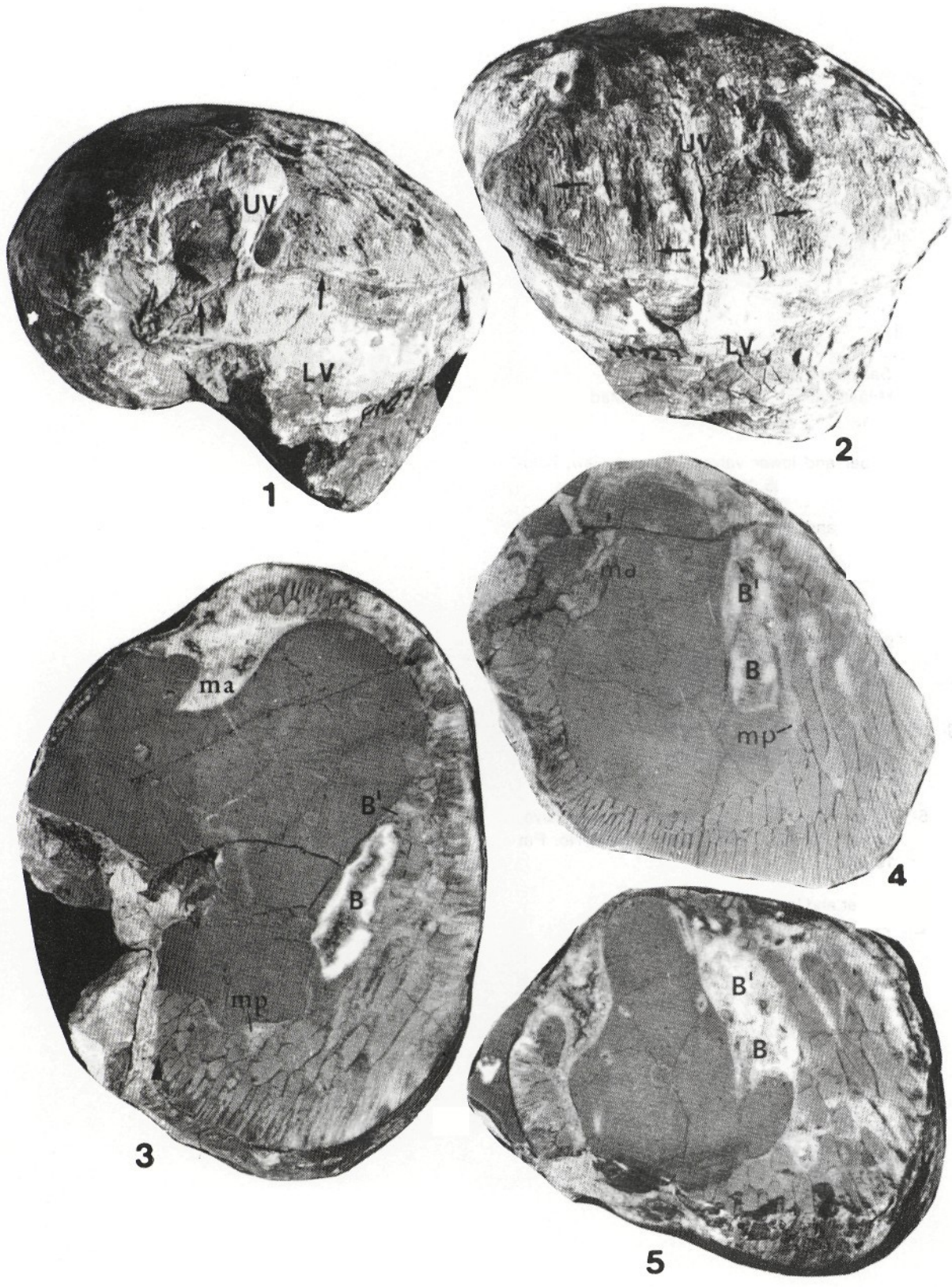


PLATE-III

Fig. 1 -5- *Sabinia ornata* n. sp.

Maastrichtian, Sirataşlar ridge, Maden, Bayburt.

Fig. 1- Upper and lower valves, external view, holotype, No. Pm 25, X0.5.

Fig. 2- Upper and lower valves, view of the siphonal region, holotype, No. Pm 25, X0.6. Note the radial canals (arrow) of the upper valve.

Fig. 3- Lower valve, external view of the siphonal region, paratype, No. Pm 14, X1. Note the costae of the interband (I) showing the resemblance with those others costae.

Fig. 4- Lower valve and partly preserved upper valve, view of the siphonal region, paratype, No Pm 16.X0.5.

Fig. 5- Lower valve and partly preserved upper valve, external view of the siphonal region, No. Pm 18, X0.9.

UV, LV : Upper and lower valves.

S, E : Posterior and anterior siphonal bands.

I : Interband.

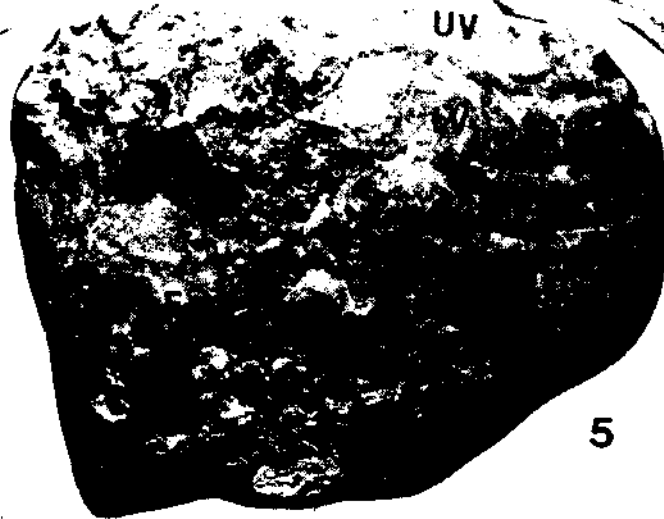
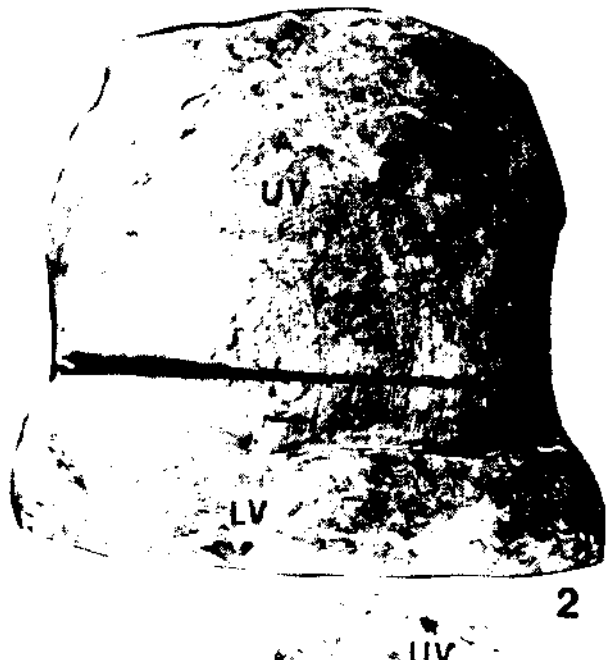
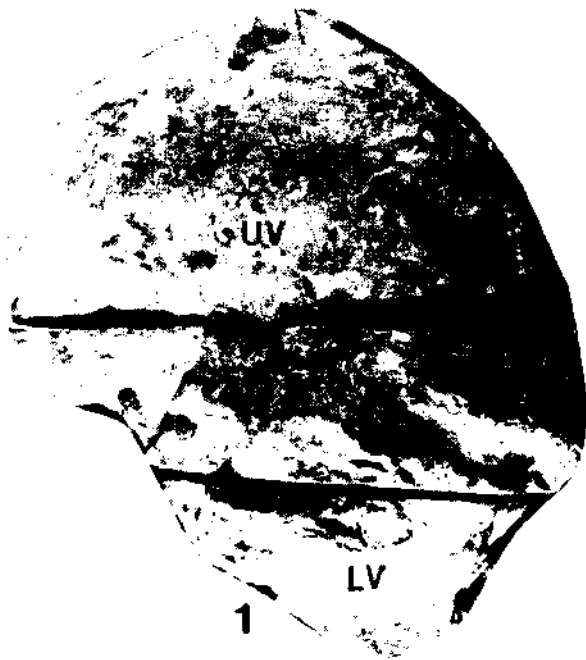


PLATE-IV

Fig. 1-4- *Sabinia ornata* n. sp.

Maastrichtian, Sirataşlar ridge, Maden, Bayburl.

Fig. 1- Lower valve, Transverse section below 15 mm of the commissure, holotype, No. Pm 25, X0.7. Compare the canals (r, f, plg, q) with the text-fig. 4.

Fig. 2- Lower valve, transverse section below 8 mm of the commissure, paratype, No. Pm 26, X0.8. Compare with the text-fig. 5.

Fig. 3- Lower valve, transverse section, commissure unknown, paratype, No. Pm 14, X1.2. Note the rectangular canals (r).

Fig. 4- Upper valve, transverse section above 10 mm of the commissure, holotype, No. Pm 25, X0.7. The section of the upper valve's beak (bk) is also seen. Compare with the text-fig. 6.

Fig. 5- *Hippurites sulcatoides* Douville

Maastrichtian, Sirataşlar ridge, Maden, Bayhurl. Lower valve, transverse section, commissure unknown, No. Pm 6, X1.3. The ligamental ridge shows a slight bending inward. The posterior pillar is short while the anterior is slightly narrow-necked.

L : Ligamental ridge.

Sp, Ep : Posterior and anterior pillars.

CV : Central cavity.

mp : Posterior myophore.

B, B', N : Teeth.

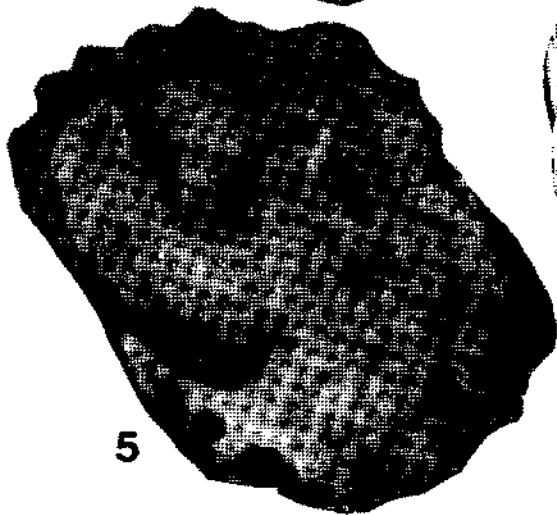
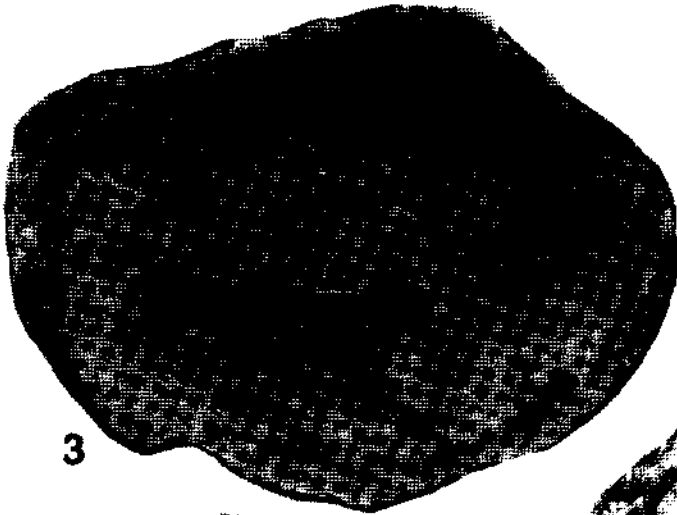
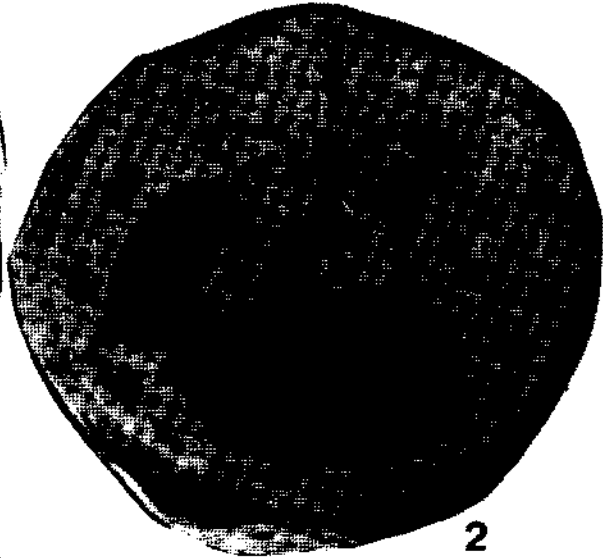
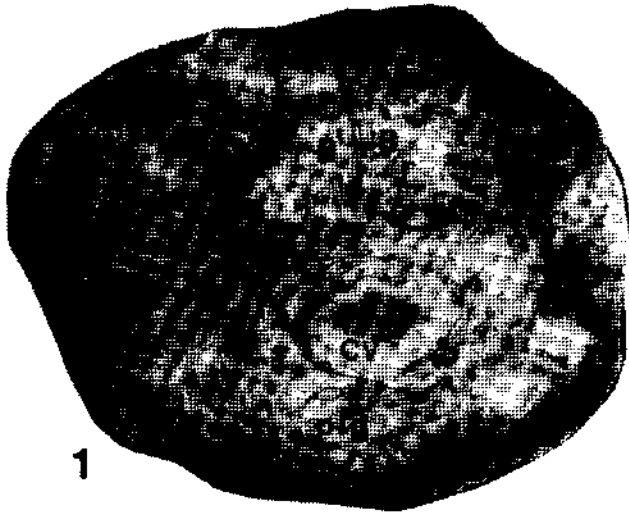


PLATE -V

- Fig. 1 -2- *Sabinia ornata* n. sp.
Maastrichtian, Sırataşlar ridge, Maden, Bay-
burt.
- Fig. 1- Lower and partly preserved upper valve, view
of the posterior side very near to the cardinal
area, paratype, No. Pm 26, X0.6. Note the la-
mellae (arrow) densely imbricated around cardi-
nal area
- Fig. 2- Lower valve, external view of the siphonal re-
gion, paratype, No. Pm 15, X0.8.
- Fig. 3- *Vaccinites ultimus* Milovanovic
Maastrichtian, Sırataşlar ridge, Maden, Bay-
burt. Lower valve, transverse section, commis-
sure unknown, No. Pm 12 X0.9.
- Fig. 4- *Joufia cappadociensis* (Cox)
Maastrichtian, Sırataşlar ridge, Maden, Bay-
burt. Upper valve, transverse section nearer the
commissure, No. Pm 22, X0.8. The cardinal
area is well preserved. Note the canal layer
consisting of a single row radial canals.

UV, LV : Upper and lower valves.

S, E : Posterior and anterior siphonal bands.

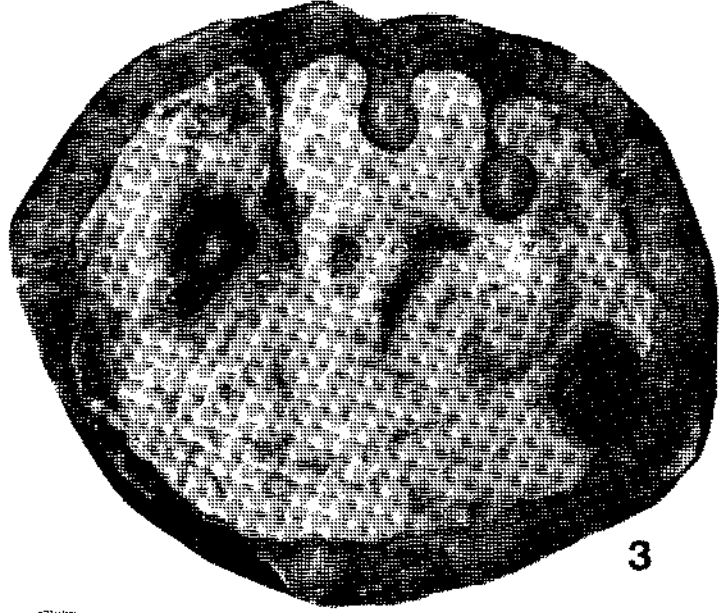
I : Interband.

L : Ligamental ridge.

B, B' : Teeth.

Sp, Ep : Posterior and anterior pillars.

mp, m : Posterior and anterior myophores.



THE LATE MIOCENE PERISSODACTYLA IN SAZAK (KALE-DENİZLİ)

Tanju KAYA*

ABSTRACT. - A new mammalian fauna is recognized in the southwest of Sazak (Kale-Denizli). *Hipparion matthewi* Abel and *Ceratotherium neumayri* (Osborn) are described and compared with similar forms from Turkey and Eurasia. The Perissodactyla is indicative of a late Late Miocene (Middle Turolian) age. The paleoecologic characteristics suggest a steppe environment with patches of bushes.

INTRODUCTION

The objective of this paper is to describe the Perissodactyla of a new fauna in Sazak, and to discuss their biochronological and the paleoecological aspects.

There is no published data which is directly concerned with the geology of the Sazak area (Kale-Denizli). Regional studies have dealt with some units, which in part may be correlatives of the Neogene continental deposits in the Sazak area (e.g. Nebert, 1956; Yalçınlar, 1951; Taner, 1975). Becker-Platen et al. (1975) recorded *Hipparion* sp., *Diceros neumayri* (Osborn) and *Chilotherium schlosseri* (Weber) in Mahmutgazi (Çal-Denizli), with reference to the Kınık and Garkın fauna

groups. Staesche and Sondaar (1979) recognized *Hipparion matthewi* Abel in Mahmutgazi, and suggested a Middle Turolian age. Gökçen (1982) recorded a lower shallow marine and an upper continental Neogene sequence in the surroundings of Muğla-Denizli, and established 10 lithologic subdivisions ranging in age from Early Aquitanian to Pontian, on the basis of ostracods. The Sarayköy lignites are late Middle Miocene and early Late Miocene in age (E. Akyol, 1992, oral communication).

The fossils presented in this paper have been recovered from the continental strata exposed at the Kapuşçabaşı Mevkii, between Kurt Tepe and Yayla Tepe, 1 km. southwest of Sazak (Kale) (Fig. 1).

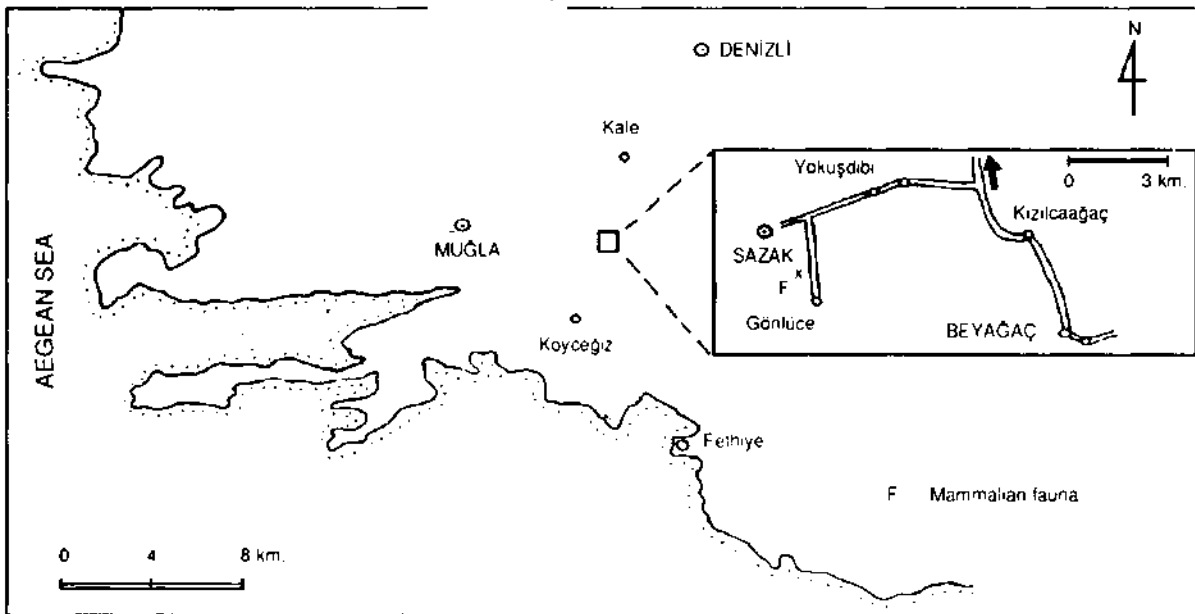


Fig. 1- Location map.

The osteological and odontological terms and systematics used for Hipparion and Ceratotherium follow those of Forsten (1968), Gromova (1952) Prothero and Schoch (1989) and Heissig (1972, 1989), and Klaitz (1973). The geological scale is according to Steininger et al. (1989). Mammalian zones are according to Mein (1975). Measurements are given in mm. The material is stored in the Natural History Museum (İzmir).

Abbreviations used in this work are: breadth (br); diameter (dia); metacarpal (Mc); Denizli-Kale-Sazak (DKS); Çanakkale-Gülpınar (ÇG); Muğla-Yatağan-Eski Bayırköy (MYB); Muğla-Yatağan-Salihpaşalar (MYS); Afyon-Sandıklı-Garkın (ASG); Uşak-Eşme-Akçaköy (UEA); Samos 5 (S), Pikermi (P), Saloniki (Sq), Halmyropotamos (H)-Greece; Upper Maragha-Persia (M); Fort Ternan-Kenya (F).

STRATIGRAPHY

Becker-Platen (1970) subdivided the Neogene deposits of southwest Anatolia into four major rock units, in ascending order: the Helvetian-Tortonian Turgut unit (limnic-fluviatile), the Sarmatian-Pontian Sekköy unit (limnic), the Pontian Yatağan unit (terrestrial-fluviatile), and the Dasian Milet unit (limnic). The Yatağan unit, which is widely exposed in southwest Anatolia, consists of two parts: a lower part of gray clayey limestone, interstratified tuffite and claystone, and an upper part of tuffite, brownish limny mudstone, conglomerate, claystone and gray limestone. The fossils of this study have been recovered from the brownish claystone layers in the upper part of the Yatağan unit.

The studied section of the Yatağan unit corresponds to Taner's (1975) early Early Pliocene deposits with *Radix (Adelinella) phrygovata* Oppenheim and late Early Pliocene strata with *Didacna (Pontalmyra) tosunlari* Taner, to Gökçen's (1982) Pannonian and Pontian deposits with *Cypria* sp. and *Darwinula* brew's Straub, to Atalay's (1980) Bayır member, and to Hakyemez's (1989) Yatağan formation.

PALEONTOLOGY

Order : Perissodactyla Owen, 1848
 Suborder : Mesaxonia Marsh, 1884
 Infraorder : Hippomorpha Wood, 1937
 Superfamily : Equoidea Gray, 1821
 Family : Equidae Gray, 1821
 Subfamily : Equinae Gray, 1821

T r i b e :: Hippotheriini Bonaparte, 1850

Genus : Hipparion de Christol, 1832

Type species : *Equus primigenius* Von

Meyer, 1829

Hipparion matthewi Abel,

1926

Pl. I, fig. 1,2

Material

Juvenile right mandibular fragment with DP₂-DP₄ (DKS-1); left astragalus (DKS-2); left calcaneum (distal part) (DKS-3).

Description

DP₂-DP₄.- The height of the ramus is 28 mm. under the middle of DP₂ and 37 mm under the middle of DP₄. The teeth are high-crowned. The external depression between the protoconid and the hypoconid is shallow. The enamel of the borders of the anterior and posterior fossetula is slightly crenellated. The protostylid and the ectostylid have not reached the occlusal surface. The cement and the enamel are thick.

Astragalus.-The astragalus is small. On the plantar view there are three facets for the calcaneum. Proximally the ectal facet meets the trochlea in an acute edge. There is a gap on the lateral part. The ectal facet meets the small and the long calcaneal facet in a blunt crenet. The sustentacular facet is long and convex in proximo-distal direction. It extends all along the height of the astragalus. The distal surface is occupied by the navicular facet, which is convex in dorso-plantar direction. The cuboid facet is quadrate-shaped and small, it forms almost a right angle with the navicular facet. The medial tuber is rounded.

Calcaneum-The calcaneum and the astragalus belong to the same individual. The tuber calcanei is broken. On the dorsal view the sustentaculum tali forms an acute elbow. There are three articulation facets for the astragalus. The ectal facet is proximally convex, distally concave. The calcaneal facet is narrow and long towards the distal direction. The sustentacular facet is long and concave in proximo-distal direction. The distal facet (for the cuboid) is quadrate-shaped, ending rather abruptly in the plantar direction. The lateral surface of the calcaneum is rough.

Comparisons

In respect to the morphology and size of the teeth and bones, *Hipparion matthewi* from Sazak is similar to those from Samos 5 (Werhli, 1941; Sondaar, 1971), Saloniki (Arambourg and Piveteau, 1929; Forsten, 1968), Upper Maragha (Bernor, 1978), Gülpınar (Kaya, 1986) and Salihpaşalar (Kaya, 1991) (Table 1,2,3).

Table 1- Measurements of DP₂-DP₄ of *Hipparion matthewi*

	DKS-1	Samos 5	
		Sondaar, 1971	Werhli, 1941
DP ₂ length/width	27/9	-	-
DP ₃ length/width	24/8	-	-
DP ₄ length/width	26/6	-	-
DP ₂ -DP ₄ length	77	80.5	69

H. matthewi is a small Hipparion. The size of *H. matthewi* is close to *H. gromovae* Villalta and Crusafont from Valdecebro (Spain) (Sondaar, 1961: astragalus height 43.5 mm., astragalus breadth distal articulation surface 32.7 mm.) and *H. macedonicum* Koufos from Ravin des Zouaves (Greece) (Koufos, 1987a: astragalus height 41.5 mm., astragalus breadth distal articulation surface 32 mm.). *H. matthewi* is smaller than *H. elegans* Gromova from Pavlodar (Siberia) (Forsten, 1968: astragalus height 47.4 mm., astragalus breadth distal articulation surface 35 mm.). *H. matthewi* is different from very small-sized *H. periafricanum* Villalta and Crusafont from Valdecebro (Sondaar, 1961: astragalus height 30.5 mm., astragalus breadth distal articulation surface 22.6 mm.).

Suborder : Ceratomorpha Wood, 1937
 Family : Rhinocerotidae Gray, 1821

Table 2- Measurements of astragalus of *Hipparion matthewi*. Samos5, Saloniki and Upper Maragha are taken from Forsten (1968)

	DKS 2	ÇG	MYS	S	Sq	M
a Maximum length	45	46	43	49.2	39.7	45.6
b Length at the internal trochlea	44	41	42	-	-	-
c Length at the external trochlea	39	31	38	-	-	-
d Maximum breadth	39	36	41	-	-	-
e Breadth of the distal facet	32	36	31	36.8	30.5	34.8
f Diameter of the distal facet	24	28	22	-	-	-
g Minimum breadth at the trochlea	19	21	20	-	-	-
e - x 100	71.1	78.2	72	74.7	76.8	76.3
a						

Table 3- Measurements of calcaneum of *Hipparion matthewi*

	DKS-3	ÇG	MYS
a Distal breadth	34	-	34
b Distal diameter	38	37	36
c Diameter of the corpus	32	-	31
d Breadth of the corpus	13	14	13
d - x 100	40.6	-	41.9
c			

Subfamily : Rhinocerotinae Gray, 1821
 Tribe : Dicerotini Groves, 1983
 Genus : *Ceratotherium* Gray, 1867
 Type species : *Ceratotherium simum* (Burchell, 1817)
Ceratotherium neumayri (Osborn, 1900) Geraads, 1988
 Pl. I, fig. 3, 4, 5

Material

Right carpal-4 (DKS-4), right metacarpal-III (DKS-5)

Description

Carpal-4.- The dorsal surface of the Sazak specimen is very large and flat. The ulnar facet slightly encroaches upon the dorsal surface. The posterior parts of proximal facets are free of grooves. The above mentioned characteristics belong to Rhinocerotini (Heissig, 1972).

The ulnar facet is convex in antero-posterior direction. It is lacking a volar appendix. An acute angle exists between the ulnar and intermedium facets. The intermedium facet is concave vertically, and separated from the carpal-3 facet by an acute ridge. There is a dorsal groove in medio-lateral direction in the middle of the dorsal surface.

On the medial view the carpal-3 facet is quadrate-shaped, smooth and deeper than it is wide.

The metacarpal-III facet is slightly concave and narrow in dorso-volar direction. The Mc-IV facet is convex transversely, and broad in front. It is narrow in dorso-volar direction. The Mc-V facet is concave and narrower than the Mc-IV facet in dorso-volar direction. The Mc-V facet is separated from the volar projection by a deep groove.

The protuberance is broad and rounded proximo-distally as well as transversely. The volar projection ends bluntly.

The medial tuber is situated below the cret between the ulnar and intermedium facet, and well developed. The lateral tuber is slightly developed and situated on the farther lateral part of the dorsal surface.

Metacarpal-III- The carpal-4 and the metacarpal-III belong to the same individual. The proximal end is narrower than the distal one. The proximal tuberosities are flat. A shallow groove separates the tuberosities, The medial tuberosity spreads in the middle and lateral parts of the bone. The lateral tuberosity is small and situated below the cret between the carpal-3 and carpal-4 facets. The above mentioned characteristics belong to Rhinocerotini (Heissig, 1972).

The proximal mam facet for the carpal-3 is triangular-shaped and deep. It is narrow and concave -in medio-lateral direction. Its hind part is turned medially. There is a triangular-shaped hump between the volar Mc-IV facet and carpal-3 facet. The carpal-4 facet is convex and deep. It is separated from the carpal-3 facet by an acute cret.

On the lateral view, the Mc-IV facet consists of two separate facets. The distance between these facets is 9 mm. The dorsal Mc-IV, facet is vertical, triangular-shaped and concave. The volar one is rounded, concave and isolated.

Table 4- Measurements of carpal-4 of Dicerotini. ASG, MYB, *D. neumayri* (Heissig, 1975b); *P. Rhinoceros pachygnathus* (Gaudry, 1862); *P. Diceros pachygnathus* (Guérin, 1980)

	DKS-4	ASG	MYB	P	P
a Maximum breadth	71	69	70	67	71
b Height	42	56	52	58	47
c Diagonal diameter	82	81	.	96	95 75
d Diameter	57				71 75
e Br/dia of the intermedium facet	39/31	36.34	31 31		.
f Br/dia of the ulnar facet	26/27	44 34	32		.
g Br/dia of the Mc-III facet	22:18				.
h Br/dia of the Mc-IV facet	31:27	34	37		.
i Br/dia of the Mc-V facet	22 17	23			.
a					
- x 100	86 5	85 1		69 7	74 1
c					
b					
- x 100	51 2	69 1		60 4	49
c					

Mc-II facet is deep in dorso-volar direction and narrow vertically.

A shallow groove with proximo-distal extension exists above the dorsal part of the distal trochlea. On the volar view the sagittal keel is sharp. The shaft is flat and rough on both sides. The volar part of the distal trochlea bears two vertical grooves.

Comparisons

The carpal-4 of *C. neumayri* from Sazak resembles those of *Diceros neumayri* (Osborn) from Garkin and Eski Bayırköy (Heissig, 1975b), *Rhinoceros pachygnathus* Wagner from Pikerimi (Gaudry, 1862), and *Diceros pachygnathus* (Wagner) from Pikerimi (Guerin, 1980) in shape as well as in size (Table 4).

The carpal-4 from Sazak is larger than Rhinocerotini type 1 and 2 from Siwalik (Pakistan) (Heissig, 1972; type 1 breadth 51 mm., height 42 mm., diameter 54 mm.; type 2 breadth 57 mm., height 47 mm., diameter 62 mm.). The size of the Sazak material is intermediate between *Dicerorhinus sumatrensis* (Fischer) from Sumatra (Hooijer,

1966: maximum breadth 61 mm.) and *Dicerorhinus ringstroemi* Arambourg from Shansi (China) (Hooijer, 1966: maximum breadth 78 mm.).

The carpal-4 from Sazak is similar to Rhinocerotini type 1 by the presence of the narrow Mc-IV and Mc-V facets in dorso-volar direction, and by having a deep groove between the Mc-V facet and volar projection. The Mc-V and Mc-IV facets are deep in Rhinocerotini type 2 (Heissig, 1972). These facets are independent surfaces in *Brachypotherium brachypus* (Lartet) from Sansan (Klaits, 1973). *C. neumayri* is close to the Rhinocerotini type 2 by the absence of the volar appendix of the ulnar facet (Heissig, 1972).

The dorsal surface of carpal-4 is very large and flat, whereas it is small and flat in Elasmotheriini, and it is very narrow and high in Aceratheriini (Heissig, 1976; Yan and Heissig, 1986).

The Mc-III from Sazak resembles *C. neumayri* from Salihpaşalar, *D. neumayri* from Garkin (Heissig, 1975b), and *D. pachygnathus* from Pikerimi (Guenn, 1980) in shape as well as in size (Table 5). The Sazak specimen is larger than *D. neumayri* from Eşme-Akçaköy (Heissig, 1975b) (Table 5).

Table 5- Measurements of metacarpal-III of Rhinocerotinae. MYS, *C. neumayri*; ASG, UEA, *D. neumayri* (Heissig, 1975b); P. *D. pachygnathus* (Guerin, 1980); H, *D. orientalis* (Melentis, 1970); F, *P. mukirii* (Hooijer, 1968)

	DKS-5	MYS	ASG	UEA	P	H	F
a	195	-	181		-	-	-
b	178	-	164		188.4	170	152
c	64	67	72	(62)	63.2	58	56
d	47	47	59	49	53.5	53	43
e	41	46	46	38	-	-	-
f	45	43	58	47	-	-	-
g	25	20	26	24	-	-	-
h	26	24	29	27	-	-	-
i	53	58	59	-	62.5	51	42
j	17	19	22	-	24.4	22	21
k	66	-	76	-	70.5	63	52
l	51	-	56	-	55.0	-	47
m	34	-	50	-	46.9	40	37
i							
- x 100	29.7	-	35.9	-	33.1	30	-
b							
k							
- x 100	37.0	-	46.3	-	37.4	37	-
b							

a- Maximum length, b- median length, c- proximal breadth, d- proximal diameter, e- breadth of the carpal-3 facet, f- diameter of the carpal-3 facet, g- breadth of the carpal-4 facet, h- diameter of the carpal-4 facet, i- breadth in the middle of the shaft, j- diameter in the middle of the shaft, k- distal breadth, l - breadth at the trochlea. m- diameter at the trochlea

The Sazak material is longer than *Dicerorhinus orientalis* (Schlosser) from Halmyropotamos (Melentis, 1970) and *D. sumatrensis* (Hooijer, 1966: median length 158 mm, distal breadth 59 mm). The measurements of the proximal and distal ends are similar (Table 5). The Mc-III of *C. neumayri* is shorter than that of *D. orientalis* from Shansi (Ringström, 1924: median length 187 mm., distal breadth 68 mm.). The Mc-III from Sazak is relatively longer than that of *Paradicerus mukirii* Hooijer (Hooijer, 1968) from Fort Ternan (Table 5).

PALEOECOLOGY

The fossils occur in lenticular masses of brownish claystones. The bones have been accumulated by fluvial transport. The connected skeletal parts may suggest slight water movements, or a short fluvial transport.

H. matthewi is a steppe species: (Forsten, 1968). Its teeth structure and gracile bones are indicative of adaptation to a xerophytic environment. *C. neumayri* (Heissig, 1975a) and the other faunal elements, *Pachytragus* sp. and *Gazella* sp. (Berg, 1975) suggest, as a whole, a habitat of open country and shrub. The paleoecologic characteristics of the fossils suggest a steppe environment with patches of bushes.

The above environmental evaluation is compatible with the steppe-like to semi-arid conditions proposed by Benda and Meulenkamp (1990) for the Turolian in western Anatolia on the basis of Kızılhisar pollen association.

AGE

In western Anatolia, the strata with *H. matthewi* (e.g. Mahmutgazi-Denizli; Eski Bayırköy, Bayırköy, Salihaşalar, Şerefköy, Akkavak-Muğla; Kemiklitepe-Uşak; Karain, Taşkınpaşa-Nevşehir; Ebiç-Kayseri; Kavakdere, Evciköy-Ankara) are of Turolian age (Becker-Platen et al., 1975; Atalay, 1980; Kaya, 1991). The above mentioned faunas have usually been considered to be correlative of the Kınık fauna group (MN 12) (Staesche and Sondaar, 1979; Kaya 1991). The Upper Maragha and Samos 5 faunas with *H. matthewi* were assigned to Middle-Late Turolian MN 12, MN 13, respectively by Steminger et al. (1989). *H. matthewi* has also been recorded from the Pontian of Ploski Blagoev-

radsko, from the Meotian of Ezerovo (Bulgaria), and from the Turolian of Beluska and Vozarzi (Macedonia) (Forsten, 1978a; Forsten and Garevski, 1989).

C. neumayri is known in Late Miocene (Vallesian and Turolian) faunas (Heissig, 1975a), and exhibits an increase in size in its evolutionary trend. The small specimens occur in the Vallesian of Eşme-Akçaköy and the Lower Turolian of Kayadibi, and the large-sized ones are present in the Lower Turolian of Garkın and the Middle Turolian of Kınık. Strong specimens are known in the Late Turolian Amasya fauna.-The measurements of the Sazak specimens indicate a Middle-Late Turolian age.

In conclusion, the Perissodactyla of Sazak may indicate a Middle Turolian age.

RESULTS

The Perissodactyla in Sazak, which are recognized in the upper part of the Yatağan unit, include *Hipparion matthewi* Abel and *Ceratotherium neumayri* (Osborn). *H. matthewi* is similar to those of Çanakkale, Muğla, Samos 5 and Upper Maragha. *C. neumayri* resembles those of Afyon, Muğla and Pikerimi. The size of *C. neumayri* indicates a high evolutionary level. These fossils are of a late Late Miocene age (Middle Turolian). The paleoecological characteristics are indicative of a steppe environment with patches of bushes.

ACKNOWLEDGEMENT

I thank Ali Tıkım (Sazak-Denizli), who has informed me about the fossiliferous exposures, Mualla Gürle (İzmir) for the drawing and Erol Şanlı (İzmir) for the photographs.

Manuscript received May 29, 1992

REFERENCES

- Abel, O.. 1926, Die Geschichte der Equiden auf dem Boden Nordamienkas: Verh. zool. Ges. Wien, 74-75, 159-164.
- Arambourg, C. and Piveteau, J., 1929, Les vertebres du pontien de Salonique: Ann. Paleontol., XVIII, 59-138.

- Atalay, Z., 1980, Muğla-Yatağan ve yakın dolay karasal Neojen'inin stratigrafi araştırması: TJK Bull, C 23, 93-99, Ankara.
- Becker-Platen, J.D., 1970, Lithostratigraphische untersuchungen in Kanozoikum Sudwest-Anatoliens (Turkei): Beih. Geol. Jb., 97, 1-244.
- ; Sickenberg, O. and Tobien, H., 1975, Die Gliederung der Kanozoischen Sedimente der Turkei nach Vertebraten-Faunengruppen: Geol. Jb., B 15, 1-100.
- Benda, L. and Meulenkamp, J.E., 1990, Biostratigraphic correlations in the eastern Mediterranean Neogene: Newsl. Stratigr., 23, 1,1-10.
- Berg, D.E., 1975, Miozane Boviden (excl. Ovivovinen) aus der Turkei: Geol. Jb. B 15, 157-158.
- Bernor, L., 1978, The mammalian systematics biostratigraphy and biochronology of Maragha and its importance for understanding Late Miocene Homioid zoogeography and evolution: Ph. D. Univ. California, 314.
- Forsten, A.M., 1968, Revision of the Palearctic *Hipparion*: Acta Zool. Fennica, 119, 1-134, Helsingfors.
- , 1978a, A review of Bulgarian *Hipparion*: Geobios, 11 (1), 31-41.
- Forsten, A. and Garevski, R., 1989, Hipparions/mammalia, Penssodactyla from Macedonia/Yugoslavia: Geol. maced., T 3, Nr. 2, 159-206.
- Gaudry, A., 1862, Animaux fossiles et geologie de l'Attique: F. Savy., LXXV, 476, Paris.
- Geraads, D., 1988, Revision des Rhinocerotinae (Mammalia) du Turolien de Pikermi. Comparaison avec les formes voisines: Ann. Pal., 74, 1, 13-41.
- Gökçen, N., 1982, Denizli ave Muğla çevresi Neojen istifinin ostrakod biyostratigrafisi: Yerbilimleri, 9, 111-131, Ankara.
- Gromova, V., 1952, Le genre *Hipparion*: Inst. Paleont. Acad. Sci. URSS 36. Translated from Russam by St. Aubin., C.E.D.P.; 12, 1-288.
- Guerin, C., 1980, Les Rhinoceros (Mammalia, Perissodactyla) du Miocene terminal au Pleistocene superieur en Europe occidentale, comparaison avec les especes actuelles: Doc. Lab. Geol. Fac. Sci., 79, 1-421, Lyon.
- Hakyemez, H.Y., 1989, Geology and stratigraphy of the Cainozoic sedimentary rocks in the Kale-Kurbalik area, Denizli, Southwestern Turkey: MTA Bull., 109, 1-14, Ankara.
- Heissig, K., 1972, Palaontologische und geologische Untersuchungen im Tertiär von Pakistan. 5. Rhinocerotidae (Mamm.) aus der unteren und mittleren Siwalik-Schichten. Abh. Bayer. Akad. Wiss. Math. Nat. Kl. N.F., Heft 152, 1-112, München.
- , 1975a, Rhinocerotidae aus dem Jungtertiär Anatoliens: Geol. Jb., B 15, 145-151.
- , 1975b, Rhinocerotidae aus dem Jungtertiär Anatoliens. 600 p., (unpublished), Müniç.
- , 1976, Rhinocerotidae (Mammalia) aus der *Anchitherium-Fauna* Anatoliens: Geol. Jb., B 19, 3-121.
- , 1989, The Rhinocerotidae: 399-417. In Prothere, D.R. and Schoch, R.M. (eds). The evolution of Perissodactyls, Oxford Univ. 537p.
- Hooijer, D.A., 1966, Miocene Rhinoceroses of East Africa: Bull. Brit. Muş 13, 2(Foss. Mamm. Afr. 21) 117-190, London.
- , 1968, A Rhinoceros from the Late Miocene of Fort Ternan, Kenya: Zoologische Mededelingen, Deel, 43, 6, 77-92.
- Kaya, T., 1986, Çanakkale ve çevresi Perissodactyla fosilleri: Doktora Tezi, 229p. (unpublished), Izmir.
- , 1991, Muğla yöresindeki Genç Miyosen yaşlı memeli faunasındaki Perissodactyla bulguları: Suat Erk Sempozyumu, Ankara.
- Klairs, B.G., 1973, Upper Miocene rhinoceroses from Sansan (Gers.) France: The manus: Jour. Paleontology, 47, 315-327, Kansas.
- Koufos, G.D., 1987a, Study of the Turolian Hipparions of the lower Axios valley (Macedonia, Greece). Geobios, n. 20, 3, 293-312.
- Mein, P., 1975, Resultats du Groupe de travail des Vertebres: In Senes, J., (ed), "Report on Activity of R.C.M.N.S. Working Group", Reg. Comm. Med. Neogene Stratigraphy, 78-81.

- Melentis, J.K., 1970, Die Pikermifauna von Halmyropotamos (Euboa, Griechenland): Ann. Geol. Des. Pays, Hellen, I serie, 19, 283-411, Athen.
- Nebert, K., 1956, Denizli-Acıgöl mevkiinin jeolojisi. 1/ 100.000'lik Denizli 105/1, 105/2 ve Isparta 106/1 paftalarının sahası içinde yapılan jeolojik harita çalışmaları hakkında rapor: MTA Rep., 2509, 107p. (unpublished) Ankara.
- Osborn, H.F., 1900, Phylogeny of the Rhinoceroses of Europe: Bull. Amer. Mus. Nat. Hist., 8, 229-267, New York.
- Prothero, D.R. and Schoch, P.M., 1989, Classification of the Perissodactyla: In Prothero, D.R. and Schoch, R.M. (eds). The evolution of Perissodactyls, Oxford Univ., 537p.
- Ringstrom, T.J., 1924, Nashorher der Hipparion-Fauna Nord-Chinas: Pal. Sinica, C, 1, 1, 1-159, Peking.
- Sondaar, P.Y., 1961, Les *Hipparion* de l'Aragon meridional: Estudios Geol., 17, 209-305, Madrid.
- Sondaar, P.Y., 1971, The Samos *Hipparion*: Proc. Kon. Neder. Akad. Wetensch., B74, 4, 417-441, Amsterdam.
- Staesche, U. and Sondaar, P.Y., 1979, *Hipparion* aus dem Valesium und Turolium (Jungtertiar) der Turkei: Geol. Jb., B 33, 35-79, Hannover.
- Steininger, F.F.; Bernor, R.L. ve Fahlbush, V., 1989, European Neogene marine/continental chronologic correlations: European Neogene mammal chronology, 15-46, New York.
- Taner, G., 1975, Denizli bölgesi Neojenin paleontolojik ve stratigrafik etüdü III: MTA Bull., 85, 45-66, Ankara.
- Werhli, H., 1941, Beitrag zur Kenntniss der Hipparionen von Samos: Pal., Zeitschr., Bd., 22, 321-386, Berlin.
- Yalçınlar, I., 1951, 1961 yazında arazi çalışmalarına ait rapor: MTA Rep., 3261 (unpublished), Ankara.
- Yan, D. and Heissig, K., 1986, Revision and autopodial morphology of Chinese-European Rhinocerotid genus *Plesiaceratherium* Young 1937: Abh. Bayer. Staatsslg. Palaont. hist. Geol., 14, 81-110. Zitteliana.

PLATE

PLATE-I

Hipparion matthewi Abel 1926

Fig. 1- Juvenile right mandibular fragment with DP₂-DP₄
(DKS-1) (occlusal view) (X1)

Fig. 2- Left astragalus+calcaneum (DKS-2, DKS-3) (dorsal view) (X1)

Ceratotherium neumayri (Osborn, 1900)
Geraards, 1988

Fig. 3- Right carpal-4 (DKS-4) (distal view) (X1)

Fig. 4- Right metacarpal-III (DKS-5) (dorsal view) (X1/2)

Fig. 5- Right metacarpal-III (DKS-5) (volar view) (X1/2)



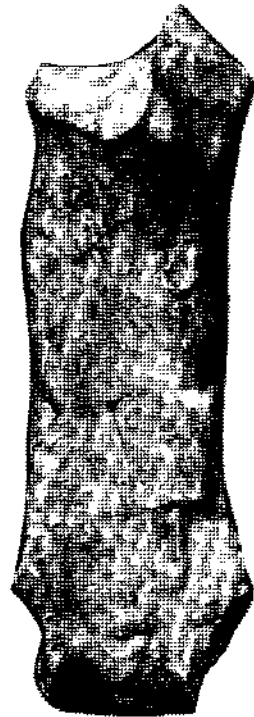
1



2



4



5



3

STRATIGRAPHY OF THE EASTERN SECTION OF THE PASINLER-HORASAN (ERZURUM) REGION

CevdetBOZKUŞ***

ABSTRACT— In the eastern part of the Pasinler-Horasan Neogene basin, the lowermost section consists generally of tuffs, andesites and basalts. This association is nomenclated as "Karakurt volcanics" They are underlain by an ophiolitic melange of Lower Cretaceous age which is unconformably overlain by the Oligocene Çayarası formation consisting of clastic rocks. The basin is bounded by sinistral strike-slip faults controlling sedimentation of various continental detritic rocks. These are distinguished as Aras and Horasan formations, both Pliocene in age, representing respectively marls and claystones of deep lagoonal environment, conformably overlain by fine grained sediments. Terrace gravels, alluvial fans and colluvium represent the Quaternary sedimentation.

GRAIN SIZE ANALYSIS OF SOME OLISTOSTROMES BETWEEN BALKUYUMCU AND ALCI (SW ANKARA)

Engin OLGUN* and Teoman NORMAN*

ABSTRACT. Sedimentary features and the detailed grain size analyses of six olistostromes (debris flows) have been examined; they are located between Alcı and Balkuyumcu villages, 40 km. southwest of Ankara. Photograph-grid method and sieving methods are used for gram size distribution analyses. The distribution of clast sizes within olistostromes are shown as histograms and cumulative curves. After calculating the main gram size parameters, their relations with respect to each other are examined on distribution diagrams (scatter diagrams). So, some of the distinguishing characteristics of olistostrome clast size distributions have been established. Studies on the clast size distribution and clast roundness indicate that, olistostromes are, in general, very poorly sorted, either negatively or positively skewed, mostly platykurtic. Clasts are angular to sub angular. Generally, scatter plots of grain size parameters of olistostromes are distinct when compared with other sedimentary deposits.

INTRODUCTION

Olistostromes are considered to be submarine debrisflow deposits with heterogeneous material in different sizes ranging from clay to block. Grain size analyses have been carried out on six different olistostromes, occurring in an area covering 17 square

kilometers, located between Alcı and Balkuyumcu villages, 40 km southwest of Ankara (Fig.1).

Each olistostrome has been sampled for grain size distribution at four, close but separate, localities. The sampling has been carried out at two levels: 1. Photographic grid sampling, 2. Sieve

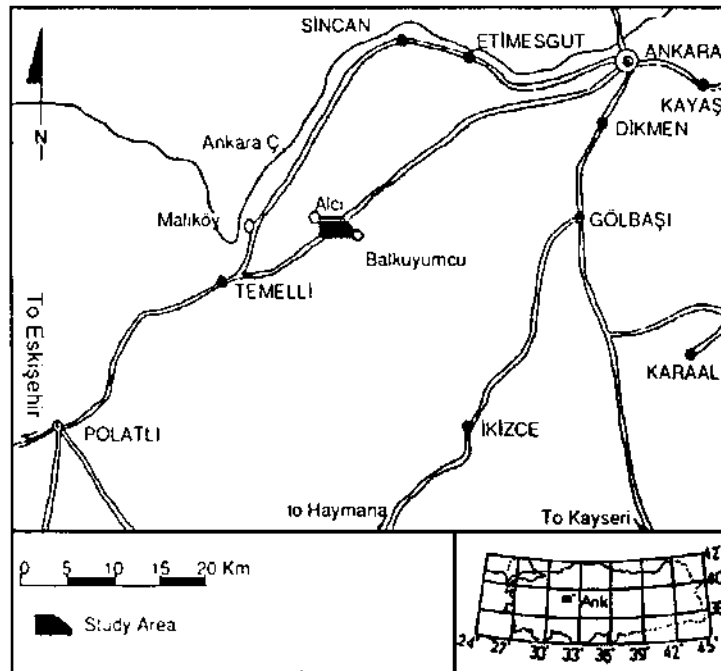


Fig. 1- Location map of the study area.

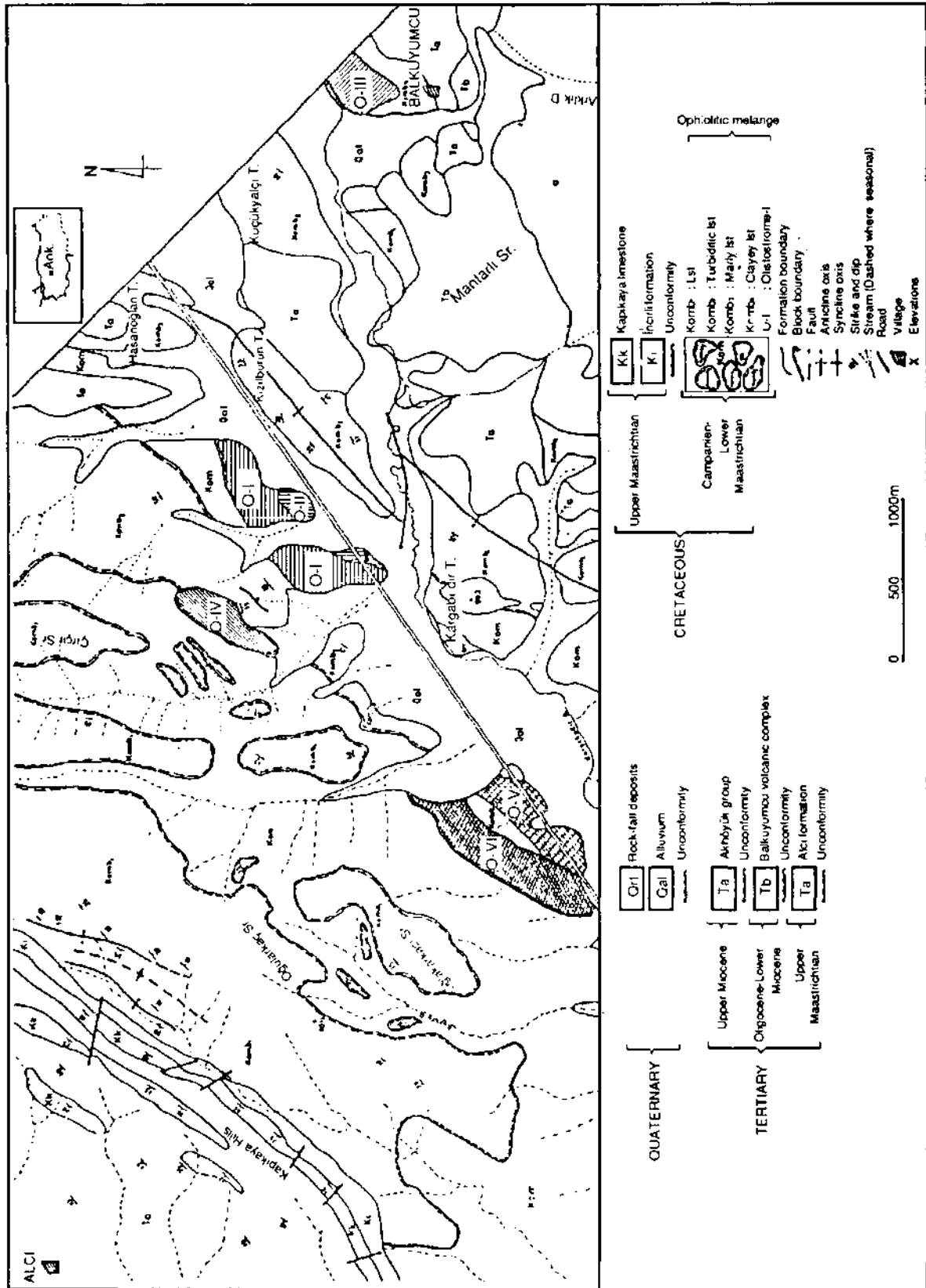


Fig. 2. Geological map of the study area (Modified from Kocyigit and Lunel, 1987; Lunel, 1987).

sampling of matrix material. In addition, 70 thin sections of clasts and matrix material have been studied to identify the ages of olistostromes. During the studies of grain size distribution, the standard model analysis technique is applied to determine the volumetric distribution of different clasts within the matrix of olistostromes.

Flores (1955) first defined the term "olistostrome", from the Greek words "olistomai" (to slide) and "strome" (accumulation) as "accumulation due to sliding". Flores argued that olistostromes are sufficiently continuous to be mappable, lithologically heterogeneous, more or less admixed, showing no true bedding, consisting of rocks accumulated as a semifluid body. Other related studies are made by several workers; Marchetti (1957), Gansser (1959), Hoedemaker (1973), Hsü (1974), Gökçen and Şenalp (1975), Koçyiğit (1979), Norman (1975 and 1979) and Bayraktutan (1982). Recently, olistostromes are defined as a sedimentary deposit consisting of a chaotic mass of intimately mixed heterogeneous materials (such as blocks and muds) that accumulated as a semifluid body by submarine gravity sliding or slumping of unconsolidated sediments (Jackson and Bates, 1980).

Some grain size distribution studies have been made by Passega (1957 and 1977) Folk (1954, 1964 and 1980), Folk and Ward (1957), Folk and Mason (1958), Friedman (1961, 1962 and 1967), Sahu (1964), Visher (1969), Buller and Mc Manus (1972) for river, dune, beach and turbidite sediments, using different grain size distribution parameters. One study (Gökçen and Özkaya, 1981) deals with the discrimination of olistostromes and turbidites by some sedimentary parameters; otherwise, very little published work on the distribution of grain size properties of olistostromes is available.

STRATIGRAPHIC POSITIONS, AGES GEOMETRIES AND THICKNESSES OF OLISTOSTROMES STUDIED

The oldest rock units are the Late Jurassic to Early Cretaceous limestones in the study area (Lünel, 1987). They are observed as megablocks (olistolith sizes larger than 500 m) and olistostromes within an ophiolitic melange which also consists of different sizes of blocks of radiolarian chert, serpentinite and pillow basalts (Koçyiğit and Lunel,

1987). These different blocks are seen in a fine grained matrix composed of greenish to gray colored shales, sandstones and pelagic mudstones. The studied six olistostromes are all situated in the ophiolitic melange and appear as blocks and lenses (Fig. 2). Where the boundary relations are clear, the olistostromes are seen to be conformable with the sedimentary rock units above and below (Fig. 3). In the northern part, the units of the ophiolitic melange are unconformably overlain by thick continental and shallow marine deposits of Tertiary age. In the southern part of study area, (Fig. 3), they are unconformably overlain by Tertiary volcanics and Pliocene clastic deposits.

Two types of olistostromes (matrix supported and clast supported) are recognized in the study area. Matrix supported olistostromes are O-I, O-II, O-V and O-VI, in which the clasts are dispersed in a fine grained matrix forming lobe or lens shape features (olistostromes are briefly denoted as "O"). Clast supported olistostromes are O-III and O-IV, in which the clast framework accommodates little amount of matrix. Matrix supported olistostromes have generally a polygenic composition, having different limestone clasts together with many ophiolitic constituents of Late Cretaceous age (Santonian-Early Maastrichtian). On the other hand, clast supported olistostromes are monogenic consisting of only limestone clasts with ages ranging from Late Jurassic (Oxfordian-Tithonian) to Early Cretaceous (Berriasian-Hauterivian) (Olgun, 1988).

In the field, O-I is about 35 m. in thickness and its length is 1 km (Fig. 2). In O-I, a lobe shape is recognized and its longitudinal section shows a "snout" like feature towards west. Generally, coarse clasts are observed at this "snout" part, showing reverse grading. O-II shows a parallel trend to O-I and it is 15 m. thick and 300 m. long. O-III is interbedded with marly limestones around Balkuyumcu village. Its thickness is 28 m. and length is 400 m. O-IV is observed as a lens; its lateral extension is 600 m. and thickness is 20 m. O-V is, also, lens shaped, with a thickness of 18 m. and length 650 m. O-VI occurs parallel to O-V; it is about 25 m. in thickness and 1 km. in length. These olistostromes generally show a lateral extension in NE-SW direction. No clast preferred orientation or internal structure, except reverse gradation, is detected.

AGE	ROCK UNITS	THICKNESS (m)	LITHOLOGY	DESCRIPTION
QUATERNARY	ALLUVIUM	> 10		Alluvium and Rock-Fall deposits
UPPER MIOCENE	AKHÖYÜK GROUP	~ 35		Claystones and Marls Lacustrine limestones
OLIGOCENE - LOWER MIOCENE	BALKUYUMCU VOLCANIC COMPLEX	~ 40		Andesitic and basaltic flows
PALEOCENE	ALCI FORMATION	145		Chaotic breccia
				Reefal limestone olistoliths
				Volcanic sandstone
				Conglomeratic sandstone
UPPER MAASTRICHTIAN	KAPIKAYA LIMESTONE	30		Fossil bearing reefal limestone
	INCIRLI FORMATION	35		Marl Sandstone, graded bedded Conglomerates
MIDDLE CAMPANIAN - LOWER MAASTRICHTIAN	OPHICLITIC MELANGE	?		Pelagic limestone blocks Mixture of serpentinite (s), radiolarite (r) and basic-ultrabasic rocks (v). Lenses of olistostromes Olistostromes interbedded with limestone

Fig. 3- Generalized stratigraphic section of the study area (Modified from Koçyiğit and Lünel, 1987; and Lünel, 1987).

GRAIN SIZE ANALYSES OF OLISTOSTROMES

a) Method: Since the olistostromes have very coarse size clast fractions (larger than any mesh or hole size of the available sieves) it is necessary to study their size distributions on photographs of outcrops in the field (Olgun, 1988).

To study the whole size range (mud to block) of an olistostrome, the "photograph-grid method"

and the "sieving method" are combined to obtain the full grain size distribution.

Four photographs are obtained of each olistostrome outcrop (a scale is included in the photographs). In the laboratory, photographs are projected onto a grid of 50x50 cm. area, providing 400 grid points 2.5 cm. apart. On the image over the gridded screen, at each grid point, the longest and the shortest diameter of each clast is measured and cover-

ted to length measurements in the field, based on the scale included on the photograph. Then, to obtain the clast size the geometrical mean of its diameters is calculated by \sqrt{dlxds} ; dl= the longest diameter (mm.), ds= the shortest diameter (mm.). Standard modal analysis technique (Chayes, 1956) is applied to determine the areal distribution of this clast size within the total amount. In this way, for each size class, a frequency (%) is obtained leading to the size distribution of the total sediment in the photograph. This process is repeated for all the photographs of the same outcrop.

In this study, the clast sizes between -2f (4mm.) and -10f (1024 mm.) are analyzed at 1f intervals, based on Wentworth grade scale. The counted grid points of clasts falling into the same size are added to obtain the proportion at that size class within the total area (i.e. the total number of points in the grid area). This proportion is used as the basis to calculate the size class distribution in the same area.

In the projected photographs, the grains finer than -2f (4mm.) are not clearly recognisable to make size measurements on them; this fraction is considered the "pan" fraction of the analysis. Sieving method is applied to this size fraction (represented by matrix) in order to separate them into different size classes. The sediment samples (matrix) are collected within the same locality of photographs. The sieve analysis is carried out using a stack of 7 sieves with apertures ranging from -1.0f (2 mm.) down to 5.0f (0.031 mm.) based on Wentworth grade scale. Then, each sieve fraction is weighed and the percentage sieve fractions are calculated to obtain the grain size distribution in the sieved sample.

Each olistostrome comprises two different sets of data: from grid analyses on photographs, and from sieve analyses. The former measures size distribution by the number of grid points which gives areal proportions. The latter is based on the weight distribution of each size fraction which is weighed and calculated to obtain the size distribution in the sample. Since areal percentages in the first method are proportional to the volumetric percentages (Chayes, 1956), and the weight percentages of the second method are also proportional to the vo-

lometric percentages, the data of the two methods used on the same sample can be combined on volumetric percentage basis to obtain total grain size distribution of the olistostrome on a single data sheet (Table 1). During this combination, sieve results of each matrix sample are multiplied by certain conversion factors to bring them into the same range as photographic grain size analyses. The combined data results are used to obtain the class percentage and cumulative percentage values, repeated at four localities on each of the six olistostromes. Histograms and cumulative curves of olistostromes are constructed and evaluated according to these results.

b) Results: Generally, bimodality is characteristic for all size distribution of the olistostromes studied (Fig. 4). The most common model size ranges for coarse materials are between -9.5f and -5.5f (boulder to pebble), and for finer (matrix) materials 0.5f and 4.5f (coarse sand to coarse silt). The general trend is almost trimodal for the histograms of O-II and O-IV. Third mode value between coarse and fine size concentrations range from -2.5f to -1.5f (pebble to granule) with a relatively low concentration value, the histograms of O-VI have an appearance of unimodal trend except for several small submode values.

The cumulative curves of O-I, O-II, O-IV and O-V show three different populations of grain size distribution. These separate populations (especially fine and coarse populations) are easily identified with their mean and standard deviation on the log-probability plot (Fig. 5). Generally, the coarse populations range between -13f (2048 mm.), and -50(32 mm.), and fine populations between -10 (2 mm.) and 4.5f (0.044 mm.). After constructing cumulative curves for each olistostrome, percentile values $f_1, f_5, f_{16}, f_{25}, f_{50}, f_{75}, f_{84}$ and f_{95} , are read off to calculate grain size parameters, such as first percentile (C), median (M), mean size (Mz), sorting (G₁), skewness (SK₁) and kurtosis (KG), as proposed by Folk and Ward (1957) (Table 2 and 3). The first percentile values of the olistostromes range from -12.85f (7500 mm.) to -7.20f (150 mm.) with an average of -9.97f (1000 mm.). The mean size values of the olistostromes range from -6.420 (86 mm.) to -1.83f (3.5 mm.) with an average of -3.79f (14 mm.). The sorting values

Table 1- Combined data results for photograph-grid and sieving methods.

SIZE		TOTAL COMBINED DATA																	
Class	mm.	phi(φ)	CLISTOSTROME - I						OLISTOSTROME - II										
			%	Cum %	%	Cum %	%	Cum %	%	Cum %	%	Cum %	%	Cum %					
GRAVEL	1024	-10	-	-	-	22.00	22.00	-	-	-	-	-	-	-	-	-	-		
	Boulder	-9	13.00	-	-	8.50	10.75	32.75	6.50	6.50	-	-	-	-	-	-	-		
	Cobble	256	-8	10.00	23.00	8.50	24.25	32.75	6.50	6.50	-	-	-	-	-	-	-	-	
		128	-7	6.00	29.00	15.75	43.50	43.50	7.25	13.75	-	-	-	-	-	-	-	-	
	Pebble	64	-6	9.75	38.75	21.25	45.50	52.25	11.25	25.00	9.50	9.50	11.50	16.50	13.75	29.75	12.00	28.50	
		32	-5	4.75	43.50	12.75	58.25	5.00	57.25	15.50	40.50	20.75	30.25	5.50	24.00	5.25	35.00	6.75	35.25
		16	-4	3.75	47.25	4.50	62.75	1.50	58.75	3.00	43.50	15.25	45.50	3.25	27.25	2.50	37.50	3.75	39.00
		8	-3	2.25	49.50	3.25	66.00	1.00	59.75	1.75	45.25	5.25	50.75	2.25	29.50	2.00	39.50	1.75	40.75
		4	-2	2.25	51.75	1.25	67.25	0.75	60.50	1.75	47.00	4.12	54.87	5.54	35.04	1.59	41.09	8.46	49.21
		2	-1	1.74	53.49	1.77	69.02	0.50	61.00	0.88	47.88	3.45	58.32	4.54	39.58	6.17	47.26	3.68	52.89
SAND	V. Coarse	0.0	2.71	56.20	1.82	70.84	2.73	63.73	2.06	49.94	3.28	61.60	4.17	43.75	2.27	49.53	6.10	58.99	
	Coarse	0.50	12.12	68.32	9.86	80.70	13.05	76.78	12.24	62.18	3.91	65.51	14.21	57.96	5.20	54.73	7.27	66.26	
		0.25	13.69	82.01	7.82	88.52	7.12	83.90	18.63	80.81	13.18	78.69	14.21	73.17	13.49	68.22	10.78	77.04	
	Fine	0.125	6.22	88.23	3.34	91.86	6.63	90.53	5.49	86.30	8.62	87.31	15.81	87.98	9.06	77.28	12.47	89.51	
		0.0625	5.34	93.57	3.72	95.58	5.97	96.50	8.70	95.0	5.97	93.28	8.29	96.27	16.12	93.40	6.73	96.24	
	MUD	Coarse silt	4.0	6.19	99.76	4.32	99.90	3.20	99.70	4.92	99.92	5.12	98.40	3.32	99.59	5.81	99.21	3.54	99.78
medium silt and clay		5.0	0.24	100.00	0.10	100.00	0.30	100.00	0.08	100.00	1.60	100.00	0.41	100.00	0.79	100.00	0.22	100.00	

Continued to Table 1

SIZE		TOTAL COMBINED DATA																
		OLISTOSTROME - III						OLISTOSTROME - IV										
Class	mm.	phi(D)	% Cum %	% Cum %	% Cum %	% Cum %	% Cum %	% Cum %	% Cum %	% Cum %	% Cum %	% Cum %	% Cum %					
GRAVEL	1024	-10	-	-	-	-	-	-	-	-	-	-	-					
	Boulder	512	-9	-	-	-	-	-	-	-	-	-	-					
	Cobble	256	-8	-	-	-	-	-	-	-	-	-	1.50	1.50				
		128	-7	-	-	-	-	-	11.00	11.00	2.00	2.00	-	11.50	13.00			
	Pebble	64	-6	10.00	6.50	4.00	4.00	3.75	3.75	16.00	27.00	10.75	12.75	3.75	19.50	32.50		
		32	-5	23.25	29.00	35.50	30.00	34.00	27.75	16.75	43.75	16.75	29.50	17.50	21.25	8.00	40.50	
		16	-4	20.25	53.50	22.00	57.50	28.75	62.75	26.50	8.75	52.50	15.50	45.00	12.25	33.50	6.75	47.25
		8	-3	7.25	60.75	8.75	66.25	6.25	69.00	6.50	2.25	54.75	7.25	52.25	8.50	42.00	1.50	48.75
	SAND	4	-2	2.50	63.25	1.75	68.00	3.00	72.00	3.00	13.50	68.25	2.25	54.50	2.25	44.25	0.25	49.00
		2	-1	3.70	66.95	4.10	72.10	3.67	75.67	4.59	6.90	75.15	14.33	68.83	9.96	54.21	9.23	58.23
V. Coarse		1	0.0	3.05	70.00	3.02	75.12	3.45	79.12	4.50	2.07	77.22	1.71	70.53	3.50	57.71	6.09	64.32
		0.50	1.0	7.39	77.39	6.06	81.18	5.57	84.69	6.91	2.71	79.93	3.52	74.06	3.02	60.73	3.78	68.10
Medium		0.25	2.0	6.06	83.45	5.62	86.80	4.58	89.27	4.55	5.40	85.33	8.14	82.20	6.63	67.36	7.78	75.88
		V. Fine	0.125	3.0	6.38	89.83	5.34	92.14	4.73	94.00	5.73	7.11	92.44	7.02	89.22	9.56	76.92	11.61
MUD			0.0625	4.0	4.62	94.45	3.80	95.94	2.56	96.56	3.05	5.73	98.17	9.60	98.82	8.52	85.44	9.48
		0.031 and clay	5.0	3.97	98.32	2.82	98.76	2.10	98.66	2.06	1.80	99.97	1.18	100.00	14.56	100.00	3.03	100.00
				1.68	100.00	1.24	100.00	1.34	100.00	1.11	0.03	100.00	-	-	-	-	-	-

SIZE		TOTAL COMBINED DATA													
		OLISTOSTROME - V						OLISTOSTROME - VI							
Class	mm.	phi(φ)	% Cum %	% Cum %	% Cum %	% Cum %	% Cum %	% Cum %	% Cum %	% Cum %	% Cum %	% Cum %	% Cum %		
GRAVEL	1024	-10	-	-	-	-	-	-	-	-	-	-	-		
	Boulder	512	-9	-	24.00	-	-	-	-	-	-	-	-	-	
		256	-8	27.50	26.75	50.75	25.50	25.50	22.00	22.00	-	-	-	9.50	
	Cobble	128	-7	15.25	42.75	9.50	60.25	22.75	48.25	13.50	35.50	8.50	8.00	-	1.75
		64	-6	21.25	64.00	9.25	69.50	17.50	65.75	14.50	50.00	5.25	13.75	4.75	12.75
	Pebble	32	-5	10.00	74.00	5.50	75.00	9.00	74.75	8.00	58.00	10.75	24.50	11.75	24.50
		16	-4	2.25	76.25	1.00	76.00	1.75	76.50	2.25	60.25	13.50	38.00	10.75	35.25
	SAND	8	-3	1.25	77.50	0.75	76.75	1.25	77.75	0.50	60.75	9.50	47.50	9.00	44.25
		4	-2	1.50	79.00	0.75	77.50	1.00	78.75	0.29	61.07	9.46	56.96	9.39	53.64
		2	-1	0.38	79.38	0.67	78.17	0.34	79.09	0.43	61.47	11.12	68.08	11.33	64.97
V. Coarse		1	0.0	0.91	80.29	1.10	79.27	1.16	80.25	2.58	64.05	7.09	75.12	7.43	72.40
		0.50	1.0	5.66	85.95	5.52	84.79	5.31	85.56	9.77	73.82	8.53	83.70	8.07	80.47
Medium		0.25	2.0	6.09	92.04	6.43	91.22	5.95	91.51	11.03	84.85	4.28	87.98	4.38	84.85
		0.125	3.0	3.05	95.09	3.79	95.01	3.27	94.78	7.12	91.97	4.97	92.95	6.38	91.28
MUD		0.0625	4.0	2.54	97.63	2.57	97.58	2.44	97.22	4.09	96.06	4.25	97.20	6.07	97.30
		0.031	5.0	2.19	99.82	2.20	99.77	2.56	99.78	3.64	99.70	2.77	99.97	2.62	99.92
medium silt and clay				0.18	100.00	0.22	100.00	0.22	100.00	0.30	100.00	0.03	100.00	0.08	100.00

range between -3.00 (8 mm.) and -5.00 (32 mm.), the results fall into very poorly to extremely poorly sorted category (Terminology from Folk, 1980), with an average of -3.900 (15 mm.). The bimodality is contributing greatly to the very poor sorting (Fig. 4). The skewness values of the olistostromes range from -0.462 (strongly coarse skewed) to 0.774 (strongly fine skewed) with an average of +0.29 (fine skewed). Nearly symmetrical distribution with zero skewness is also present. O-I, O-II have both positive and negative skewness values, while O-III, O-IV, O-V and O-VI have positive skewness. The kurtosis values range from 1.301 (leptokurtic) to 0.563 (very platykurtic) with an average of 0.806 (platykurtic) (Folk, 1980).

In order to establish the nomenclature of the major textural groups of sediments forming the olistostromes, the proportions of gravel, sand and mud, calculated from each olistostrome sample, are plotted in a ternary diagram (Fig. 6), proposed by Folk (1954). The sediments of olistostromes are mixtures of gravel, sand and relatively minor amounts of mud, and vary from sandy gravel to muddy sandy gravel as seen in the triangular diagram. The most striking feature is the, high amount of gravel size material which is generally more than the sum of other sediment types. The average values between 49.51 % and 74.53 % in the olistostromes studied. Average sand fractions range from 25 %-35 % and mud fractions from 2.64 %-5.20 %. The dominant mud class is coarse silt.

The clast roundness measurements are made on projected photograph samples, (two from each olistostrome, Table 4). The average roundness class intervals is computed by multiplying the mid points of the-roundness class intervals with the areal percentage values of those roundness classes (Powers, 1953). The computed results fall in partly angular to sub-angular (1.95-2.79) range.

DISCUSSION AND INTERPRETATION OF THE RESULTS

Grain size parameters are environmentally sensitive and combination of these parameters may permit separation and identification of different deposits (Mason and Folk, 1958). Different combinati-

ons of grain size parameters are plotted against each other, such as mean size (Mz) - sorting (G), mean size (Mz)-skewness ((SK_i), mean size (Mz)-kurtosis (KG_i), skewness (SK_i), kurtosis (KG_i), median (M)-first percentile (C) and median (M)-quartile deviation (QDa), and compared with the same parameter combinations from previously known environments. In the plots of mean size (Mz)-sorting (G_i), mean size (Mz)-skewness (SK_i), sorting (G_i)-skewness (SK_i), the plots of olistostromes are seen at the outside of previously constructed trends (Figure 7, 8 and 9). In the scatter diagram of quartile deviation (QDa) versus median (M), the plots of olistostromes occur within an envelope which is different from the envelopes of flaxoturbidites and proximal-distal turbidites (Fig. 10).

CONCLUSIONS

The conclusions reached in this study may be outline as follows:

1. Both bimodal and trimodal grain size distributions are characteristic for the studied olistostromes and the bimodality contributes to the very poor sorting. Skewness is not a significant parameter for olistostromes, varying in a wide range from strongly coarse skewed to strongly fine skewed. On the other hand, the kurtosis values are in platykurtic range due to poor sorting and polymodal nature; this may be considered one of the characteristic feature of olistostromes.
2. The sediment types of olistostromes vary from sandy gravel to muddy sandy gravel, in which the average mud fraction is less in amount than gravel and sand.
3. Scatter plots of grain size parameters fall generally outside the limits of river, beach and dune environments of several previous workers. However, plots of quartile deviation (QDa) versus median (M) seem to hold the best promise for distinguishing olistostromes from deposits of other environments.
4. The average roundness values of clast constituents of olistostromes range from angular to subangular.

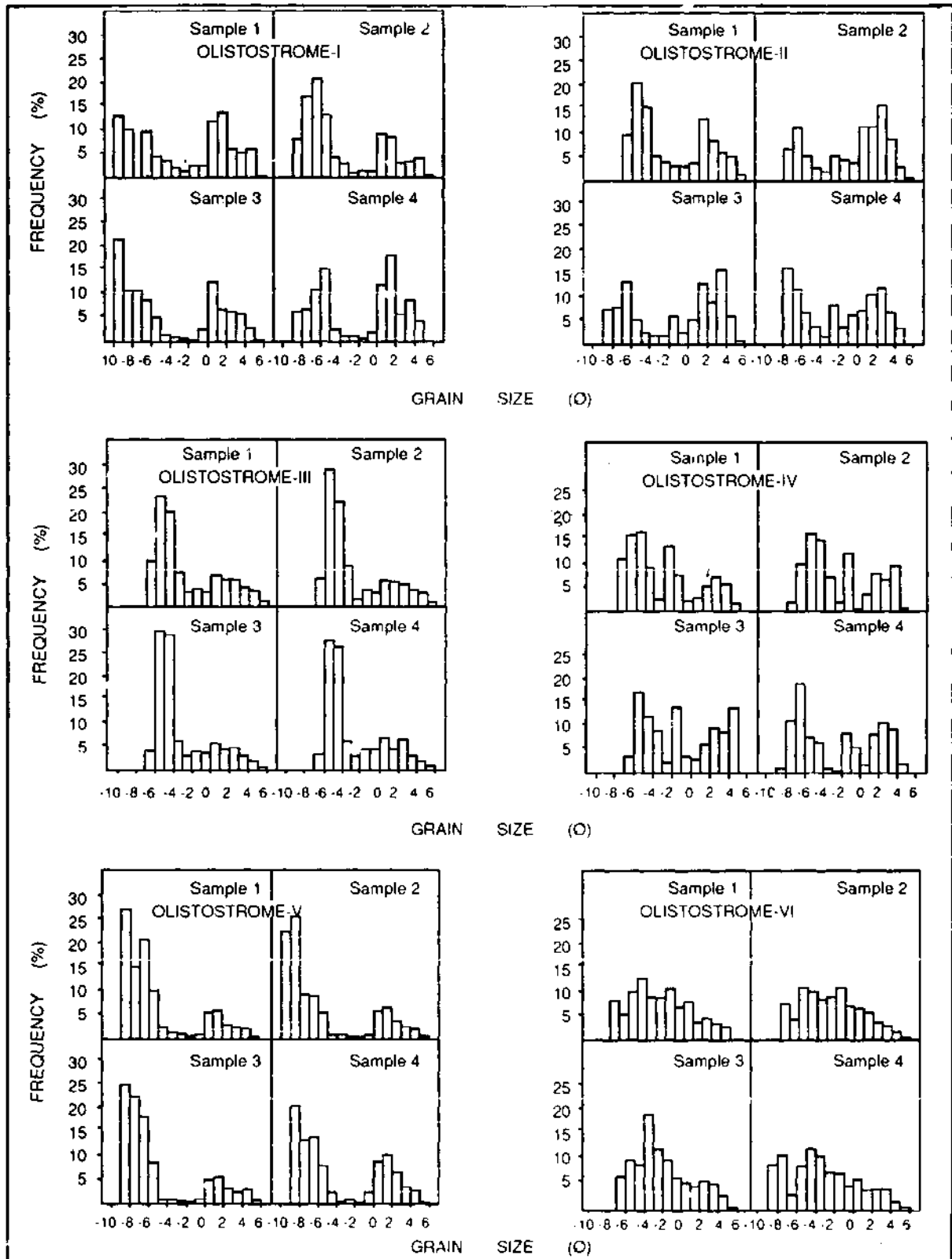


Fig. 4- Grain size distribution histograms of olistostromes (Four samples from each olistostrome unit).

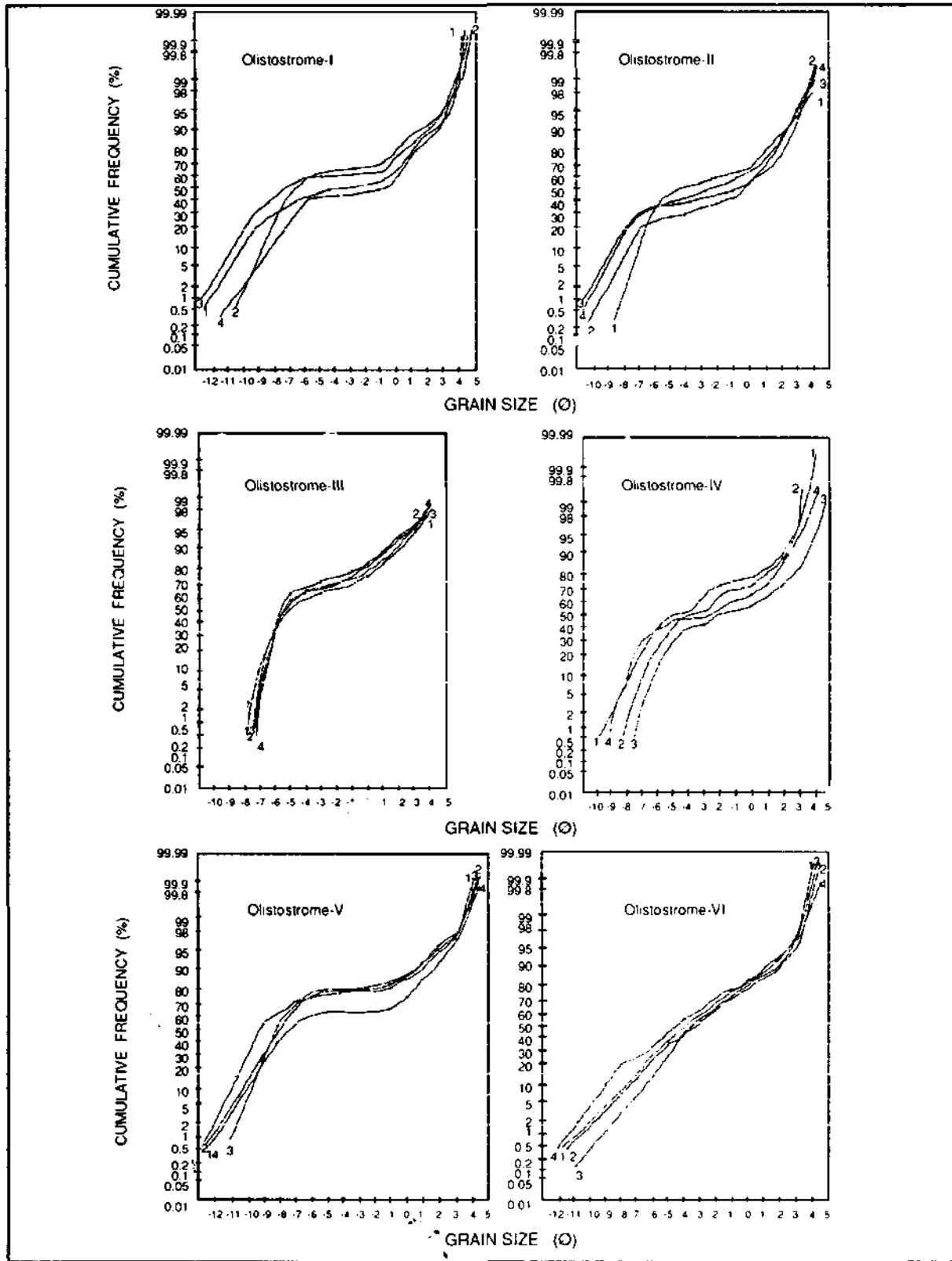


Fig. 5- Cumulative curves of olistostromes (Combined results of grain size analysis by photograph-gind method and sieve method). Four samples per olistostrome.

Table 2- Results of grain size distribution percentiles.

P E R C E N T I L E S								
<i>Olistostrome No.</i>	<i>O1</i>	<i>O5</i>	<i>O16</i>	<i>O25</i>	<i>O50</i>	<i>O75</i>	<i>O84</i>	<i>O95</i>
	-12.20	-10.95	-9.75	-8.80	-4.00	0.45	1.20	3.35
	-12.40	-9.60	-8.35	-8.00	6.80	0.55	0.25	2.65
	-12.85	-11.50	-10.40	-10.00	-7.40	-0.30	0.95	2.80
	-10.90	-9.20	-7.80	-7.15	-1.00	0.95	1.70	3.20
II	-8.15	-7.30	-6.70	-6.30	-4.20	0.50	1.35	3.00
	-9.60	-8.10	-7.15	-5.50	-0.35	1.30	1.90	2.80
	-10.75	-9.30	-8.10	7.30	1.00	1.65	2.25	3.00
	-10.20	-9.20	-8.10	7.20	2.90	0.90	1.60	2.90
III	-7.65	-7.30	-6.70	6.25	5.10	0.20	1.20	3.20
	-7.30	-7.00	6.60	6.35	5.40	0.70	0.80	2.90
	-7.25	-7.00	-6.30	6.10	-5.60	2.20	0.25	2.60
	-7.20	-6.95	6.20	6.00	5.40	1.05	0.50	2.80
IV	-8.00	-8.40	7.60	7.10	5.35	1.60	0.95	2.55
	-8.20	7.50	6.70	6.20	4.30	0.10	1.30	2.70
	-7.45	6.80	6.00	5.45	2.40	1.95	2.90	3.85
	9.20	8.60	8.00	7.50	3.00	0.90	1.70	2.95
V	-12.15	-10.90	9.40	9.05	7.70	4.95	-0.20	2.20
	-12.40	-11.50	10.20	10.00	9.00	6.00	0.15	2.30
	-11.00	-10.20	9.20	8.95	7.90	4.00	0.10	2.15
	-11.80	-10.70	9.20	8.70	7.90	0.25	1.00	2.80
VI	-10.90	8.40	6.80	6.00	3.70	1.20	0.20	2.60
	10.50	-8.30	6.60	5.90	3.20	0.60	1.00	2.80
	9.20	7.20	5.70	5.00	3.55	0.95	0.70	2.90
	-11.20	9.40	8.35	6.90	4.40	1.70	0.30	2.55

Table 3- Grain size distribution parameters (in ϕ units).

<i>Olistostrome no</i>	<i>First Percentile (c)</i>	<i>Median (m)</i>	<i>Mean Size (Mz)</i>	<i>Sorting (σ_s)</i>	<i>Skewness (SK₁)</i>	<i>Kurtosis (KG)</i>
I	-12 20	4 00	4 18	4 83	0 008	0 611
	-12 40	6 80	4 97	3 95	0 507	0 652
	-12 85	7 40	5 62	4 89	0 509	0 573
	-10 90	1 00	2 37	4 24	0 375	0 622
II	-3 15	4 20	3 18	3 57	0 395	0 597
	-9 60	0 35	1 87	3 91	0 462	0 656
	10 75	1 00	2 28	4 45	0 361	0 563
	10 30	2 90	3 13	4 26	0 057	0 612
III	-7 65	5 10	3 50	3 57	0 587	0 711
	-7 30	5 40	3 73	3 35	0 676	0 682
	-7 25	5 60	3 88	3 09	0 747	1 009
	7 20	5 40	3 70	3 15	0 722	0 807
IV	8 80	5 35	4 00	3 80	0 458	0 816
	8 20	4 30	3 23	3 55	0 386	0 664
	7 45	2 40	1 83	3 84	0 183	0 590
	-9 20	3 00	3 10	4 18	0 000	0 564
V	-12 15	7 70	5 77	4 12	0 640	1 200
	-12 40	9 00	6 42	4 46	0 774	1 301
	-11 00	7 90	5 73	4 03	0 723	0 960
	11 80	7 00	5 07	4 40	0 589	0 592
VI	10 90	3 70	3 43	3 42	0 130	0 939
	-10 50	3 20	2 93	3 58	0 094	0 858
	9 20	3 55	2 81	3 13	0 303	1 022
	-11 20	4 40	4 15	3 97	0 125	0 942

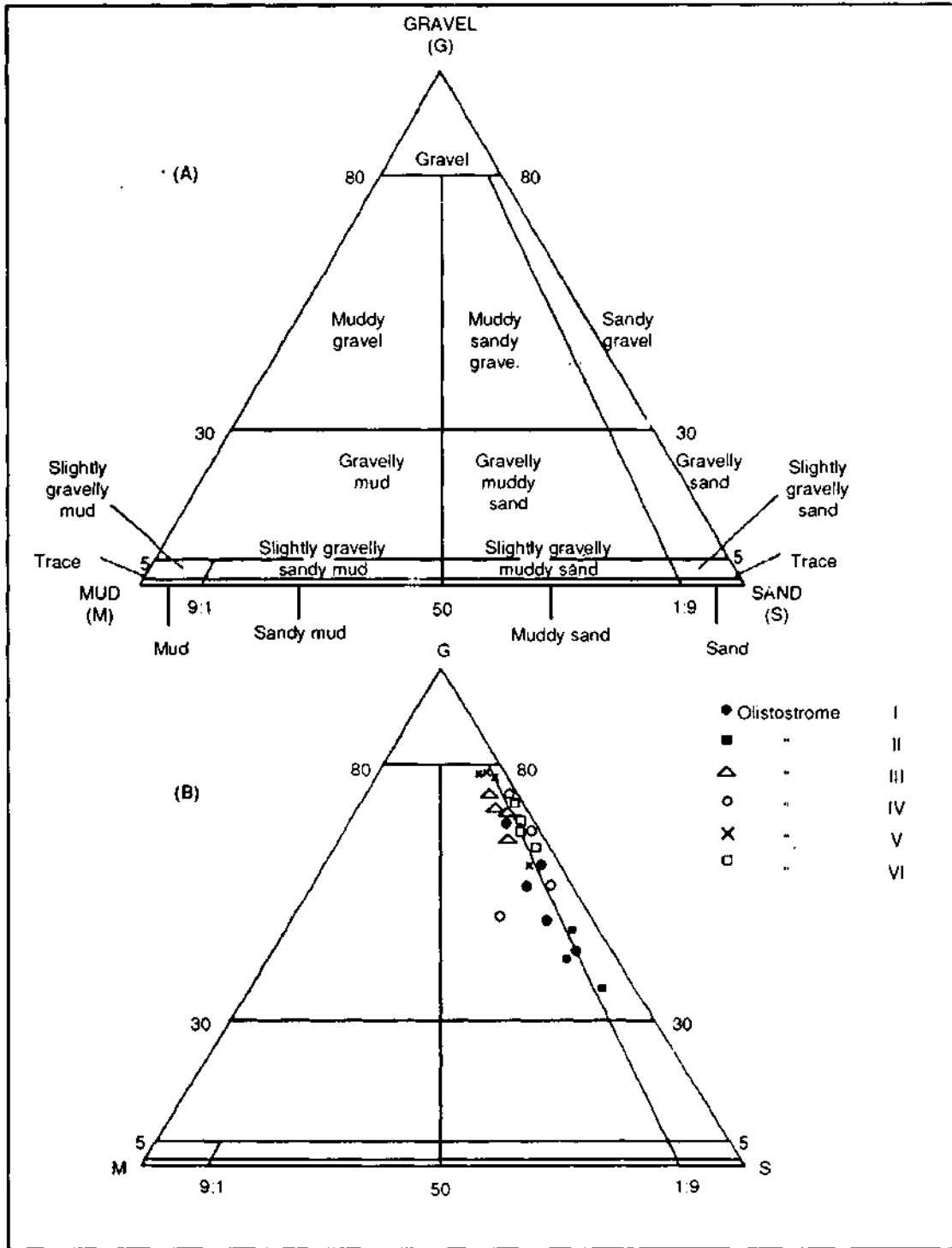


Fig. 6- A. Ternary classification of grain sizes in clastic rocks (Folk, 1954); 1. Gravel, 2. Muddy gravel, 3. Muddy sandy gravel, 4. Sandy gravel, 5. Gravelly mud, 6. Gravelly muddy sand, 7. Gravelly sand, 8. Slightly gravelly sand, 9. Slightly gravelly sandy mud, 10. Slightly gravelly muddy sand, 11. Slightly gravelly sand, 12. Mud, 13. Sandy mud, 14. Muddy sand, 15. Sand.
 B. Distribution of sediment types in six olistostromes.

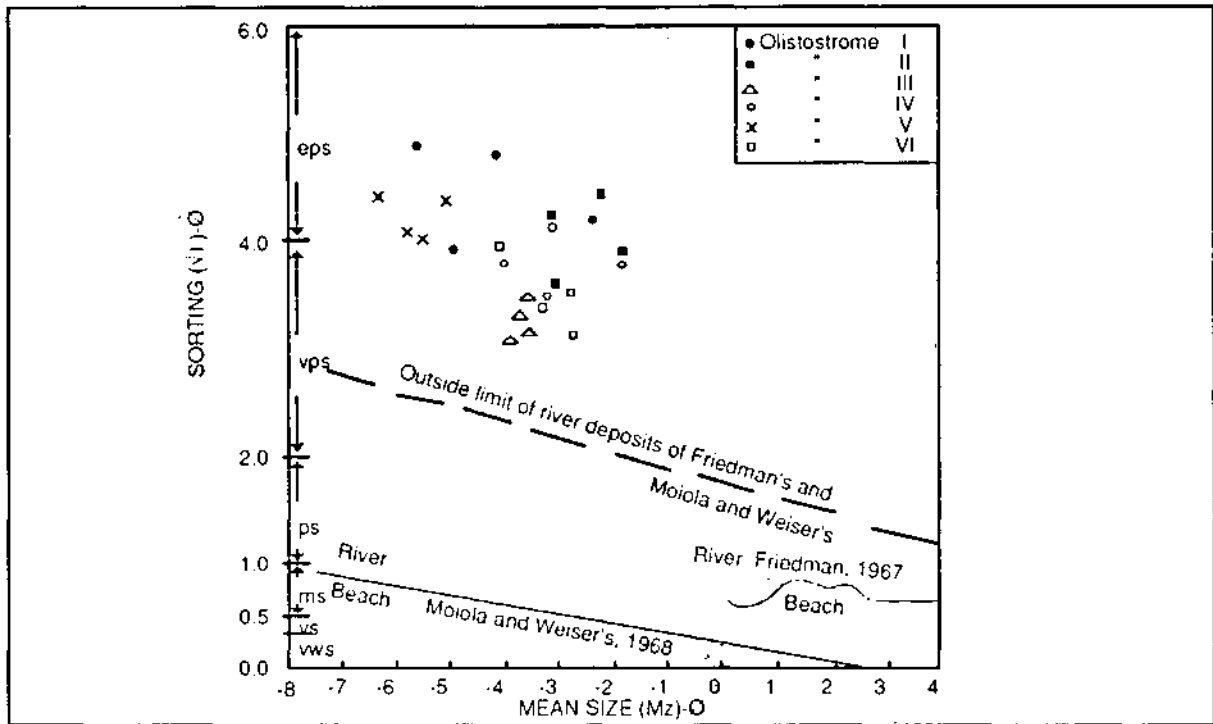


Fig. 7- Scatter diagram of Mean size (Mz)-Sorting (G₁), (vws: very well sorted, ws: well sorted, ms: moderately sorted, ps: poorly sorted, vps: very poorly sorted, eps: extremely poorly sorted).

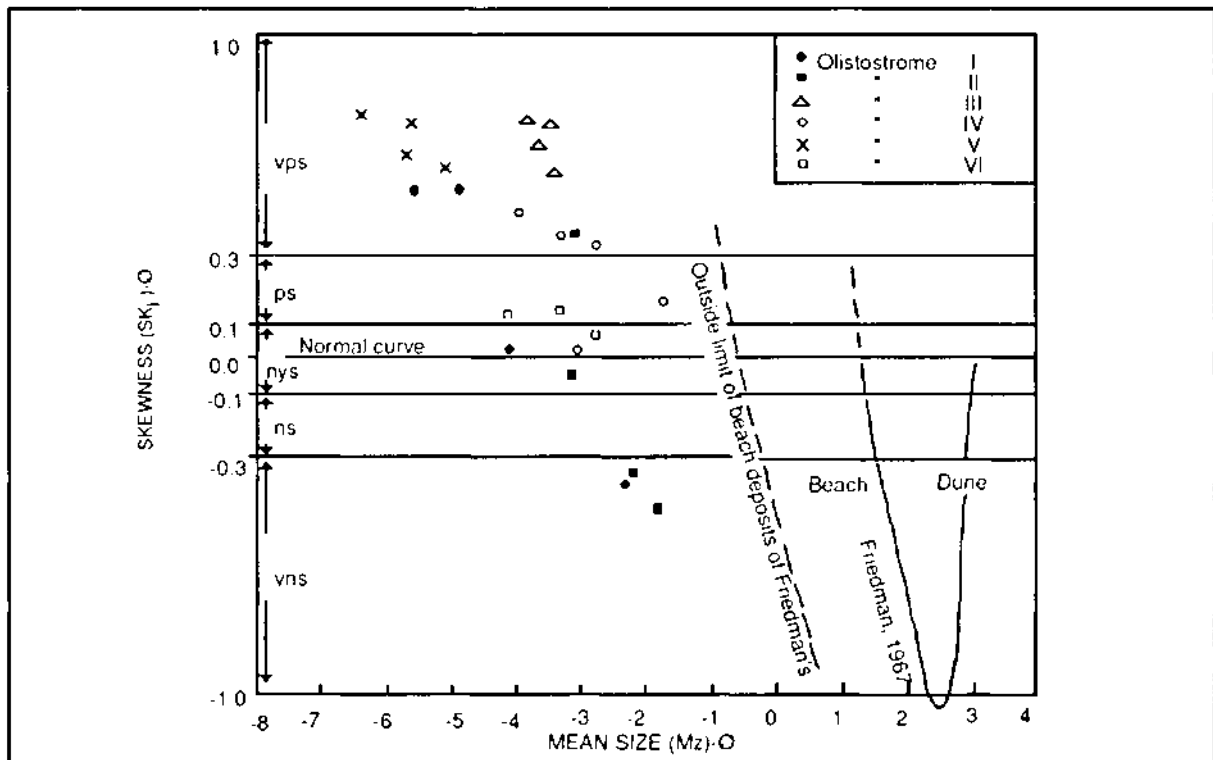


Fig. 8- Scatter diagram of Mean size (Mz)-Skewness (SK₁), (scs: strongly coarse skewed, cs: coarse skewed, ns: near symmetrical, fs: fine skewed, sts: strongly fine skewed).

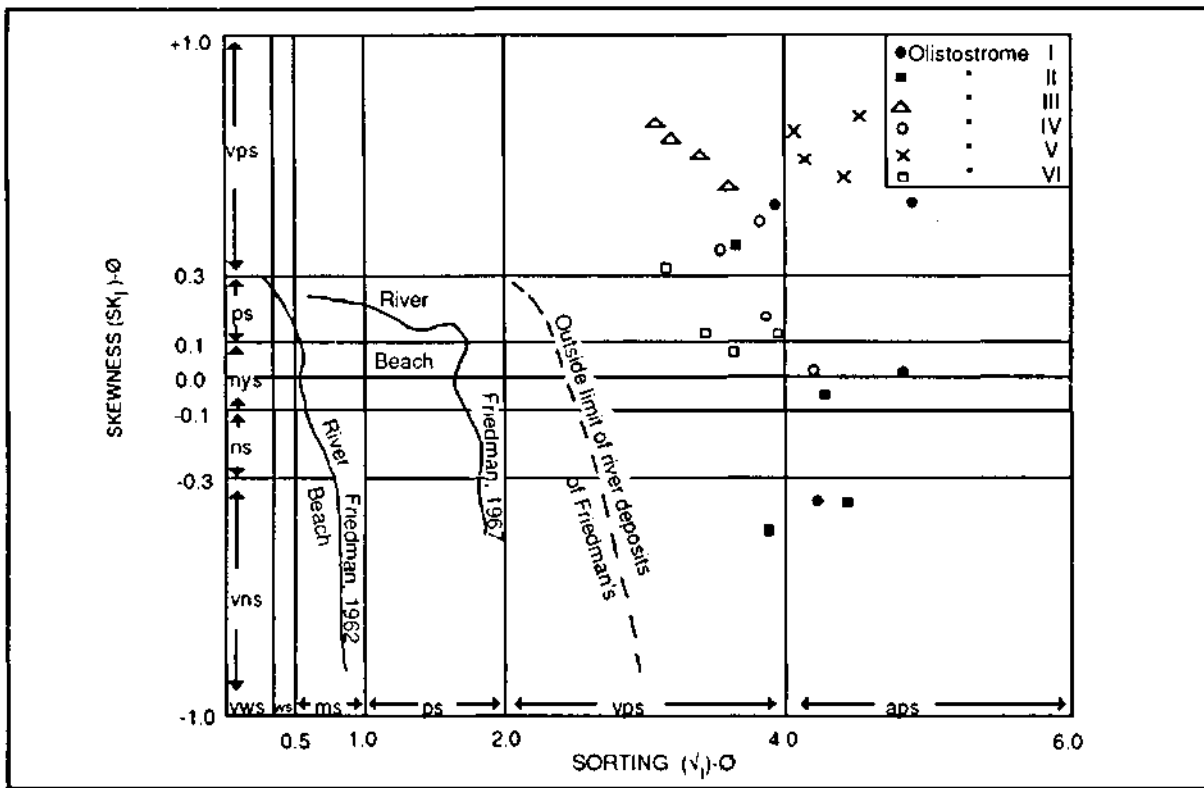


Fig. 9- Scatter diagram of Sorting (G)-Skewness (SK) (vws: very well sorted, ws: well sorted, ms: moderately sorted, ps: poorly sorted, vps: very poorly sorted, eps: extremely poorly sorted and scs: strongly coarse skewed, cs: coarse skewed, ns: near symmetrical, fs: fine skewed, sfs: strongly fine skewed).

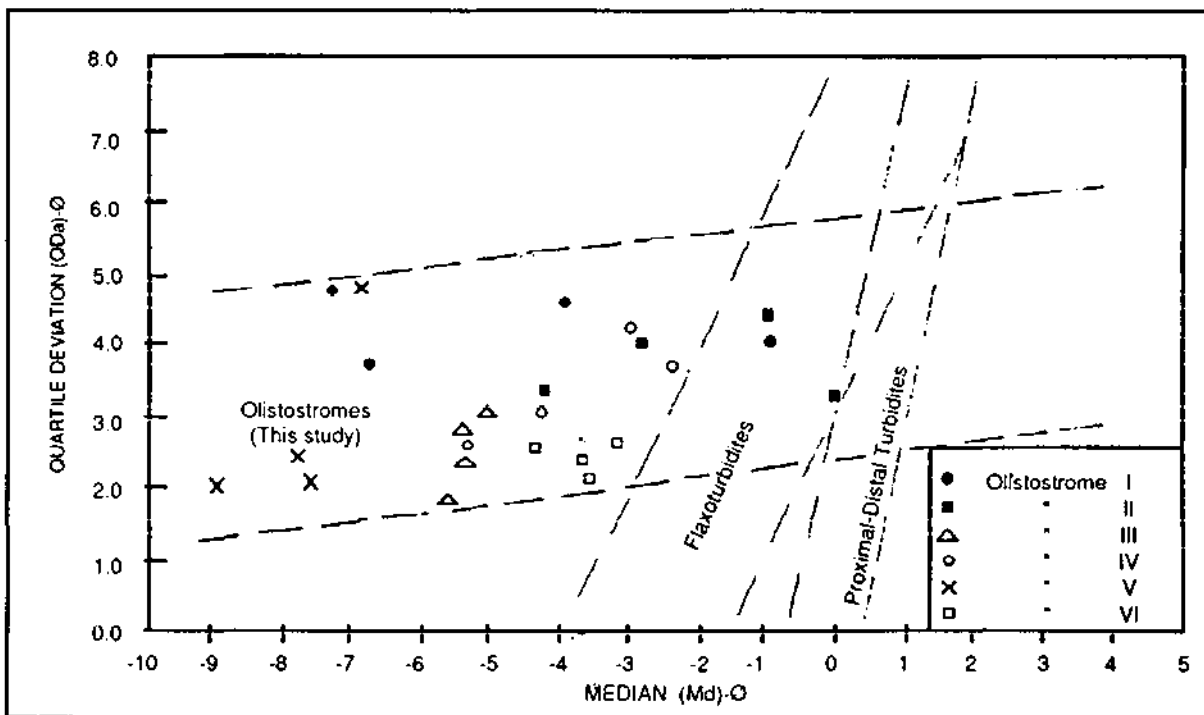


Fig. 10- Scatter diagram of Median (M)-Quartile deviation (QDa) (Based on Buller and Mc Manus, 1972).

REFERENCES

- Bayraktutan. M.S., 1982, Narman (Erzurum) havzasının Miyosen'deki sedimentolojik evrimi: Atatürk Üniv. doktora tezi, 283 (unpublished).
- Buller, AT. and McManus, I., 1972, Simple metric sedimentary statistics used to recognize different environments: *Sedimentology*, 18, 1-21.
- Chayes, F., 1956, *Petrografik Modal Analysis, An Elementary Statistical Appraisal*: John Wiley and Sons Inc., 356, Newyork.
- Flores, G., 1955, Discussion in Beneo, E., -les Resultats des etudes pour la recherche petrolifere en Scile (Italie): *Proc. 4th World Petrol. Congr. Rome*, sect. 1, 259-275.
- Folk, R.L., 1954, The distinction between grain size and mineral composition in sedimentary nomenclature: *Jour. Geol.*, 62, 344-359.
- , 1964, A review of grain size parameters: *Sedimentology*, 6, 73-93.
- , 1980, *Petrology of sedimentary rocks*: Hemphill Pub. Co., Austin, 182, Texas.
- and Ward, W.L., 1957, Brazos river bar; A study in the significance of grain size parameters: *Jour. Sed. Petr.*, 27, 3-26.
- and Mason, C.C., 1958, Differentiation of beach, dune and aeolian ftot environments by size analysis: *Jour. Sed. Petr.*, 28, 211 -226.
- Friedman, G.M., 1961, Distinction between dune, beach and river sands from their textural characteristics: *Jour. Sed. Petr.*, 31, 514-529.
- , 1962, On sorting, sorting coefficient and the log-normality of the grain size distribution of sandstones: *Jour. Geol.*, 70, 734-753.
- , 1967, Dynamic processes and statistical parameters compared for size frequency distribution of beach and river sands: *Jour. Sed. Petr.*, 37, 327-354.
- Gansser, A., 1959, Ausseralpine ophiolith problem: *Eclogae Geol. Helv.*, 52, 2, 327-354.
- Gökçen, S.L. and Şenalp, M., 1975, Kayma oluşukları, olistostromlar ve turbidit fasiyelerinin ayırıcı ana jeolojik, sedimantolojik ölçütleri: TÜBİTAK, V. Bilim Kongr. Tebliğ. 56-59.
- , and Özkaya, I., 1981, Olistostrom ve turbidit fasiyelerinin diskriminant analizi ve ayırımı: *Yerbilimler*, 8, 1-26.
- Hoedemaeker, P.J., 1973, Olistostromes and delapsional deposits and their occurrences in the region of Moratall (Prov. of Muncia, Spain): *Scripta Geol.*, 19, 1-207.
- Hsu, K.J., 1974, Melanges and their distinction from olistostromes: modern and ancient geosynclinal cementation: *Spec. Publ. Soc. econ Paleont. Miner.*, 19, 321-333.
- Jackson, J.A., and Bates, R.L., 1980, *Glossary of Geology*: American Geological Institute Falls Church, 751, Virginia.
- Koçyiğit, A., 1979, Çördük olistostromlari: *Türkiye Jeol. Kur. Bült.*, 22, 1, 59-68.
- and Lünel, AT., 1987, Geology and tectonic setting of Alcı region: *Ankara, M.E.T.U. Jour. Pure. Appl. Sci.*, 20, 35-59.
- Lünel, AT., 1987, Petrology of Balkuyumcu volcanic complex-Ankara, M.E.T.U. *Jour. Pure. Appl. Sci.*, 20, 67-136.
- Marchetti, M.P., 1957, The occurrence of slide and flow-age materials (olistostromes) in the Tertiary series of Italy", 20th Int. Geol. Congr. Mexico City, 1956, Sec. 5, 1, 209-225.
- Moiola, K.J., and Weiser, D., 1968, Textural parameters-an evaluation: *Jour. Sed. Petr.*, 38, 45-53.
- Norman, T., 1975, Flow features of Ankara melange: 9th Int. Congr. on sedimentology, Nice (France), 4, 261-269.
- , 1979, On the defination of melange formation: *Geocoome-I*, 581-593.
- Olgun, E., 1988, Sedimentary features of some Jurassic-Cretaceous olistostromes between Alcı and Balkuyumcu, SW of Ankara: A Master's Thesis in Geol. Eng. M.E.T.U. 103,(unpublished).
- Passega, R., 1957, Texture as characteristic of clastic deposition: *Bull. Am. Assoc. Petrol. Geol.*, 69, 1952-1984.
- , 1977, Significance of CM diagrams of sediment deposited by suspension, *Sedimentology*, 24, 723-733.
- Powers, M.C., 1953, A new roundness scale for sedimentary particles: *Jour. Sed. Petr.*, 23, 117-119.
- Sahu, B.K., 1964, Depositional mechanisms from the size analysis of clastic sediments: *Jour. Sed. Petr.*, 34, 73-83.
- Visher, G.S., 1969, Grain size distribution and depositional processes: *Jour. Sed. Petr.*, 39, 1074-1106.

ÇAN (ÇANAĞKALE), ORHANELİ VE KELES (BURSA) LİNYİT AÇIK OCAK İŞLETMELERİNDEKİ SEDİMANTER İSTİFİN KİL SEDİMANOLOJİSİ

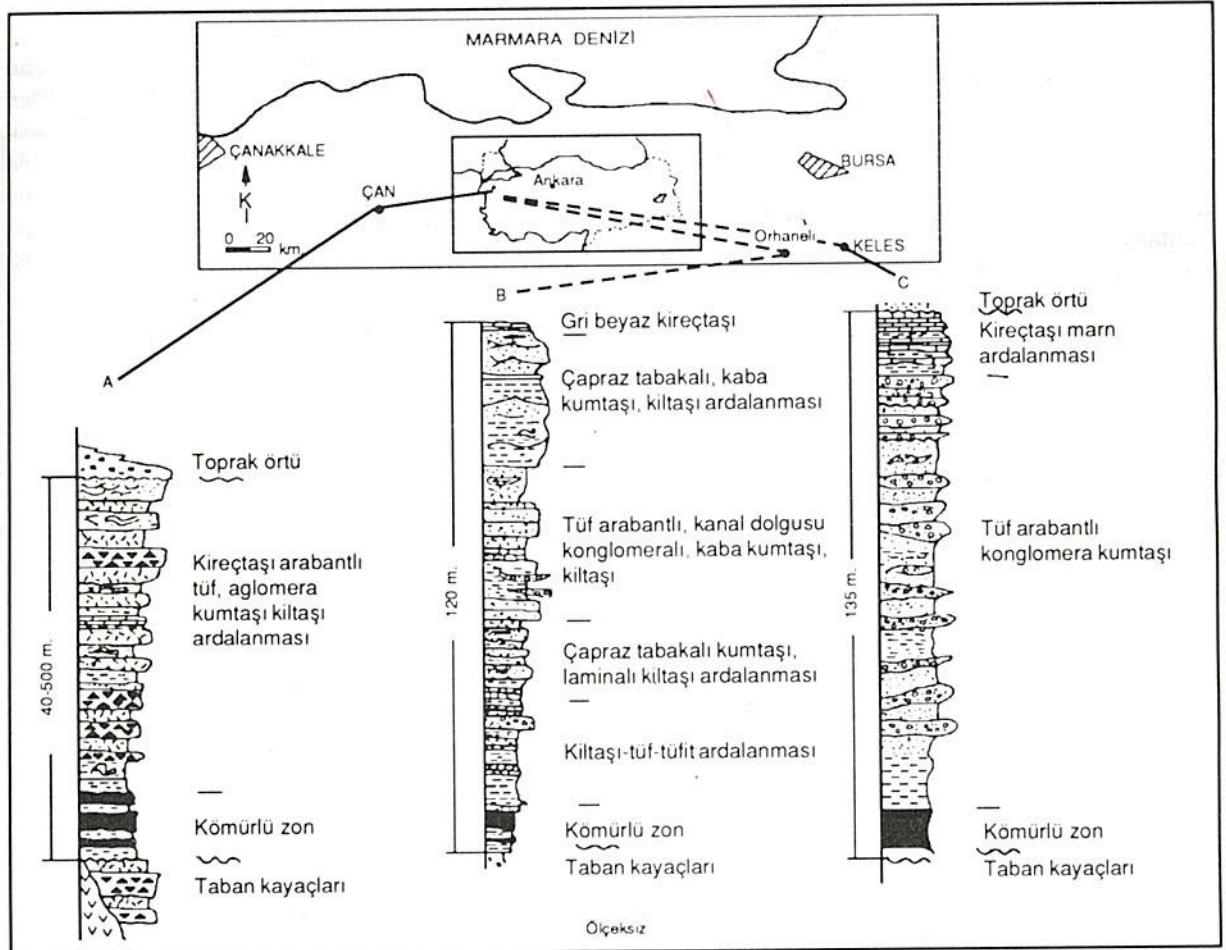
Emel BAYHAN*, Abdurrahim ŞAHBAZ* ve Sezai GÖRMÜŞ*

ÖZ_ Çan, Orhaneli ve Keles yörelerindeki Miyosen yaşlı kömürlü sedimanter istifin kil fraksiyonu ayrılarak simektit, illit, kaolinit ve klorit parajenezi saptanmıştır. Monomineralik simektitlerde ana element çözümlenmeleri yapılarak bunların dioktaedrik (baydelit), trioktaedrik (saponit) karakterinde olduğu belirlenmiş ve oluşumları irdelenmiştir. Tüflü serilere bağlı simektitler volkanik malzemenin bozunması sonucu; killi-karbonatlı serilere bağlı simektitler ise ya kırıntılı yerinde neoformasyonu ya da kırıntılı simektitlerin transformasyonu ile oluşurken, illit ve klorit ise metamorfik kayalardan türemişlerdir.

GİRİŞ

Çan (Çanağkale), Orhaneli ve Keles (Bursa) çevresindeki (Şek. 1) Miyosen yaşlı sedimanter istifte stratigrafik kesitler ölçülmüş ve örnek alınarak mikromineralojik analizler yapılmıştır. Bu çalışmada,

bölgede detaylı çalışmalar yapan Kulaksız ve diğerlerinin (1991) tanımladığı çökel istifi kullanılmıştır (Şek. 1). Keles bölgesinde Yiğitel ve diğerleri (1989) tarafından çökel istifin yaşı Miyosen, Orhaneli bölgesinde ise benzer istif Orta-Üst Miyosen, Çetin (1985) olarak belirlenmiştir.



Şek. 1- Çalışma alanlarının genelleştirilmiş çökel istifi ve lokasyonları. A: Çan; B: Orhaneli; C: Keles.

Çalışmanın amacı, inceleme alanı içindeki kırıntılı istifin kil mineral parajenezini ve bunların kimyasal özelliklerini saptayarak, istifin paleoklimatolojik, paleotopografik koşullarını açıklamaya çalışmaktır.

STRATİGRAFİ

Çan bölgesi: Bu bölgede kömürlü zonu da içine alan Neojen yaşlı istifin altında andezit, kaolinleşmiş tuf ve aglomeralardan oluşan taban kayaları yer almaktadır (Şek. 1a). Çalışma alanı içinde bazı lokalitelerde taban kayaları içinde metamorfikler ve spilitler de gözlenmiştir. Bu taban üzerine açılmal uyumsuzlukla gri, kahve, kırmızı renkli laminalı kil taşlarının arabant halinde gözlemlendiği, kalınlığı 35 metreye kadar ulaşan kömürlü zon yer almaktadır.

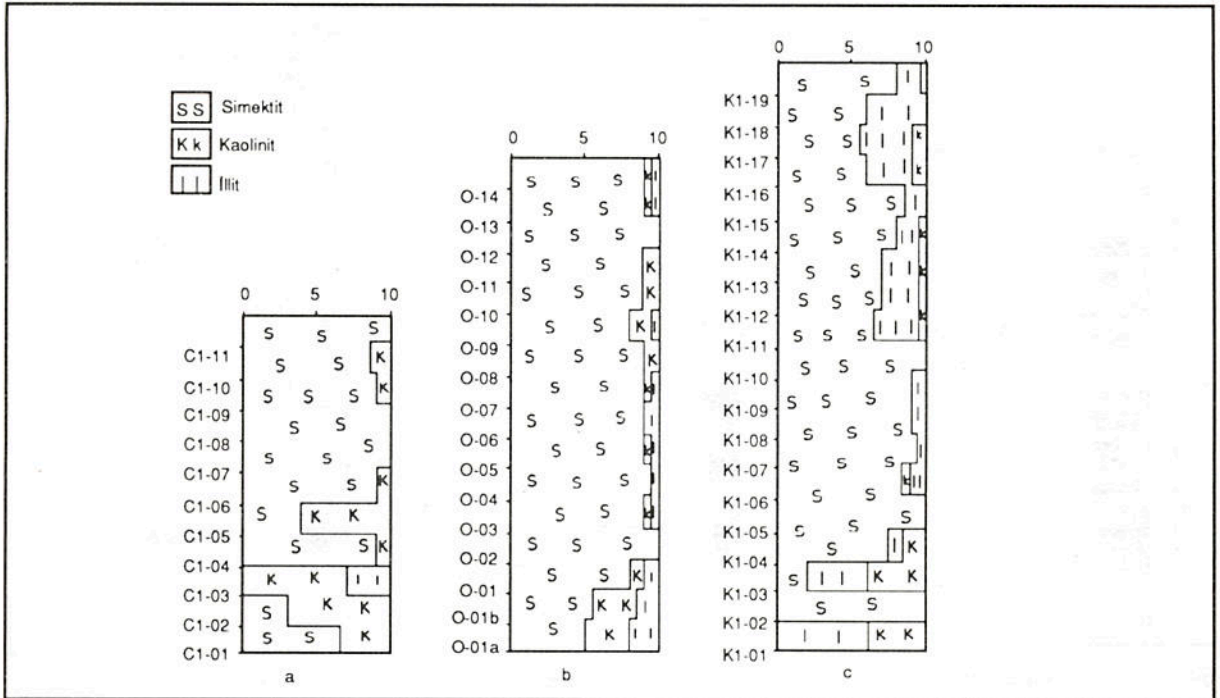
Orhaneli bölgesi: Bölgenin çökel istifi Şekil 1b de görülmekte olup, Neojen yaşlı istifin altında kristalize kireçtaşı ve serpantinlerden oluşan taban kayaları bulunmaktadır. Taban kayaların üzerinde kiltası, tuf, tufit ardalımalı bir seviye bulunmakta ve bu seviyenin içinde iki ayrı zon halinde kömür yer almaktadır. İstif üste doğru kanal dolgusu konglomeralar, tuf arabantlı kiltaları ve kaba taneli kumtaşları ile devam etmektedir. Çapraz tabakalı çakıllı kumtaşı ve kiltası ardalıması bu seviyenin

üstünde yer almakta olup, ince bir kireçtaşı seviyesinden sonra bulunduğu yerlerde alüvyon tüm seviyeleri diskordan olarak örtmektedir.

Keles bölgesi: Çökel istifi Şekil 1c de görülen bu bölgede en altta taban kayaları olarak isimlendirilen Paleozoyik yaşlı metamorfik kayalar ile rekristalize kireçtaşları yer almaktadır. Taban kayalarının üzerine açılı diskordansla Neojen yaşlı kömürlü zon gelmektedir. Kömürlü zonun üstünde genel olarak konglomera, kaba kumtaşı ve silttaşı ardalımasından oluşan bir istif devam etmektedir. Bu istif içinde yer yer anahtar seviye olarak izlenen tuf arabantları mevcuttur. Konglomera, kumtaşı ve silttaşı ardalımasından oluşan bu seviyenin üzerinde ince bir kireçtaşı-marn ardalıması yer almakta olup, istifin en üstünde gözlenebildiği yerlerde toprak örtüsü bulunmaktadır.

MATERYAL VE YÖNTEM

Çalışma alanı içerisinde üç ayrı lokalitede Neojen yaşlı kömürlü zonu da kapsayan tüm istiften ölçülü kesitler boyunca alınan örneklerin kil fraksiyonundan itibaren X-ışınları difraktometresi ile Gündoğdu ve Yılmaz'a (1984) göre kil minerallerinin yarı kantitatif yüzdeleri saptanmıştır. Ayrıca kil fraksiyonu içinde monomineral olarak bulunan simektitlerin kimyasal analizleri yapılarak ana element oksit



Şek. 2- Çan, Orhaneli ve Keles yörelerinde kil minerallerinin dağılımı.

değerleri belirlenmiş ve yapısal formülleri hesaplanmıştır.

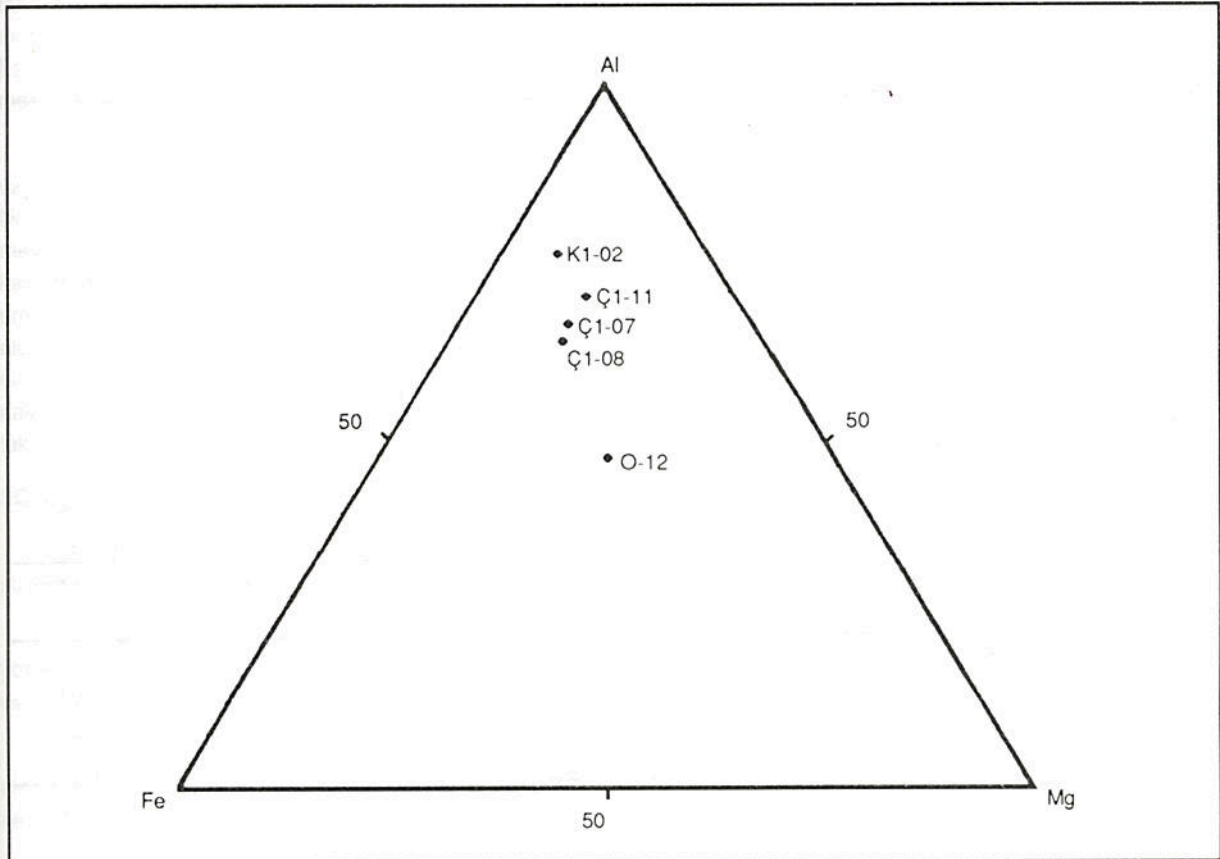
KİL MİNERALLERİ

Çan bölgesi: Bu yörede ölçülü kesit boyunca alınan örneklerin kil fraksiyonunda simektit, kaolinit, illit mevcut olan minerallerdir (Şek. 2a). Bölgede egemen kil minerali olan simektit tüm örneklerde mevcuttur. Simektit örneklerin bir kısmında monomineral olarak diğer bir kısmında da en az 3 bolluğunda bulunmaktadır. Kaolinit kömürlü zonun hemen altındaki örneklerde 3.5 bolluğunda, hemen üstündeki örneklerde ise 7.0 bolluğuna yükselmekte iken daha üst seviyelerdeki örneklerde 1.0-2.0 arasında değişen bolluklarda bulunmaktadır. İstiften alınan bir örnekte saptanan illit 2.0 bolluğunda, klorit ise eser miktarda mevcuttur.

Orhaneli bölgesi: Bu yöredeki örneklerin kil fraksiyonunda simektit egemen olarak bulunmak-

tadır (Şek. 2b). Analizi yapılan tüm örneklerde saptanmış olan simektit 8-10 arasında değişen bolluklarda mevcuttur. Bu bölgedeki kayaç örneklerinde bulunan diğer kil mineralleri ise kaolinit ve illittir. Kaolinit örneklerde 1.0-3.5, illit 1.0-2.0 arasında değişen bollukta ve klorit ise eser miktarda bulunmaktadır.

Keles bölgesi: Diğer bölgelerde olduğu gibi Keles bölgesinde de egemen kil minerali simektittir. Simektit tüm örneklerde 2-10 arasında değişen bolluklarda bulunmaktadır. 1-6 arasında değişen bollukta illit, örneklerde saptanan ikinci önemli mineraldir. Simektitin monomineral olarak bulunduğu örneklerin dışındaki diğer incelenen örneklerde bulunan illitin bolluğunda Çan ve Orhaneli bölgelerine göre bu yöredeki örneklerde artış gözlenmiştir. Kaolinit ise 0.5-3 bolluğunda mevcut olup, klorit, Çan ve Orhaneli bölgelerinde olduğu gibi eser oranda bulunmaktadır.



Şek. 3- Simektitlerin Al-Fe-Mg üçgenindeki konumları.

SİMEKTİTİN JEOKİMYASI ile DİĞER KİL MİNERALLERİNİN OLUŞUMU

Çan, Orhaneli ve Keles bölgelerinden alınan örneklerin mikromineralojik incelenmesi sonucunda, monomineral olarak simektitin bulunduğu beş örneğin (Ç-7, Ç-8, Ç-11, K-2, O-12) ana element çözümlenmeleri yapılmıştır. Bu örneklerin $d_{(060)}$ parametreleri toz örnekten itibaren X-ışınları difraktometresi ile ölçülmüş, analiz sonuçları Calilere ve Henin'e (1963) göre değerlendirilerek, bunların dioktaedrik ve trioktaedrik olarak belirlenen simektitlere uygunluk gösterdikleri saptanmıştır. Bu simektitlerin ana element analiz sonuçları Çizelge 1 de, Al-Fe-Mg diyagramındaki dağılımları ise Şekil 3 te verilmiştir. Dioktaedrik karakterdeki örnekler baydelit bileşiminde olup, miktarı 1.33-1.55 arasında değişen Al, oktaedrlerin ana katyonudur. Oktaedrlerde bulunan diğer katyonlar ise Mg, Fe ve Ti'dir.

Baydelitlerde oktaedrik katyon toplamı 2.00-2.07 arasında değişmektedir. Diğer taraftan bir örnek ise (O-12) ise trioktaedrik simektit olup, saponitik karakterdeki bu örneğin Al-Fe saponit olduğu belirlenmiştir. Benzer Al-Fe saponitler Bigadiç, (Gündoğdu, 1985), Emet (Yalçın ve Gündoğdu, 1985) ve Burdur (Bayhan, 1992) yörelerinde de bulunmuştur. Bu tip saponitik simektitin oktaedrik katyon toplamı 2.28'dir. Bu durum oktaedrlere önemli miktarda Al ve Fe girmesi ile açıklanabilmektedir.

Millot (1964), Grim (1968) ve Gündoğdu'nun (1982) belirttiği gibi tüflere bağlı bulunan dioktaedrik simektitlerin, volkanik malzemenin bozunması sonucunda oluştuğu düşüncesi göz önüne alınarak Çan bölgesindeki dioktaedrik simektitlerin de benzer bir mekanizmanın ürünü olabileceği düşünülmektedir.

Çizelge 1- Simektitlerin kimyasal analiz sonuçları ve yapısal formülleri

	Yöre Örnek No	Çan Ç1-7	Çan Ç1-8	Çan Ç1-11	Keles K1-2	Orhaneli O-12
%	SiO	62.6	59.45	62.59	61.88	51.86
O	Al ₂ O ₃	18.67	19.63	20.11	21.06	16.9
K	TiO ₂	0.8	0.59	0.7	0.55	0.59
S	Fe ₂ O ₃	5.99	7.14	4.88	3.01	9.2
I	MnO	0.04	0.08	0.03	0.01	0.11
T	MgO	3.41	3.56	3.31	3.64	9.12
L	CaO	1.43	1.55	1.1	1.15	2.37
E	K ₂ O	1.17	1.33	1.13	0.07	1.2
N	Na ₂ O	0.23	0.23	0.31	0.06	0.47
M	P ₂ O ₅	0.04	0.04	0.02	0.03	0.06
E	H ₂ O	9.04	8.06	8.87	8.94	10.5
	Top.	103.42	101.66	103.05	100.4	102.38
Tetraedral	Si	3.96	3.84	3.95	3.96	3.51
	Al	0.04	0.16	0.05	0.04	0.49
Oktaedral	Al	1.35	1.33	1.44	1.55	0.86
	Ti	0.04	0.03	0.03	0.03	0.03
	Fe	0.29	0.35	0.24	0.14	0.47
	Mg	0.32	0.34	0.31	0.35	0.92
Yapraklar Arası	Ca	0.1	0.11	0.07	0.08	0.17
	Na	0.03	0.03	0.04	0.06	0.06
	K	0.1	0.11	0.09	0.07	0.1

Tüflü birimlere bağlı olan simektitlerin dışında killi-karbonatlı birimlere bağlı olan simektitlerin ise epijenetik olarak oluşabilecekleri Singer (1984) tarafından belirtilmektedir. Orhaneli ve Keles yöresinde de killi-karbonatlı birimlere bağlı olan simektitler de epijenetik olup kırıntılı malzemenin itibaren oluşmuş olmalıdır.

Orhaneli yöresinde bir örnekteki (O-12) simektitin saponit karakterinde olduğu saptanmıştır. Killi-karbonatlı birimlere bağlı olarak bulunan saponitler ya kırıntılı malzemenin yerinde neoformasyonu ile ya da kırıntılı simektitlerin transformasyonu ile oluşmaktadır. Orhaneli yöresindeki simektitin Al-Fe-Ti gibi çözünlürlüğü düşük olan elementlerce zengin olması, Ataman (1966) ve Trauth (1977) tarafından da belirtildiği gibi, kırıntılı malzemenin transformasyonu ile saponitin oluştuğunu düşündürmektedir.

Simektitin dışında her üç yörede de belirlenen kil minerallerinden kaolinit feldispatlı kayaçların düşük pH'lı ortamda alterasyonu ile oluşmuştur. Illit, tabandaki metamorfik kayaçlardan türemekte ve muskovitlerin kil boyu bileşenini teşkil etmektedir. Eser miktardaki klorit ise taban kayaçları olan metamorfik kayaçlar ile ofiyolitlerden türemişlerdir.

İncelenen yörelerde kömür oluşumunun varlığı, kil minerallerinden kaolinitin mevcut olması, Neojen devresinde kuzey-kuzeybatı Anadolu'daki mevcut göl ortamlarında çökelen kırıntılı kayaçların kaynak bölgesinin sıcak ve yağışlı bir iklim ile iyi drenajlı, penneplen topografyaya sahip bir bölge olduğunu düşündürmektedir. Bu yorum Şahbaz ve Görmüş'ün (1992) Keles yöresindeki yaptıkları kaynak bölge ve çökeltme ortamı çalışmalarını da desteklemektedir.

SONUÇ

Bu çalışma sonucunda elde edilen bulguları şu şekilde belirtebiliriz:

1. Simektit hâkim kil minerali olarak üç yörede de tespit edilmiş ve az olarak illit, kaolinit ve eser halde klorit bulunmuştur.
2. Çalışma alanı içindeki simektitlerde ana element çözümlenmeleri yapılarak bunların baydelit ve saponit karakterinde olduğu saptanmıştır.
3. Tüflere bağımlı simektitlerin volkanik malzemenin bozunması sonucu, killi karbonatlı birimle-

re bağlı simektitlerin epijenetik ve kırıntılı simektitlerin transformasyonu sonucu oluştuğu düşünülmektedir.

4. Kil parajenezinde mevcut olan illit ve kloritler taban kayaçlardan türemiştir.

5. Simektit ve illitlere eşlik eden kaolinitler feldispatça zengin kayaçların düşük pH, sıcak iklim ve iyi drenajlı ortamda alternasyonu ile oluşmuştur.

KATKI BELİRTME

Yazarlar TKİ-MLİ Çan, Keles, Orhaneli Müessese Müdürlüğü ile Jeoloji Mühendisi Melih Özdoğan'a teşekkür ederler.

Yayına verildiği tarih, 23 Kasım 1992

DEĞİNİLEN BELGELER

- Ataman, G., 1966 Geochimie des mineraux argileux dans les Bassins sedimentaires marins. Etudes sur le bassin Triassique du Jura: Mem. Serv. Carte Geol. Alsace Lorrain, 25, 237 s.
- Bayhan, E., 1992, Burdur civarı Üst Kretase-Tersiyer yaşlı simektitlerin dağılımı ve özellikleri: MTA Derg. 114, 111-118.
- Calillere, S. ve Henin, S., 1963, Mineralogie des argiles. Masson, Paris, 355 s.
- Çetin, A., 1985, Harmancık-Kozluca (Bursa-Orhaneli) dolayının jeolojisi ve linyit olanakları: MTA, Rap. 7660, (yayımlanmamış), Ankara.
- Grim, R.E., 1968, Clay mineralogy: Mc. Graw Hill, New York. 569 s.
- Gündoğdu, M.N., 1982, Neojen yaşlı Bigadiç sedimanter baseninin jeolojik, mineralojik ve jeokimyasal incelenmesi: H.Ü. Doktora tezi, 386 s. Ankara.
- , 1985, Bigadiç gölsel baseninde karbonat mineraleri ile simektitlerin dağılımı: II. Ulusal Kil Sempozyumu Bildirileri, H.Ü. 123-140.
- ve Yılmaz, O., 1984, Kil mineralojisi yöntemleri: I. Ulusal Kil Sempozyumu Bildirileri. C.Ü. 319-330.
- Kulaksız, S.; Görmüş, S.; Şahbaz, A.; Aksoy, H.; Şentürk, A. ve Güner, I., 1991, TKİ, ÇLL., Çan Bölgesi Açık Ocak İşletmesi yapısal jeoloji, hidrojeoloji ve zemin etüdüleri nihai raporu: HÜTE Rap. 67 s.

- Kulaksız, S.; Görmüş, S.; Şahbaz, A.; Aksoy, H.; Şentürk, A. ve Gürer. İ., 1991, TKI, MLI Keles Bölgesi Açık Ocak İşletmesi yapısal jeoloji, hidrojeoloji ve zemin etüdüleri nihai raporu: HÜTE Rap. 53 s.
- _____; _____; _____; _____; _____ ve _____, 1991, TKI, MLI Orhaneli Bölgesi Açık Ocak İşletmesi yapısal jeoloji, hidrojeoloji ve zemin etüdüleri nihai raporu: HÜTE Rap. 52 s.
- Millot, 1964, Geologies des Argiles: Masson et Cie, 499s, Paris.
- Singer, A., 1984, The paleoclimatic interpretation of clay minerals in sediments: A review: Earth Sci. Rev. 21, 251-293.
- Şahbaz, A. ve Görmüş, S., 1992, Keles (Bursa) Linyit açık ocak işletmelerindeki Miyosen yaşlı istifin stratigrafik, sedimentolojik ve tektonik incelenmesi: C.Ü. Dergisi, Seri A, Yerbilimleri C.Q, S-1, 41-48.
- Trauth, N., 1977, Argiles évaporites dans la sédimentation carbonate continentale et epicontinentale Tertiaire, Bassin de Paris, de Mormogion et de salinelles (France) de Jbel Ghassool (Maroc): Mem. Sci. Geol. 49, 195 s.
- Yalçın, H. ve Gündoğdu, M.N., 1985, Emet gölsel Neojen Baseninin kil mineralojisi: II. Ulusal Kil Sempozyumu Bildirileri, H.Ü., 155-170.
- Yiğitel, İ.; Altınay, A. ve Özcan, K., 1989, Bursa, Keles, Davutlar kömür sahası jeoloji raporu: MTA Rap., 8767, (yayımlanmamış), Ankara.

TEK BORAT PARÇALANMASI YÖNTEMİ KULLANILARAK REFRAKTER SİLİKATLARDA ESAS, YAN VE İZ ELEMENT ANALİZLERİ

Bahattin AYRANCI*

ÖZ_ Oksitleyici olmayan koşullarda, indüksiyon fırını kullanılarak yapılan eritme parçalanması, refrakter bileşenler içeren örneklerin ayrıştırılmasına alternatif bir yöntem olup bu şekilde, demirin oksidasyon biçimlerinin ve diğer esas, yan ve iz elementlerin analizleri tek bir örnek parçalanması ile yapılabilir.

GİRİŞ

Silikatların esas, yan ve iz element analizleri, genel olarak ya borat parçalanması (disintegrasyon) ve presleme ile tableetlenmiş toz örneklerin XRF-tekniki ile analizi, ya da örneklerin asitle ayrıştırılması (dekompozisyonu) ile yapılmaktadır. Bileşenler aygıtsal yöntemlerle ölçülmektedir (örneğin, AAS, ICP, ICP-MS).

Borat-ergitici (flaks) kullanılarak (örneğin lityum metaborat, ergime noktası 840°C; lityum tetra-borat, ergime noktası yaklaşık 950°C) örneklerin ayrıştırılması genel olarak atmosfer koşullarında yapılmakta olup ergime sırasında valans durumları korunmamaktadır. Bundan dolayı, ek bir analitik işlem gerekli olmaktadır: Demirin oksidasyon evrelerinin elde edilebilmesi için yapılan ayrıştırmada örneğin çeyreklenmiş bir bölümü oksitleyici olmayan bir asitle ayrıştırılır.

Oksitleyici olmayan koşullarda gerçekleştirilen tek örnek parçalanması (Ayrancı, 1978), aygıtsal yöntemler kullanılarak demirin oksidasyon evrelerinin ve örnek içinde bulunan diğer bileşenlerin de saptanmasını mümkün kılmaktadır.

Refrakter bileşenler (örneğin kromit, granatlar, spineller, stavrolit, zirkonlar) içeren silikat örnekleri, asit muamelesi sırasında tamamen çözünmeyebilirler. Buna bağlı olarak, demirin valans durumu ve yine diğer bileşenlerin belirlenmesinde bazen hatalı değerler verebilir.

Bütün bileşenlerin analizleri (demirin valans durumu ve uçucu bileşenler de dahil olmak üzere)

tek bir silikat örnek çeyreğinden yapılabilir. Bu proses iki aşamada gerçekleştirilir:

1- Oksitleyici olmayan koşullarda, borat-ergitici kullanılarak örneğin parçalanması ve bunu takiben uçucu bileşenlerin (örneğin H₂O, CO₂, H₂S, SO₂) belirlenmesi,

2a- Katlaşmış ergiyiğin, demirin valans durumunu saptamak üzere oksitleyici olmayan şartlarda analizi için çözündürülmesi,

b- Demirin oksidasyon evrelerinin tespiti için katlaşmış ergiyik çeyreğinin kullanılması, geri kalan ergiyikten esas, yan ve iz elementlerin XRF ile analizi için cam disk hazırlanması, veya örnek çözeltisinden arta kalan katlaşmış ergiyiğin çözündürülmesinden sonra AAS ve ICP-MS ile bileşenlerin analizi.

Demirin valans durumunun belirlenmesi için yapılacak analizlerde refrakter silikatların ayrıştırılması için borat-flaks (NaF+B₂O₃) kullanılması, Rowledge (1934) tarafından önerilmiştir. Rowledge tekniği geliştirilmiş (örneğin Novikova 1966; Donalson, 1969) ve mikroanalizlerde kullanılmıştır (Meyrowitz, 1970). Demirin valans durumunun saptanması için kullanılabilir ve çoğaltılabilir değerlerin elde edilmesindeki zorluklar daha önce Ayrancı'da (1992) tartışılmıştır.

Bu çalışma, çok bileşenlilerin analizlerinde bir çeyreklenmiş örnek kullanılarak asit muamelesi ve eritmeyle ayrıştırma işlemlerinin bütünleştirilmesi amacıyla yapılmaktadır.

* İsveç Federal Teknoloji Enstitüsü Yerbilimleri Bölümü, Zürih (ETH-Z).

ANALİTİK TEKNİK

Asidik borat ergiticilerinin (örneğin lityum tetraborat, ergime noktası yaklaşık 950°C), parçalanma işlemi oksitleyici olmayan ortamda yapıldığı takdirde, ayrıştırma sırasında elementlerin valans değiştirmesini kolaylaştırmadığı iyi bilinmektedir (Bock, 1979). Oksitleyici olmayan koşullarda silikat örneklerinin asidik borat (örneğin lityum tetraborat) kullanılarak ayrıştırılması aynı ayrıştırma işleminden farklı aletsel yöntemlerle birçok bileşenin analizlerinin yapılmasını mümkün kılmaktadır: Parçalanma işlemi sırasında çıkan uçucu bileşenler (örneğin H_2O , CO_2 , SO_2), uygun aletler (örneğin GC, IR) kullanılarak analiz edilebilir.

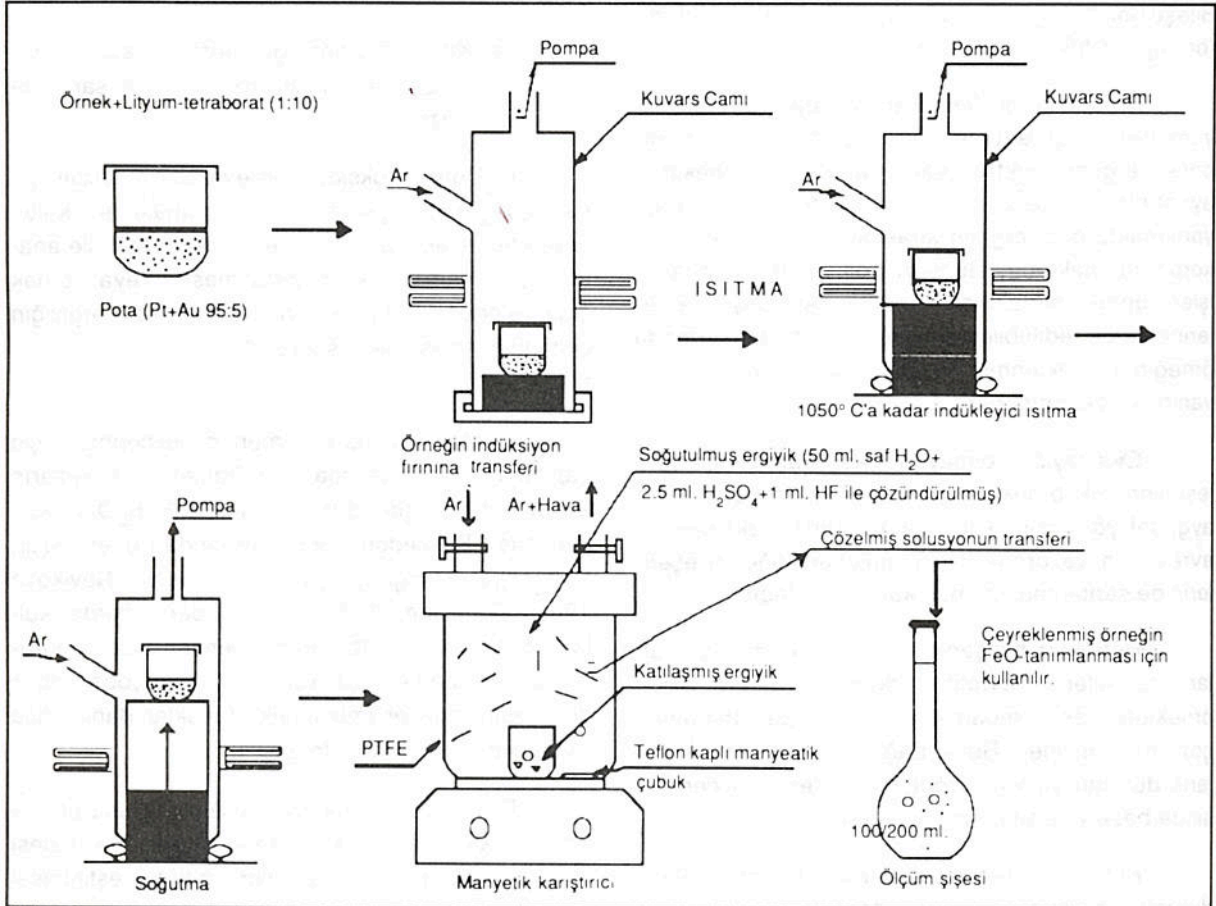
Refrakter silikatlarda sadece demirin valans durumu saptanacaksa, örneklerin asidik borat ergitici ile ayrıştırılmasının (Argon atmosferinde, Au-Pt (5:95) pota kullanılarak) indüksiyon fırınında

yapılması, tüp biçimli fırından daha uygundur (Rowledge, 1934; Groves, 1951; Donalson, 1969; Meyrowitz, 1970).

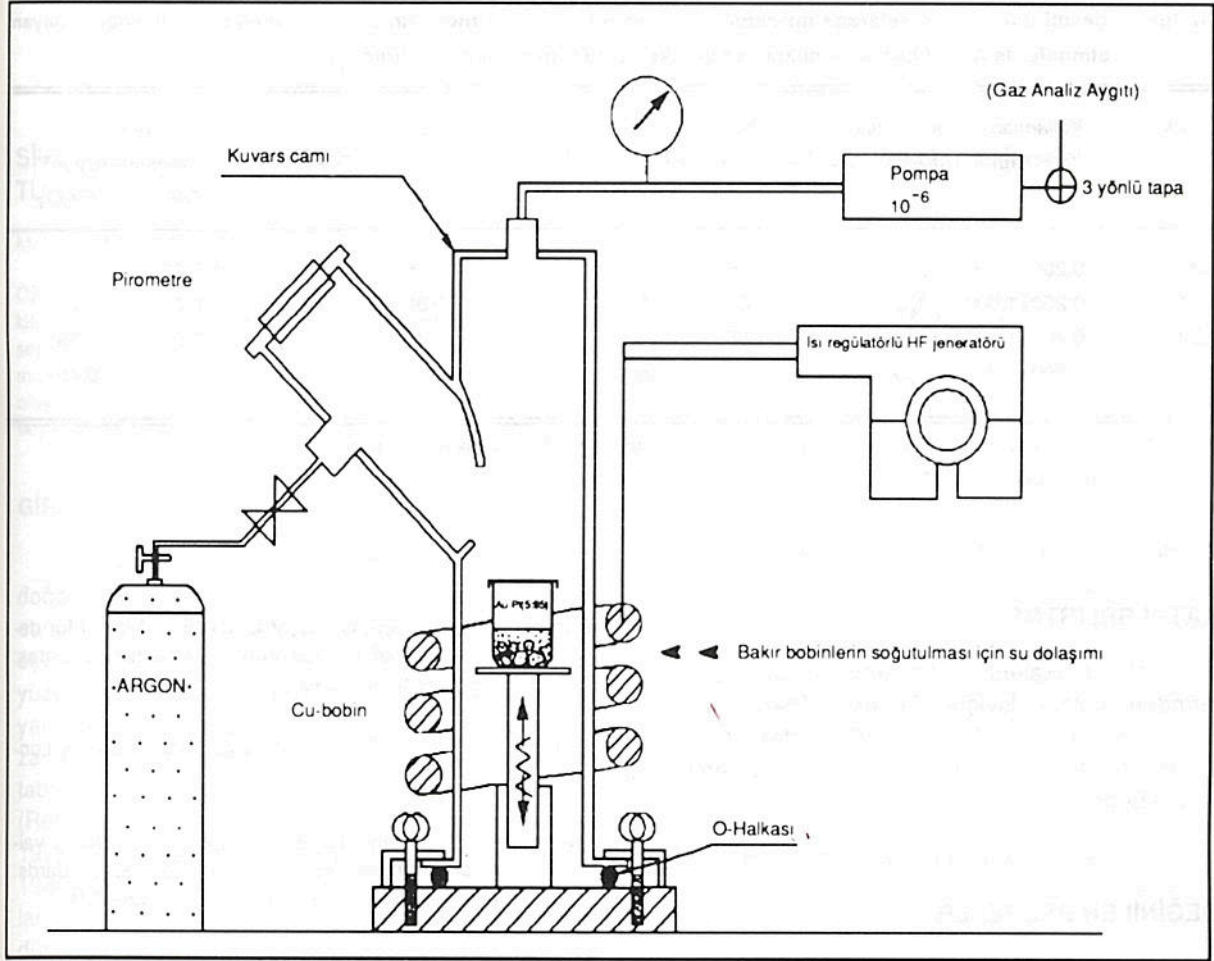
İndüksiyon fırını (Şek. 1), bir seferde yalnızca bir örneğin ayrıştırılması için kullanılabilir. Daha büyük bir indüksiyon fırını kullanılarak birden fazla örnek aynı anda ayrıştırılabilir. Buna karşılık, birçok örneğin aynı anda ayrıştırılması sırasında uçucu bileşenlerin analizlerinin yapılamayacağı da açıktır.

Örneğin ayrıştırılması

Örnek (10-1000 mg), ağırlığının 5-10 katı ağırlıkta, önceden kızdırılmış asidik borat ergitici (lityum tetraborat, ergime noktası 950°C) ile karıştırılır ve daha sonra Au-Pt potada (5:95) ilâve lityum tetraborat ile kaplanır. Tamamen kapatılmış pota daha sonra oda sıcaklığında bir indüksiyon fırınına yerleştirilir. Kuvars fırınının (Şek. 1) vakum



Şek. 1- Oksitleyici olmayan koşullarda, silikat örneklerinin ergiticilerle bozundurulmasında kullanılan bir indüksiyon fırınının şeması.



Şek. 2- Örneklerin ergitilmesi ve çözündürülmesi ile eritme bozundurmasından sonraki analizler (şematik olarak).

kilitlemesi O-halkası kullanılarak yapılır (Şek. 1 ve 2). Kapalı sistemdeki hava, 10^{-4} torr basınçla basılan AR-kalitesinde Argon gazı ile değiştirilir. Bu işlem sırasında örneğin nemi 105°C civarında Argon akışı ile giderilir.

Gaz ölçüm cihazına (örneğin; GC, IR) üç yönlü bir tıpa takılarak fırın sıcaklığı 600°C 'a kadar yükseltilir. Organik uçucu bileşenlerin uzaklaştırılması için bu gereklidir. Daha sonra fırın sıcaklığı dereceli olarak artırılarak 5 dakikalık süre içinde 1000°C 'a çıkarılır. Örneğin tamamen erimesi için, $1050-1100^{\circ}\text{C}$ 'da 2-3 dakika ısıtılması gerekmektedir. Fırın daha sonra kapatılır ve pota, fırının soğuk zonuna yükseltilir. Üç yönlü tıpa oda

atmosferine açılarak eriyik kuvvetli bir argon akımı ile yıkanır ve söndürülür (Şek. 2). Potanın oda sıcaklığına soğutulmasından sonra, üç yönlü tıpa kapatılır ve katılaşmış eriyik keki fırından alınır. Bu kekin çeyreklenmiş bir bölümü demirin oksidasyon halinin belirlenmesi için kullanılırken (Şek. 2), eritilmiş örneğin geri kalan kısmı ise diğer bileşenlerin XRF, AAS, ICP, ICP-MS ile analizi için kullanılabilir. Bu yöntem, analitik sonuçların çoğaltılabilirliğine bağlı olarak, tek analitik evrede birçok bileşenlerin analizinin yapılabilmesi açısından büyük bir avantaj sağlamaktadır (Çizelge 1). Silikat örneklerinin mikroanaliz tekniği ve rutin analizlerinde fayda sağlamaktadır.

Çizelge 1- Çeşitli uluslararası referans malzemeye ait analitik veriler. Örneklerin bozundurulması oksitleyici olmayan atmosferde Argon gazı kullanılarak ve indüksiyonlu fırında gerçekleştirilmiştir.

Örnek	Kullanılan örnek+ergitici (flaks) ağırlığı (gram)	Saptanan konsantrasyon		Hesap.*	Önerilen konsantrasyon**	
		FeO	ΣFe_2O_3	Fe_2O_3	FeO	Fe_2O_3
BM	0.200+1.000 $Li_2B_4O_7$	7.35	9.75	1.75	7.28	1.60
JB-1	0.200+1.000 $Li_2B_4O_7$	6.05	9.05	2.30	6.00	2.28
JG-1	0.200+1.000 $Li_2B_4O_7$	1.65	2.25	0.42	1.63	0.39
JR-1	0.200+1.000 $Li_2B_4O_7$	0.40	1.05	0.61	0.43	0.40

Hesap.* : Toplam demirden iki değerlikli (Fe_2O_3) demir konsantrasyonları olarak hesaplanmıştır
(Toplam demir Fe_2O_3 -FeOx 1.1113-üç değerlikli demir konsantrasyonu olarak).

Önerilen konsantrasyon** : Grovindaraju (1989).

KATKI BELİRTME

Bu makalenin hazırlanmasındaki yardımlarından dolayı İsviçre Federal Teknoloji Enstitüsü'nden (E.T.H. Zürich) Dr. G. Lister ve Dr. T. Thompson ile F. Ried, M. Roemer ve B. Zuercher'e teşekkür borçluyum.

Yayına verildiği tarih, 6 Temmuz 1992

DEĞİNİLEN BELGELER

Ayrancı, B., 1978, The major, minor and trace-element analysis of silicate rocks and minerals from a single sample solution: Schweiz. mineral. petr. Mitt. 57, 299.

—, 1992, Analysis of the oxidation states of iron in silicate rocks and refractory minerals by fusion disintegration: Kontakte (Merck), 1, 16s.

Bock, R., 1979, A handbook of decomposition methods in analytical chemistry: International Textbook Company, London.

Donalson, E.M., 1969, Study of GROVES Method for determination of ferrous iron in refractory silicates: Anal. Chem., 41, 3401.

Groves, A.W., 1951, Silicate Analysis: Allen-Unwin, London.

Govindaraju, K., 1989, 1989 compilation of working values and sample description for 272 geostandards: Geostandards Newsletter Special Issue, 13s.

Meyrowitz, R., 1970, A new semimicroprocedure for the determination of ferrous iron in refractory silicate minerals using a sodium metafluoroborate decomposition: Anal. Chem., 42, 1110.

Novikova, N. Yu., 1966, The possibility of determination iron (II) in rocks and minerals by fusion with sodium metafluoroborate: Zhur. Anal. Khim; 23, 1057.

Rowledge, H.P., 1934, New method for the determination of ferrous iron in refractory silicates: Journal Roy. Soc. W. Australia, 20, 165.

SİVRİHİSAR'DA (ESKİŞEHİR) SEDİMENTER-DİYAJENETİK OLUŞUMLU YENİ BİR LÜLETAŞI TÜRÜ

Mefail YENİYOL*

ÖZ_ Bu çalışma oluşumu, yataklanma tarzı, dokusu ve bileşimi açısından klasik yumru tipindeki lületaşlarından farklı bir lületaşını tanımlamaktadır. Bu lületaşı Sivrihisar'ın güneyinde Neojen dolomitli istifin üst kesimlerinde yer alan sedimenter sepiolitlerle birlikte bulunur. Tabakalı, mercek biçimli ve detritik kırıntılar halinde temsil edilen dolomit ve/veya kalsit minerallerinden meydana gelir. Sepiolit yeniden işlenmiş ve çökelmiş olan karbonat malzemesinden sonra diyajenez evresinde oluşmuş olup tanelerarası hacmi çeşitli oranlarda kaplar. İncelenen bu lületaşlarından en iyi nitelikte olanlar, gözenekli, hafif ve beyaz renkli olup suyla ıslatıldıklarında kolayca yontulabilmektedirler.

GİRİŞ

Lületaşı, beyaz, kompakt, hafif ve gözenekli doğal bir malzeme olup sepiolit mineralinden meydana gelir ve pipo, ağızlık ile biblo gibi bazı süs eşyalarının yapımında kullanılır. Türkiye'de yüzyıllardır bilinen ve işletilmekte olan lületaşına ait yataklar Eskişehir çevresinde bulunur. Neojen havzasının kenar kesimlerindeki bu yataklarda lületaşı taban konglomeraları içinde çakıllar halinde yer alır (Retrascheck, 1963; b; Brennich, 1965; Öncel 1971; Öncel ve Denizci, 1982; Yeniyo1 ve Öztunalı, 1985). Kayıtlara göre (Öncel, 1971) 15. yüzyıl sonlarından itibaren işletildiği bilinen bu yataklardan dünyada bilinen en kaliteli lületaşı üretilmektedir.

Yayınlanmış çalışmalardan işletilmiş oldukları bilinen ve işletilen diğer lületaşı yatakları Kenya ile Tanzanya sınırı dolayında ve bu sınırın kuzeyindeki Amboseli havzasındaki lületaşları (Stoessell ve Hay, 1978; Hay ve Stoessell, 1984) ile İspanya'da Madrid yakınındaki Vallecas'ta (Galan ve Castillo, 1984) olanlardır. Bunlardan Vallecas'ta lületaşı üretimi 16. yüzyıl sonlarından itibaren yapılmıştır. Sedimenter kökenli olan ve dünyanın bilinen en büyük sepiolit yataklarından biri olan Vallecas'taki bu yataktan halihazırda çeşitli endüstri dallarında kullanılmak üzere sepiolit üretimi yapılmaktadır. Tanzanya ve Kenya'daki lületaşı yatakları ise bulunduğumuz yüzyılın ikinci yarısının başlarında ortaya çıkmışlardır. Sedimenter kökenli olan bu yataklarda lületaşı, dolomitlerle birlikte kalış breşleri içinde düzensiz cepler ve ince damarlar halinde bulunur. İyi kalite pipo yapımında kullanılan ve halen işletilmekte olan Amboseli'deki yataktan her 1 m³

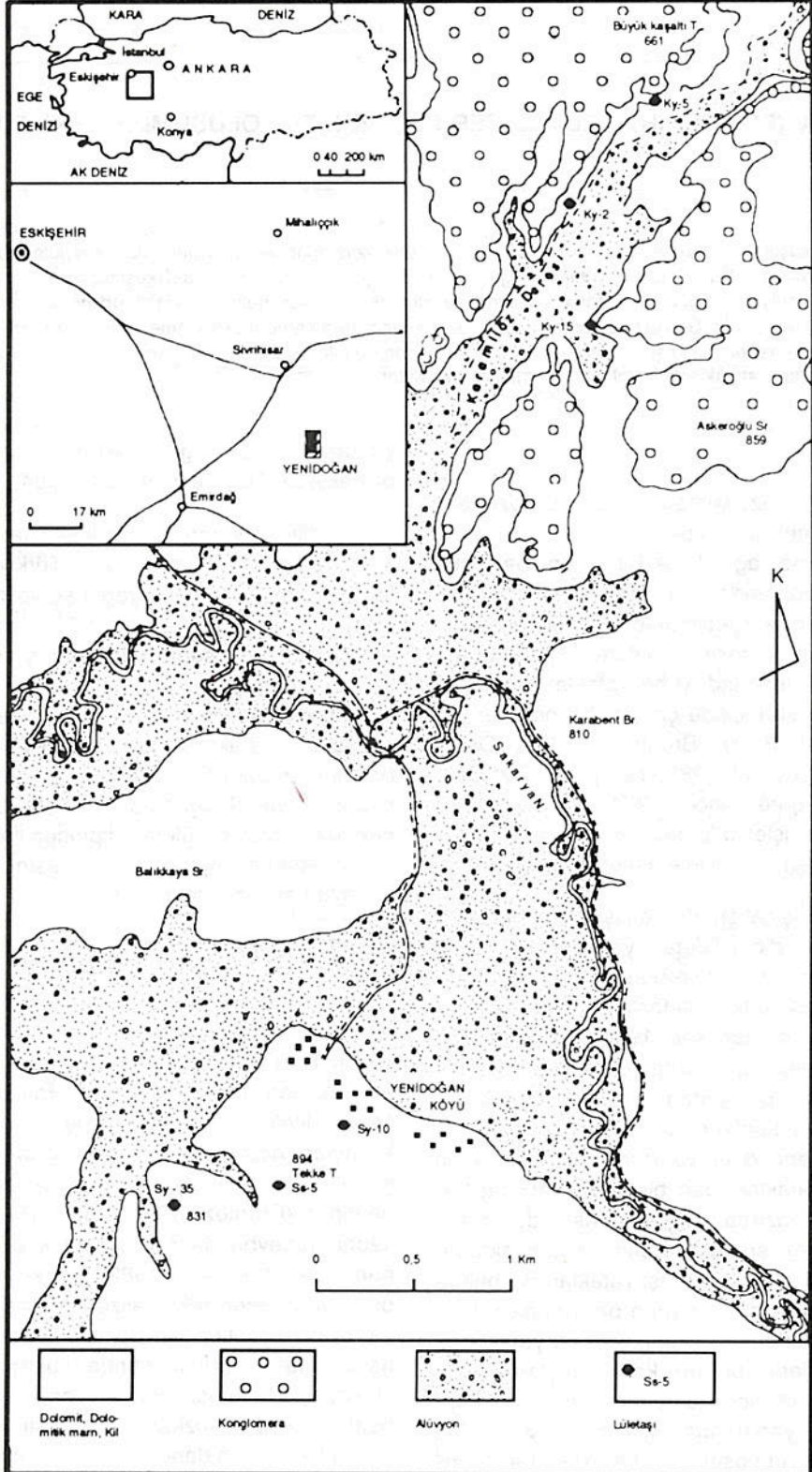
yantaştan 7.3 kg dolayında lületaşı üretilmektedir (Hay ve Stoessell, 1984).

Bilinen yumru tipteki lületaşları dışında 1960 lı yıllarda yapılan çalışmalarla Türkiye'de sediment oluşumlu ve tabaka yapılı sepiolitlerin de varlığı ortaya konmuştur (Akıncı, 1967; Öncel ve Denizci, 1982). Bu tipteki sepiolit yataklarından biri Sivrihisar ilçesinin güneyinde yer alan Yenidoğan Köyünün bitişiğinde bulunur (Şek. 1). Yeniyo1 (1992), sözkonusu yatakta ve bunun kuzeyindeki alanda tabakalı sepiolitlerle birlikte lületaşı niteliğinde malzemenin de var olduğunu saptamıştır. Bu çalışma bilinen klasik yumru lületaşı tipinden farklı bir oluşum ve yataklanma sunan bu lületaşını incelemeyi ve tanımlamayı amaçlamaktadır.

GENEL JEOLojİ

İnceleme alanı (Şek. 1) bölgesel ölçekte büyük bir yayılım gösteren Neojen havzasının çok küçük bir kesimini kaplar ve tümü Pliyosen yaşlı kayaçlardan meydana gelir. Havzanın taban ve çevre litolojisini temsil eden Tersiyer öncesi kayaçlar, alanın dışında yer alırlar ve kuzeybatı-güneydoğu gidişli morfolojik yükselteleri meydana getirirler (Erentöz, 1975). Bu yaşlı litoloji 25 km kadar güneybatıda rekristalize kireçtaşları ile serpantinitle (Yeniyo1, 1982); 7 km kadar kuzeydoğuda mermer, rekristalize kireçtaşları, gnays, şist ve granodiyoritler ile 30 km kadar kuzeybatıda aşınan Neojen örtüsü altında mostra veren ultramafik kayaçlarla temsil edilir. Pliyosen sedimentleri pe-nepnenleşmiş sözkonusu yaşlı litolojiye ait yükseltelerin sınırlandığı çöküntü alanlarındaki

* İstanbul Üniversitesi, Jeoloji Mühendisliği Bölümü, İstanbul.



Şek. 1- Yenidoğan dolayının litoloji haritası.

kimyasal göllerde, kurak ve yarıkurak iklim koşullarında çökemişlerdir (Yeniyo, 1992).

Bölgesel ölçekte olduğu gibi, incelenen alan sınırları için de Pliyosen litolojisinde egemen kayaç türleri dolomitik marnlar ve dolomitlerdir. Bu kayaçlar ve bunlarla birlikte ancak daha düşük oranlarda bulunan diğer kayaç türleri, inceleme alanının güneyinde görünür kalınlığı 200 metreyi aşan bir istif meydana getirirler (Yeniyo, 1992). Güneydoğuda, Sakarya Nehri vadi tabanından itibaren istif; volkanik malzeme (asidik tüf) ile bazan detritik arakatkılar da içeren ve sık sık silisleşmiş dolomit seviyelerinin yer aldığı bir dolomit ve dolomitik marn ardalanmasıyla başlar. Alanın sadece güneydoğu kesiminde görünen bu topluluğun üzerinde Yenidoğan köyü, Karabent Burnu ve Askeroğlu Sirtının güneydoğu kesimlerinde yayılım gösteren, Jips seviyelerinin de bulunduğu korrensitli killer ile dolomit ve dolomitik marn ardalanması yer alır.

Istifin üstünü, içinde sepiolit ile sepiolitli oluşukların da yer aldığı dolomit ve dolomitik marn ardalanmasından meydana gelen bir kayaç topluluğu temsil eder. Bu topluluk Yenidoğan Köyü dolayında 70 metreyi aşkın bir kalınlık gösterir. Tabanda magnezitli-dolomitli bir karbonat seviyesiyle başlar ve alt yarısında başlıca iki ayrı seviyede sepiolit zenginleşmesi yer alır. Her iki seviye, % 90 dan fazla sepiolit içeren "sepiolit kili" ve çeşitli oranlarda ancak % 50 den az dolomit içeren "dolomitli sepiolit" tabaka ve mercceklerinin ardalanmasından oluşur. Üstteki sepiolitli seviye alttakinden daha kalın (en çok 10 m) olup yanal yönlerde düzenli olarak ve daha geniş bir alanda yayılım gösterir. Bu seviyenin üst kesimlerinde yer yer ve lületaşını niteliği gösteren sepiolitli malzeme yer alır.

İçinde sepiolit oluşuklarının yer aldığı Pliyosen istifinin üst kesimi inceleme alanının bir çok yerinde aşınmıştır. Aşınmanın daha az olduğu ve böylece sepiolitli seviyelerin de korunabildiği bir başka kesim, alanın kuzeydoğusundaki Keremliöz Deresi dolayındadır. Burada da sepiolitinin yer aldığı kayaç topluluğu Yenidoğan köyü dolayında olduğu gibi tabanda magnezitli-dolomitli karbonat seviyeleriyle başlar, üstte doğru dolomit ve dolomitik marn ardalanmasıyla devam eder. Yenidoğan Köyünde olduğundan çok daha az kalınlıkta olan bu topluluğun üst kesimi aşınmış olup üzerinde diskordan olarak muhtemelen Üst Pliyosen veya daha genç

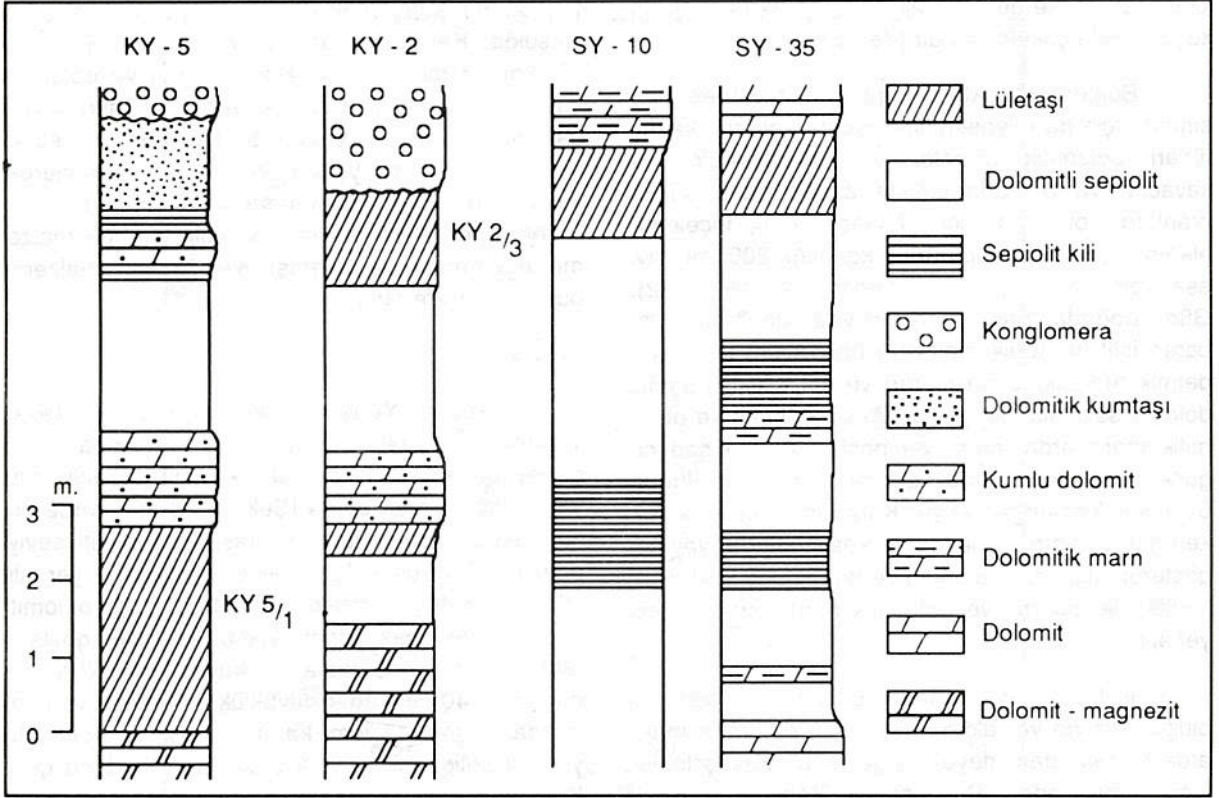
yaştaki bir konglomera seviyesi yer alır. Sepiolit oluşukları Keremliöz vadisinin yamaçları boyunca 1-15, km bir mesafede izlenir. Dolomit ve dolomitik marn ardalanmasıyla birlikte başlıca iki ayrı seviye halinde gözlenen bu oluşuklardan sepiolit kili, sadece vadinin güney yamacında ve üst kesimlerde, yayılımı az olan ince bir seviye halinde bulunur. Diğer yerlerde ise dolomitli sepiolit türünde malzeme egemendir ve lületaşını niteliğindeki malzeme bunlarla birlikte bulunur.

Lületaşını

Lületaşını, Yenidoğan köyü dolayında; Tekke Tepenin kuzeydoğusunda, batısında ve güneybatıdaki 851 m yükseklikteki tepenin batı yamacında olmak üzere (Şek. 1) üç ayrı yerde bulunmaktadır. Bu yerlerde lületaşını üst sepiolitli seviyenin en üst kesiminde merccekler halinde yer alır (Yeniyo, 1992). Lületaşını birlikte bulunduğu dolomitli sepiolitlerden bazı farklı fiziksel özellikler gösterir. Mostra verdiğinde hızla su kaybederek kurur ve bazan 30-40 cm kadar büyüklükte parçalar verecek tarzda seyrek, 1 cm kadar genişlikte konkoidal yüzeyli poligonal kuruma çatlakları meydana gelir. Kuruyken hafif ve darbeyle kuru tahta sesi veren lületaşını, beyaz, kirli beyaz renklerde, sıkı ve masif yapılıdır. Bazan çok ince kum boyutunda iri kırıntılı ve gözle görülebilecek boyutta detritik dokuludur. Bazan da submikroskopik boyutta ince taneli ve porselen görünüşlüdür. Islatılınca suda dağılmaz ve parçalara ayrılmaz, sabun görünüşü kazanır, rengi koyulaşarak kirli beyaz-çok açık bej rengini alır ve kolayca kesilip yontulabilir.

Lületaşını ve daha düşük kalitede benzeri malzeme içeren mercceklerin kalınlıkları 30 cm ile 1.4 m arasında değişir. Tabanda dolomitli sepiolit bulunur ve iki farklı tipteki malzeme arasında bir kaç santimetrelilik bir aralıkta dereceli geçiş gözlenir. Tavan da ise bazan dolomitli sepiolit (Şek. 2), genellikle tüm sepiolitli seviyenin de üst sınırını meydana getiren sert bir dolomit seviyesi yer alır. Lületaşını yanal yönlerde, ancak daha geniş aralıklarda, dolomitli sepiolite dereceli geçiş gösterir.

Lületaşını, Keremliöz vadisinin yamaçlarında dolomitli sepiolitlerle birlikte sepiolit mineralinin zenginleşme gösterdiği başlıca iki ayrı seviyede bulunur. Bazan dolomitik kumtaşını veya kumlu dolomit karakteri kazanan ince bir dolomitte birbirinden ayrılan bu seviyelerde lületaşını ayrı merccekler halin-



Şek. 2- Lületaşı düzeylerinin istiftteki yerini gösteren dikme kesitler.

de yer alır. Bu seviyelerde lületaşı niteliğindeki malzeme tabanda, tavanda veya tümünü meydana getirecek tarzda farklı stratigrafik konumlarda bulunabilmektedir (Şek. 2). Yataklanma biçimi ve fiziksel özellikleri açısından Yenidoğan Köyü dolayında bulunan lületaşlarına benzerler. Bir çok yerde ve birey mercleklerin değişik kesimlerinde, çökeltme ürünü iri birincil karbonat kırıntıları; ikincil boşluk ve gömülen organizma izi veya çatlak dolgusu olarak kalsit, dolomit bazan da kuvars içerirler. Bazan ince kum boyutlu malzeme içeren ve çıplak gözle bile gözlenen detritik dokulu olan lületaşlarının iyi nitelikli kesimleri submikroskopik boyutta çok ince taneli olup dolgu veya iri kırıntılı malzeme içermezler. Renk, genellikle beyaz ve kirli beyaz olup bazan çatlak yüzeyleri boyunca demirli suların etkisiyle açık kırmızı kahve renklerde de boyanmış olabilmektedirler.

Lületaşı karakterindeki malzeme yanal yönlerde dolomitli sepiolite dereceli geçiş gösterir. Bu yönlerdeki yayılımı birkaç on metre ilâ 300 metreyi aşan değerler arasında değişir. Düşey yönde lületaşı ya dolomitli sepiolit ile bir kaç santimetre

aralıkta gözlenen dereceli geçişlidir veya dolomit ile oldukça keskin sınırlıdır. İçinde marn ve düşük nitelikli veya nitelsiz kesimler de içeren lületaşı ve benzeri karakterde malzemenin bulunduğu mercleklerin kalınlıkları 25 cm ilâ 2.7 m arasında değişir.

BİLEŞİM DOKU VE FİZİKSEL ÖZELLİKLER

Materyal ve Metod

Analitik çalışmalarda inceleme alanında değişik yerlerden alınan 18 adet numune ve karşılaştırma yapmak üzere klasik yumru tipindeki lületaşını temsil eden bir numune incelenmiştir.

Kalitatif mineral analizleri Philips X-ışını difraktometresi ile yapılmış, doğal durumlarındaki lületaşı numunelerinin öğütülmesiyle elde edilen yönlenmemiş toz preparatlardan X-ışını difraksiyon (XRD) kayıtları alınmıştır. Kantitatif bileşimi ortaya koymak için ise oda sıcaklığında kurutulan ve toz haline getirilen numunelere IM Hcl eklenerek karbonat bünyeden çıkartılmıştır. Numuneler damıtık suyla yıkanıp tekrar kurularak tartılmış ve aradaki

ağırlık farkı numunenin içerdiği karbonat miktarı olarak hesaplanmıştır. Hem dolomit hemde kalsit içeren lületaşlarında bu iki mineralin bileşimdeki % lerini hesaplamak için; XRD kayıtlarında bu mineralere ait maksimum piklerinin şiddetleri ölçülmüş ve toplam karbonat yüzdesiyle orantı kurularak bileşimdeki oranları ortaya konmuştur (Schultz, 1964).

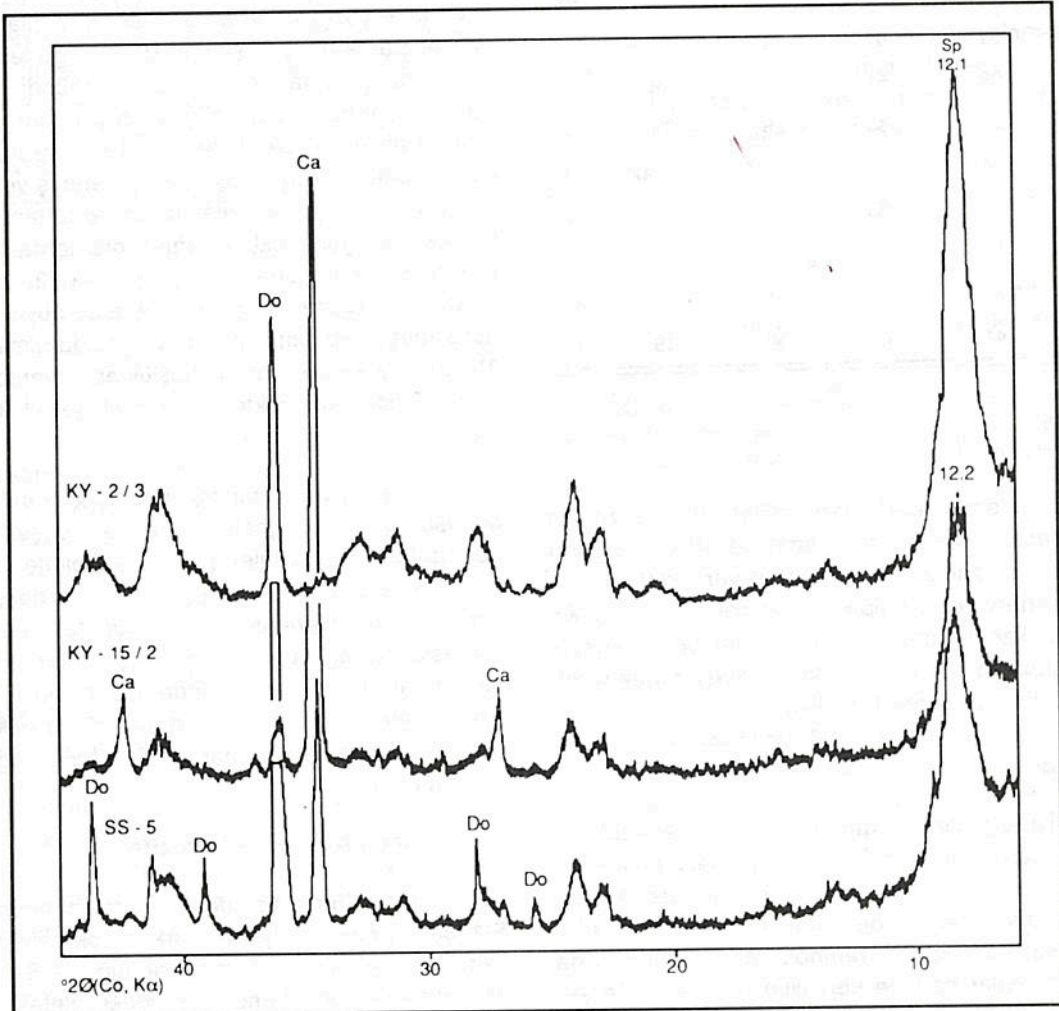
Mineralojik ve özellikle dokusal incelemeler için JSM-T330 tarama elektron mikroskobundan (SEM) yararlanılmış, analizlerde altınla kaplanmış doğal haldeki numuneler kullanılmıştır.

Porozite (gözeneklilik) ve başlıca bundan kaynaklanan hafiflik, lületaşının ticarî değerini belirleyen başlıca özelliklerdendir. Bu özellikleri kabaca ortaya koymak için, numuneler oda sıcaklığında 10

gün kurutulmuş sonra düzgün yüzeyli geometrik şekiller elde edecek tarzda kesilmişlerdir. Bu şekillerin hacimleri ve ağırlıklarından "birim hacim ağırlıkları" hesaplanmıştır. Daha sonra bu numuneler damıtık suya konarak 4 saat bekletilmiş ve gözenekleri suya doymun hale gelmesi sağlanmıştır. Sudan çıkartılan numunelerin ölçülen ağırlıkları ile bunların kuru ağırlıkları arasındaki fark porozite yüzdesi olarak kabul edilmiştir. Söz konusu fiziksel özellikler, XRD ve asitle çözündürme işlemleriyle hesaplanan mineral bileşimleri ile ilgili değerler toplu olarak Çizelge 1 de verilmiştir.

Bileşim ve Doku

XRD verilerine göre lületaşları başlıca sepiolit dolomit ve/veya kalsit minerallerinden meydana gelmektedirler (Şek. 3). Bu minerallerden sepio-



Şek. 3- Lületaşı örneklerinin XRD analiz sonuçları

lit, iyi nitelikteki lületaşlarında ana bileşen olup bileşimde % 50 den fazla oranlarda yer almaktadır. Kalsit ve dolomit, sepiolitten daha düşük oranlarda temsil edilirler. Bileşimde birlikte bulduklarında kalsit ve dolomit bolluk sırası değişir. Daha düşük sepiolit içerikli malzeme gittikçe lületaşı olarak değersiz hale gelir ve sepiolitik marn veya sepiolittli dolomit niteliği kazanır (Çizelge 1).

Çizelge 1- Lületaşların bazı fiziksel özellikleri ve bileşimleri

Numune No. (*)	Birim hacim ağırlığı (gr/cm ³)	porozite %	Sepiolit %	Dolomit %	Kalsit %
S-1	0.52	75	100	-	-
KY-15/2	0.79	88	60	10	30
KY-2/3	0.91	81	78	22	-
Ss-5	1.08	51	65	28	7
KY-3/5	0.91	43	26	74	-
KY-11/2	1.04	51	32	çok az	68
KY-7/3	1.08	55	36	-	64
KY-3/1	1.17	66	34	66	-
KY-3/2	1.22	57	31	40	29
KY-5/1	1.41	49	30	19	51

(*) S-1 Yunak lületaşı yatağından (Yeniöl ve Öztunalı, 1985), Ss-5 Yenidoğan Köyünden, KY serisi ise Keremliöz'den alınan numuneleri göstermektedir.

İncelenen lületaşları, SEM altında bazan tane destekli bazan da hamur destekli görünen kırıntılar ile tanelerarası hacimde yer alan sepiolitten meydana gelen tipik bir detritik doku özelliği gösterir. Taneler bazan köşeli, genellikle küt köşeli, yuvarlak veya yarı yuvarlaktır. Lületaşı olarak iyi nitelikteki numunelerde tane boyutlu 2-10 μ arasında değişir (Levha I, şek. 1-3) ve genellikle detritik kökenlidir.

Tane yüzeyleri genellikle sepiolitle kaplı olduklarından bunların SEM altında analiz edilmeleri güçtür. Ancak XRD analizleriyle bu kırıntılı dolomit ve kalsit bileşiminde oldukları anlaşılmaktadır. Ayrıca kalsit ve dolomit yanında daha düşük oranda ve intraklastlar halinde sepiolitin de bileşimde yer alması olasıdır. Kalsit ve dolomit genellikle sedimentasyon aşamasında kırıntılar halinde

çökelmişlerdir (Levha I, şek. 1-3; Levha II, şek. 1, 2). Bunlardan kalsit diyajenez sonrası evrelerde oluşmuş, mekik biçimli tipik kuruma çatlaklarında dolgular halinde de bulunabilmektedir. (Levha III, şek. 1). Ayrıca bazı sepiolit liflerinde SEM ile yapılan analizlerde olağanın çok üzerinde % Ca değerlerinin elde edilmesi, kalsitin geç evrelerde sepiolit liflerinin yüzeyinde ince bir film halinde de çökelmiş olabileceğini telkin etmektedir. Sözü edilen karbonatlar dışında, yine detritik kırıntılar halinde ve çok az miktarlarda magnezyumlu mikanın da (muhtemelen biyotit) bileşimde yer aldığı, gerek binoküler mikroskop gerekse SEM ile yapılan incelemelerde gözlenmiştir.

Tüm lületaşı numunelerinde sepiolit mineralinin tane çökelişinden sonra ve diyajenez evresinde oluştuğu açıkça görülmektedir. Sepiolit, lifler halinde önce tane yüzeylerine paralel, sonra bunlara dik ve ışınsal olarak büyümüşlerdir. Bu lifler genellikle 0.5-1 μ uzunluklarda ve oldukça düzgündür. Ayrıca daha geç evrede büyümüş 3.5-5 μ kadar uzunluklarda olabilen lif ve lif demetleri de vardır. Bunlar çeşitli yönlerde büyümüş ve kenetlenmiş veya birbirine paralel ve yarı paralel konumlarda tanelerarası boşlukta ve gözenekleri değişik oranlarda kaplayacak tarzda bulunurlar (Levha II, şek. 2, 3). Buna rağmen, tanelerarası gözenek hacmi büyük ölçüde korunmuş olup sepiolit lifleriyle doldurulmamış ve 15 μ büyüklüğe varan boşlukların varlığı SEM altında gözlenebilmektedir (Levha I, şek. 1-3; Levha III, şek. 1).

Klasik yumru tipindeki lületaşı çok daha farklı dokusal özellikler gösterir. Levha III, şekil 3 de görüldüğü gibi, bu lületaşının bileşiminde yer alan tek mineral sepiolittir. Değişik yönlerde gelişmiş ve birbirine kenetlenmiş lif ve lif demetleri bu lületaşlarına ağ veya sünger biçimli bir doku kazandırır. Bazı kesimlerinde ise sepiolit 4-5 μ uzunluklarda oldukça düzgün veya hafif bükülmüş, birbirine paralel ve yarı paralel lifler halinde gözlenir (Levha III, şek. 2).

Birim Hacim Ağırlık ve Porozite

Klasik yumru tipinde bir lületaşını temsil eden S-1 işaretli numune iyi kalitede ve çok hafif bir malzeme olup birim hacim ağırlığı 0.5 gr/cm³ dolayındadır. İnceleme alanındaki lületaşlarından en iyi nitelikte olanlar; Şekil 1 de Ss-5, KY-2 ve KY-15 işaretli yerlerden alınanlardır. Bu numuneler,

yumru tipteki lületaşlarından biraz daha ağır olmakla birlikte birim hacim ağırlıkları 1 gr/cm^3 dolayında veya daha düşüktür. Ölçülen porozite değerleri ise yaklaşık % 50 ilâ % 90 arasındadır. Sepiolit adsorpsiyon yeteneği yüksek olan bir malzemedir. Dağılmaya mekanik direnç göstererek hayli yüksek oranda sıvı adsorbe edebilir. Bu özelliği gözönüne alındığında, bu yöntemle hesaplanan porozitenin bir kısmının, sepiolit suyu adsorbe etmesinden kaynaklandığını özellikle sepiolit içeriği yüksek olan numuneler için dikkate almak gerekir. Ancak bu yöntemle elde edilen sonuçlar, yine de malzemenin porozitesi ile ilgili yorum ve karşılaştırma yapabilmek için yeterli olduğu kanısını vermektedir.

Yukarıda sözü edilen lületaşların sepiolit içerikleri yüksek, tane boyutları çok küçük ve 0.2-10 μ arasında değişim gösterirler. Bu nedenlerden dolayı ıslatıldıklarında düzgün ve pürüzsüz yüzey elde edebilecek tarzda kolayca yontulabilmektedirler. Bunlardan Ss-5 en iyi nitelikte olup kurduğunda çatlamamaktadır. KY-2 ve KY-15 işaretli yerlerden alınan bazı numuneler ise kuruduktan sonra çatlamakta bazıları da Ss-5 numuneleriyle benzer nitelikler gösterirler.

Çizelge 1 de yeralan ve diğer bazı lületaşı, mercerklerinden alınan numuneler, mostrada lületaşına benzer görünüş ve özellikler göstermelerine rağmen bunlar daha düşük nitelikte veya değersizdir. Poroziteleri % 40 ilâ % 65 arasında değişen bu numunelerin birim hacim ağırlıkları, genelde 1 gr/cm^3 ten daha fazladır. Sepiolit içerikleri ise % 35 ten azdır. Bunlar ya iri taneli veya bileşimlerinde çok ince tanelerle birlikte, bazan gözle görülebilecek büyüklükte olabilen kırıntılar ve ikincil karbonat dolguları içerirler. Zor yontulabilen ve yontulduklarında çentikli yüzey veren bu numuneler kuruduktan sonra genellikle çatlarlar.

BİLEŞİM DOKU VE FİZİKSEL ÖZELLİKLER ARASINDAKİ İLİŞKİ

Türkiyede yüzyıllardan bu yana tanınan ve işletilen, Neojen yaşındaki konglomeralar içinde çakıl halinde bulunan yumru tipindeki lületaşlarıdır. ıslatıldıklarında kolayca yontulabilmeleri ve pürüzsüz düzgün yüzey vermeleri, beyaz ve lekesiz olmaları, kuruyunca deforme olmamaları ve çatlamamaları ile hafif olmaları gibi özellikler, bu lületaşların ticarî değerini belirler. Bileşimleri başlıca sepiolit mineralinden meydana gelir.

Bileşimde yeralan ve özgül ağırlığı düşük (2 gr/cm^3) olan sepiolit minerali yanında hacimdeki yüksek gözenek oranı (porozite), lületaşına 1 gr/cm^3 ten daha düşük bir birim hacim ağırlığı kazandırır. Bu nedenle suya atıldığında lületaşı, gözenekleri suya doymun hale gelinceye kadar yüzer. Deniz köpüğü anlamına gelen "Meerschäum" diye adlandırılması bu nedendir. Dolomit, magnezit, kuvars ve demirli mineraller, bileşimde bulunabilen ve niteliğini etkileyebilen safsızlıklardır. Bu mineraller, lületaşında, kendisinin türemiş olduğu (Yeniol ve Öztunalı, 1985) magnezitten arta kalan bileşenlerdir ve genellikle çok düşük oranlarda bulunabilirler.

Bunlardan magnezit, sepiolitleşme prosesinin tamamlanamadığı durumlarda çeşitli oranlarda bulunabilir. Bileşimde magnezit arttıkça birim hacim ağırlığı da artar, malzeme zor yontulur ve ticarî değeri gittikçe azalır. Kuvars, ya birincil magnezit bileşiminden arta kalan ince damarcıklar veya saçınımlar ya da sepiolitleşme prosesi sonucu olarak bileşimde çeşitli biçimlerde ve oranlarda yer alan oluşuklar halinde temsil edilebilir ve yontulmayı güçleştirir. Demirli mineraller az miktarlarda bile bulduklarında lületaşının beyazlığını azaltır. İyi nitelikli bir lületaşında bu safsızlıklar bulunmaz veya çok düşük orandadır. Gözenek dağılımı homojen, sepiolit lifleri değişik yönlerde büyümüş ve kenetlenmiş olup birbirini izleyen ıslatma ve kurutma işlemlerinde çatlaklar meydana gelmez.

Bu metnin konusu olan sedimentler lületaşları, köken ve oluşumlarındaki farklılıkları nedeniyle yumru tipindeki lületaşlarından değişik bileşim ve dokusal özellikler gösterirler. Sepiolit ana mineral bileşeni olmasına rağmen önemli miktarlarda karbonat mineralleri de bileşimde yer alır. Bazı yerlerdeki infiltrasyonlar dışında demir ile karbonat minerallerinden magnezit, bileşimde hiç bulunmaz. Dolomit ile kalsit ise, ayrı ayrı veya birlikte ve değişik oranlarda bu lületaşlarında temsil edilen minerallerdir. Bileşim ve doku farklılığına rağmen incelenen lületaşları yumru tipindeki lületaşlarına benzer fiziksel özellikler gösterirler. İyi nitelikte olanları beyaz, hafif, ıslatılınca kolayca yontulabilirler ve kuruyunca çatlamazlar.

Bileşimde yeralan dolomit ve kalsit kırıntıları lületaşına beyaz renk verirler. Karbonat oranı çok düşük buna karşın sepiolit oranı çok yüksek olan numunelerde renk, gri-beyaz veya çok açık bej ton-

larını kazanır. Sepiolit başlıca diyajenez evresinde oluşmuş olup lifler halinde bulunur. Ancak sepiolit bir kısmının, kırıntılarla birlikte çökme evresinde sudan doğrudan kristalizasyonla oluşmuş olması muhtemeldir (Yeniyol, 1992). Bazı lületaşlarında çamur destekli ve düşük oranlardaki kırıntıların bulunması bu ihtimali telkin etmektedir. Diyajenez evresinde tane yüzeylerinden itibaren karşılıklı olarak büyüyen ve değişik yönlerde gelişen daha genç jenerasyon sepiolit lifleri, kenetlenerek malzemeye sıkı ve suda dağılmama özelliği kazandırmıştır. Bu özellik lületaşlarının birlikte buldukları ve diğer yönleri ile benzeri oldukları, dolomitli sepiolit olarak tanımlanan malzemeden başlıca farkını meydana getirir.

İncelenen lületaşlarının bileşiminde karbonat minerallerinin yer alması, bunların yumru tip lületaşlarına göre biraz daha ağır olmalarının nedeni-
dir.

Numunelerde yer alan karbonat ve sepiolit bağıllı bolluğundaki farklılıklar, birim hacim ağırlığını sınırlı ölçüde denetler. Hafifliği belirleyen asıl etken karbonat kırıntıları ile sepiolit liflerinin hacimdeki düzenlenme tarzları ve bunun sonucu olarak meydana gelen porozitedir. Birincil porozite; başlıca kırıntıların biçimleri, boyutları, hacimdeki dağılım ve istiflenme tarzlarıyla ilgilidir. Bu değişkenlere bağlı olarak boşlukların biçimleri, boyutları ve dağılımı da yer yer ve farklı numunelerde değişiklik göstermektedir. Öyle ki, bazan aynı dolomit içerikli olan farklı numunelerde, değişik porozite % leri sözkonusu olabilmektedir (Çizelge. 1). Diyajenez evresinde oluşan sepiolit lifleri her ne kadar birincil boşlukları değişik oranlarda kaplamışsa da, önemli ölçüde gözeneklilik, birey lifler arasında varlığını sürdürür.

Yontulabilme özelliğini denetleyen ana etken bileşimdeki sepiolit içeriğidir. Sepiolit oranının yüksek olması yanında bileşimdeki karbonat kırıntılarının çok ince boyutlarının sınırlı bir aralıkta değişim göstermesi; lületaşa kolay yontulabilme, yontulduğunda düzgün, çentiksiz ve homojen renkte yüzey elde edilebilmesini sağlamaktadır. Bunun aksine, karbonat oranı arttıkça veya çok ince karbonat kırıntıları yanında kalsitli, dolomitli damarcıklar ve iri tanelerin varlığı halinde, lületaşı zor yontulur, yontulduğunda çentikli yüzey verir. Rengi ise be-
nekli veya lekeli bir görünüştü kazanır.

Tane boyu, gözenek boyutu ile bunların dağılımlarındaki düzensizlikler, düzensiz kuruma hızı ve bunların sonucu olarak lületaşında çatlamalara neden olur. Malzemede çatlama sonuçlandırabilecek bir başka neden de bazı numunelerdeki yüksek sepiolit oranıdır. Bu mineralin yüksek adsorbsiyon yeteneği ile kurduğunda hızlı su kaybetmesi numunelerde iç ve dış kesimler arasında çatlama neden olan genleşme farkına neden olabilir. Çatlamanın meydana gelmediği numuneler; kırıntılar, gözenekler ve sepiolit haciminde oldukça düzenli dağılımlı olduğu, sepiolit içeriğinin çok yüksek olmadığı ve sepiolit liflerinin iyi kenetlen-
diği numunelerdir.

OLUŞUM

Yumru tipteki lületaşları, yakın çevrede magnezit yatakları içeren ultramafik kayaların yer aldığı, Neojen havzasının kenar kesimlerindeki konglomeralarda; yuvarlakköşeli veya yumru biçimli çakıllar halinde bulunurlar. (Petrascheck, 1963 a, b; Brennich, 1965; Öncel, 1971; Öncel ve Denizci, 1982; Yeniyol ve Öztunalı, 1985). Lületaşı oluşumu çevredeki magnezit yataklarından kaynaklanan bu çakıllardan, erken diyajenez evresinde, sedimentlerde tanelerarası boşluklarda dolaşım halinde olan Si^{4+} ve Mg^{2+} iyonları açısından zengin çözeltilerin magneziti ornatması sonucunda meydana gelmiştir (Yeniyol ve Öztunalı, 1985; Yeniyol, 1986).

İncelenen lületaşları, sedimentler sepiolitlerle birlikte Neojen sedimentasyonunun meydana geldiği alkali göl ortamının sığ kenar kesimleri ve buralardaki kısa ömürlü gölcüklerde kurak ve yarı kurak iklim, koşullarında çökelmişlerdir (Yeniyol, 1992). Kurak dönemlerde göl alanının daralmasıyla yüzeylenen ve kuruyan sedimentler, sonraki yağışlı dönemlerde yeniden taşınarak su ortamında kırıntılar halinde çökelmişlerdir. Bunu izleyen diyajenez evresinde sepiolit, gözeneklerindeki Si^{4+} ve Mg^{2+} açısından zengin çözeltilerden doğrudan kristallenme yoluyla meydana gelmiştir (Siffert, 1962; Wollast ve diğerleri, 1968; Singer ve Norrish, 1974; Khoury ve diğerleri, 1982; Abtahi, 1985; Yeniyol, 1992).

SONUÇLAR

Sivrihisar'ın güneyinde ve Neojen istifinin üst kesimlerinde yer alan sedimenter kökenli sepiolitlerle birlikte, lületaşı niteliğinde sepiolitik bir malzeme

yer almaktadır. Mercek biçimli ve tabakalı olan bu lületaşları, klasik yumru tipindeki lületaşlarından farklı bileşim ve doku özellikleri gösterirler. Detritik dokulu olan bu lületaşlarının bileşiminde % 50 den fazla sepiolit ve bundan daha az oranlarda da detritik kırıntılar halinde dolomit ve/veya kalsit bulunur.

Beyaz ve hafif olan bu lületaşları ıslatıldıklarında kolayca yontulabilirler ve kuruyunca çatlamazlar. Beyaz rengi, bileşimde yer alan karbonat içeriği ile ilgilidir. Malzemenin hafifliğini sepiolit ve karbonat bileşenlerin bağıl oranı yanında, özellikle bu minerallerin hacimdeki düzenleme tarzı ve bununla ilgili olarak meydana gelen porozite denetler. Sepiolit liflerinin iyi kenetlenmesi malzemeye suda dağılmama direnci ve özelliğini kazandırır. Kırıntıların çok ince boyutlu olması, bileşimin başlıca sepiolitten meydana gelmesi ve bu bileşenlerin hacimde oldukça homojen dağılım göstermesi ise kolay yontulmayı ve lekesez, beyaz, düzgün yüzey elde etmeyi sağlar.

İncelenen lületaşı, karbonat içermesi nedeniyle yumru tipindeki lületaşından biraz daha ağırdır. Ancak yataklanma tarzı, kendisinden daha kaliteli olan bu lületaşlarına göre bazı avantajlar sağlamaktadır. Bu lületaşından düşük maliyetle, daha kolay üretim yapılabilir ve daha büyük parçalar halinde malzeme elde edilebilir. Ayrıca birçok amaçlar için, kendisinden daha değerli olan yumru tipteki lületaşının yerine kullanılabilmesi mümkündür.

KATKI BELİRTME

Yazar; SEM analizleri için numunelerin kaplamalarını yapan Türkiye Şişe ve Cam Fabrikaları A.Ş. Araştırma Merkezinden Bülent Arman, bu analizlerin yapılmasına olanak sağlayan İ.T.Ü. Kimya ve Metallürji Fakültesinden Prof. Dr. Adnan Tekin ile analizlerde yardımları geçen Turgay Gönül ve Hüseyin Sezer'e içten teşekkür borçludur.

Yayına verildiği tarih, 16 Mart 1992

DEĞİNİLEN BELGELER

Abtahi, A., 1985, Synthesis of sepiolite at room temperature from SiO₂ and MgCl₂ solution: Clays and Clay Minerals, 20, 521-523.

Akıncı, Ö., 1967, Eskişehir l25 cl paftasının Jeoloji ve 82-97 tabakalı lületaşı zuhurları: MTA Derg., 68, 82,97.

Brennich, G., 1965, Eskişehirde lületaşı zuhurları: MTA., E.H.M. Rap. No. 87, Ankara.

Erentöz, C., 1975, 1:500 000 ölçekli Türkiye Jeoloji Haritası: Erentöz, der, MTA. yayl., 111, Ankara.

Galan, E. ve Castillo, A., 1984, Sepiolite-Palygorskite in Spanish Tertiary Basin; genetical patterns in continental environments: Singer A. ve Galan E., ed., Palygorskite-Sepiolite Occurrences, Genesis and Uses da, Developments in Sedimentology, 87-124.

Hay, R.L. ve Stoessell, R.K., 1984, Sepiolite in the Amboseli basin of Kenya: a new interpretation: Singer A. ve Galan E., ed., Palygorskite-Sepiolite Occurrences, Genesis and Uses da. Developments in Sedimentology, 125-136.

Khoury, H.N., Eberl, D.D. ve Jones, F.B., 1982, Origin of magnesium clays from the Amargosa Desert, Nevada: Clays and Clay Minerals, 30, 327-336.

Öncel, Z., 1971, Türkiye'de lületaşı madenciliği ve lületaşı işletmeciliği: MTA Rap., 5313, (yayımlanmamış), Ankara.

— ve Denizci, F., 1982, Eskişehir Bölgesi lületaşı ve magnezit etüdüleri raporu: MTA Rap., 7181, (yayımlanmamış), Ankara.

Petrascheck, W.E., 1963a, Eskişehir civarında bulunan lületaşı ve magnezit: MTA. Rap., 3441/A, (yayımlanmamış), Ankara.

— 1963b, Eskişehir civarında bulunan lületaşı yatakları: MTA. Rap., 3441/B, (yayımlanmamış) Ankara.

Schultz, L.G., 1964, Quantitative interpretation of mineralogical composition from x-ray and chemical data for the Pierre Shale: Geol. Survey Prof. Paper, 391-C.

Siffert, B., 1962, Quelques réactions de la silice en solution; La formation des argiles: Mém. Serv. Carte Geol. Alsace-Lorraine, 21, 100 p.

Singer, A. ve Norrish, K., 1974, Pedogenic palygorskite occurrences in Australia: Amer. Mineral., 59, 508-517.

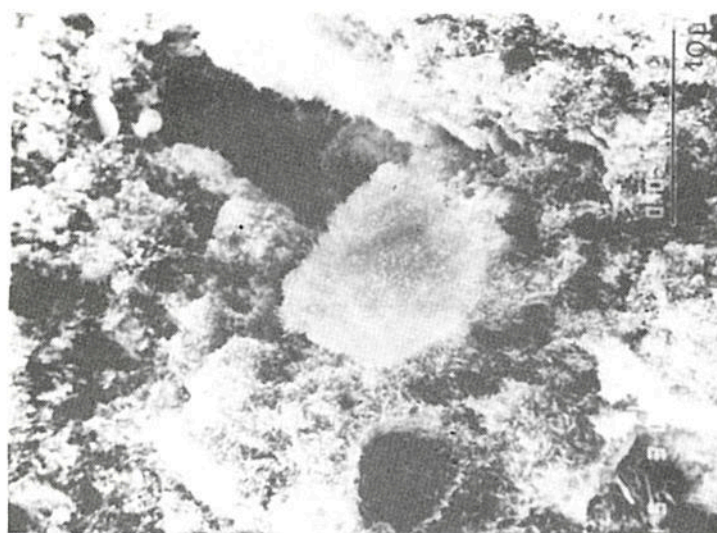
Stoessel, R.K. ve Hay, R.L., 1978, The geochemical ori-

- gin of sepiolite and Kerolite at Amboseli, Kenya: Contrib. Mineral. Petrol, 65, 255-267.
- Wollast, R., Mackenzie, F.T. ve Bricker, D.P., 1968, Experimental precipitation and genesis of sepiolite at earth surface conditions: Amer. Mineral., 53, 1645-1661.
- Yenişol, M., 1982, Yunak (Konya) magnezitlerinin oluşum sorunları, değerlendirilmeleri ve yöre kayaçlarının petrojenezi: İstanbul Yerbilimleri, 3, 21-51.
- 1986, Vein-like sepiolite occurrence as a replacement of magnesite in Konya, Turkey: Clays and Clay Minerals, 34, 353-346.
- 1992, Yenidoğan (Sivrihisar) sepiolit yatağının jeolojisi, mineralojisi ve oluşumu: MTA Derg., 114, 71-84.
- ve Öztunalı, Ö., 1985, Yunak sepiolitinin mineralojisi ve Oluşumu: Gündoğdu, M.N. ve Aksoy H., ed., II Ulusal Kil Sempozyumu bildiriler kitabında, Bizim Büro Basımevi, Ankara, 171-186.
-

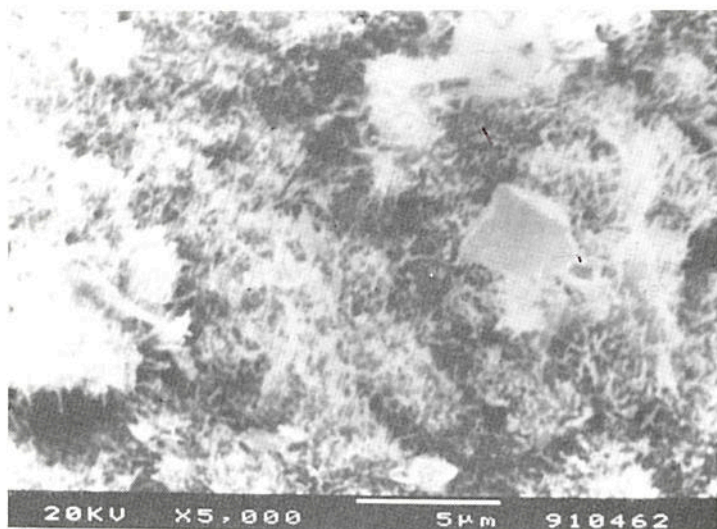
LEVHALAR

LEVHA-I

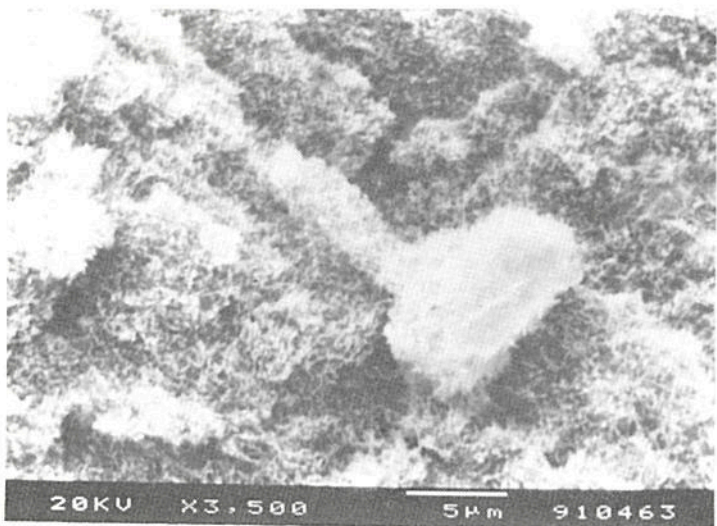
Şek.1, 2, 3- Yenidoğan Köyünden alınan Ss-5 numunesinin tarama elektron mikrografları.



1



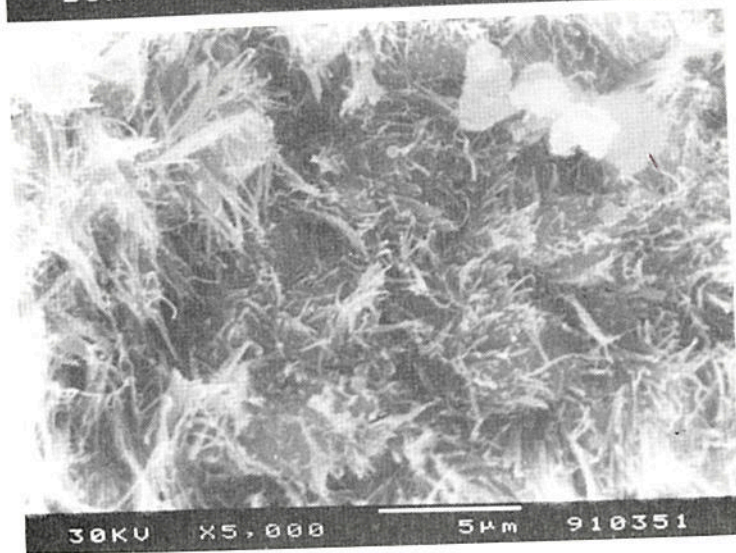
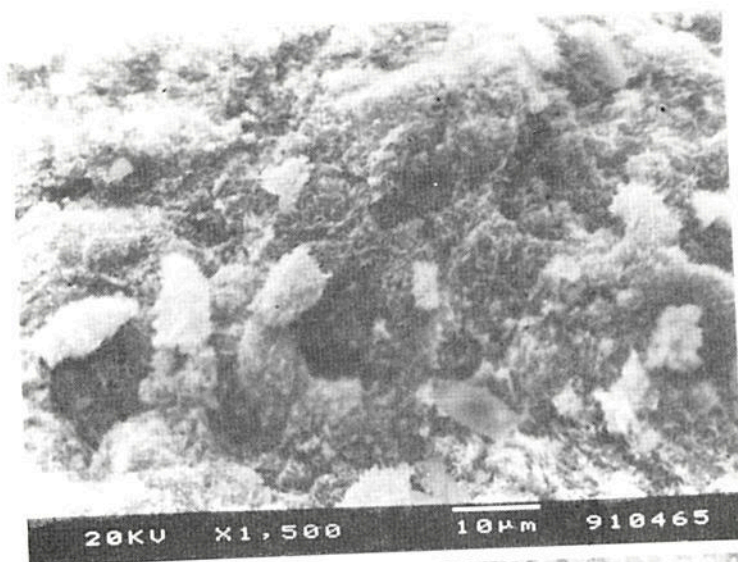
2



3

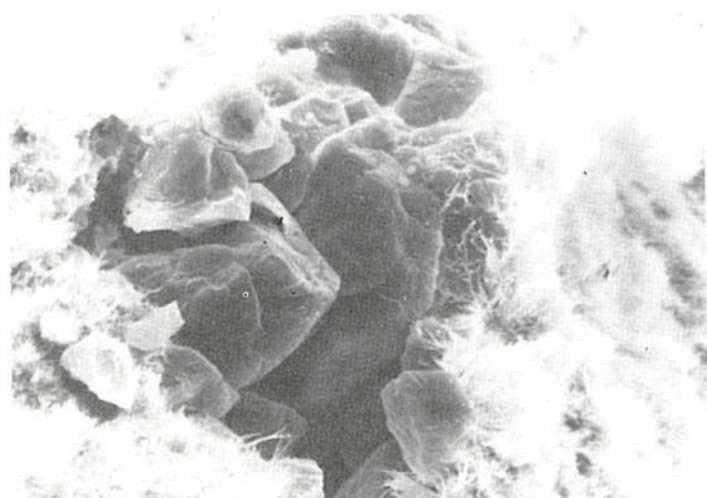
LEVHA-II

- Şek. 1- Keremliöz'den alınan KY-2/3 numunesinin tarama elektron mikrosrafı.
- Şek. 2, 3 - Keremliöz'den alınan KY-15/2 numunesinin tarama elektron mikrosrafları.



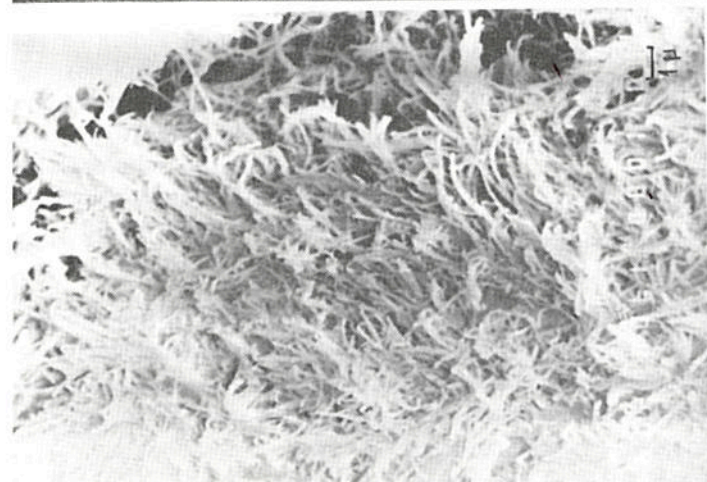
LEVHA-III

- Şek. 1- KY-15/2 numunesinin tarama elektron mik-
rografı.
- Şek. 2, 3 - Yumru tipinde bir lületaşının tarama elektron
mikrografı.

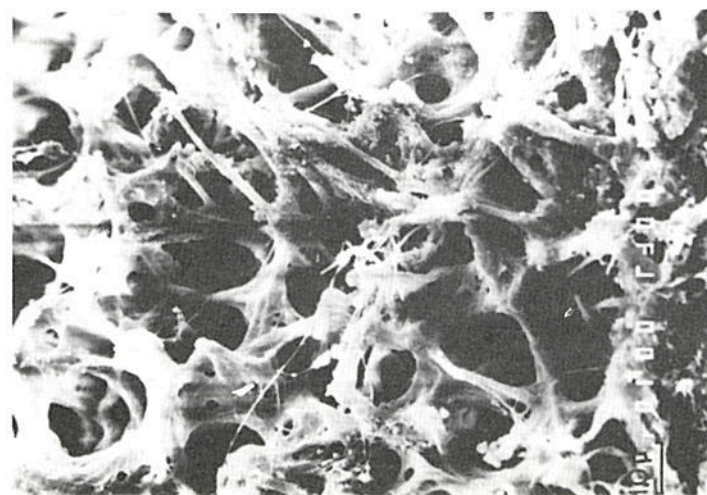


1

20KV X2,000 10µm 910354



2



3

BEYPAZARI-ÇAYIRHAN LİNYİTLERİ HÜMİK ASİTLERİNİN IR-SPEKTROFOTOMETRİK İNCELENMESİ

Gültekin KAVUŞAN*

ÖZ_ Beypazarı-Çayırhan linyit havzasında Davutoğlan ve Kuzey fayları en önemli tektonik kırıklardır. Havzada alt horizonta dar yayımlı tek bir damar, üst horizonta ise toplam kalınlığı ortalama 3 m olan iki linyit damarı mevcuttur. Bölgede yapılan ve faylara dik doğrultudaki sondajlarda kesilen alt ve üst damar horizonlarına ait linyit örneklerinden tane boyu 0.25-0.70 mm arasında kalanlardan, $ZnCl_2$ çözeltisi ($d=1.44-1.50 \text{ gr/cm}^3$) kullanılarak hüminit grubu maseralleri ayrılmışlardır. Bu maserallerce zenginleştirilmiş örnekler KOH (% 5) ile muamele edildikten sonra hümik asitler, çözeltiden konsantre HCl yardımıyla çöktürülmüştür. Elde edilen hümik asitler IR-spektrofotometresinde incelenmişlerdir. van Krevelen diyagramlarında damarların H/C oranlarının gömülme derecelerine bağlı olarak arttığı ve benzer biçimde Davutoğlan fayına yakın olan sondaj örneklerinin H/C-O/C değerlerinin, damar ortalama değerlerinden yüksek olarak yer aldıkları görülmüştür. Bu kömürleşme derecesinin artması, Davutoğlan fayının doğurduğu ısı ve tektonik basıncın artmasına bağlıdır. Örneklerde yapılan IR-spektrofotometrik incelemelerde, $1600-1620 \text{ cm}^{-1}$ bantında yoğun bir aromatikleşme olduğu, $>C=C<$ bağlarının hümik asitlerin yapısında buldukları, $2800-3000 \text{ cm}^{-1}$ bantındaki absorpsiyona dayanarak yine hümik asitlerin yapısında simetrik ve asimetrik CH_2 ve CH_3 gruplarının yer aldıkları saptanmıştır.

GİRİŞ

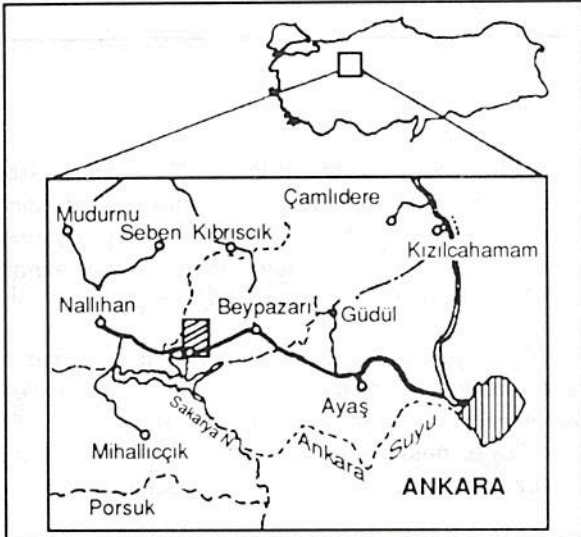
Beypazarı-Çayırhan bölgesinde alt ve üst damar horizonu olarak iki kömür horizonu bulunmaktadır. Alt damar horizon kalınlığı 1.30-11.15 m arasında değişir. Üst damar horizonu ise alt damar horizonunun ortalama 150 m üzerinde yer alır ve iki damardan oluşmuştur. Damarlar ortalama olarak 1.50-2.50 m arasında değişmektedir. Arada bulunan arakesme kalınlığı 1.00 ile 10.00 m arasında değişir.

Bölgedeki en önemli kırıklar Davutoğlan ve Kuzey faylarıdır. (Şek. 1). Davutoğlan fayı bir bindir-

me fayı, Kuzey fayı ise sondajlar civarında gravite fayı olarak gözlenir. Davutoğlan fayının atımı 70-110 m arasında değişir. Kuzey fayının atımı, doğuda 20, m den daha fazladır (Aslan, 1975; Siyako, 1983; Yağmurlu ve diğerleri 1988; Kavuşan, 1991, 1993).

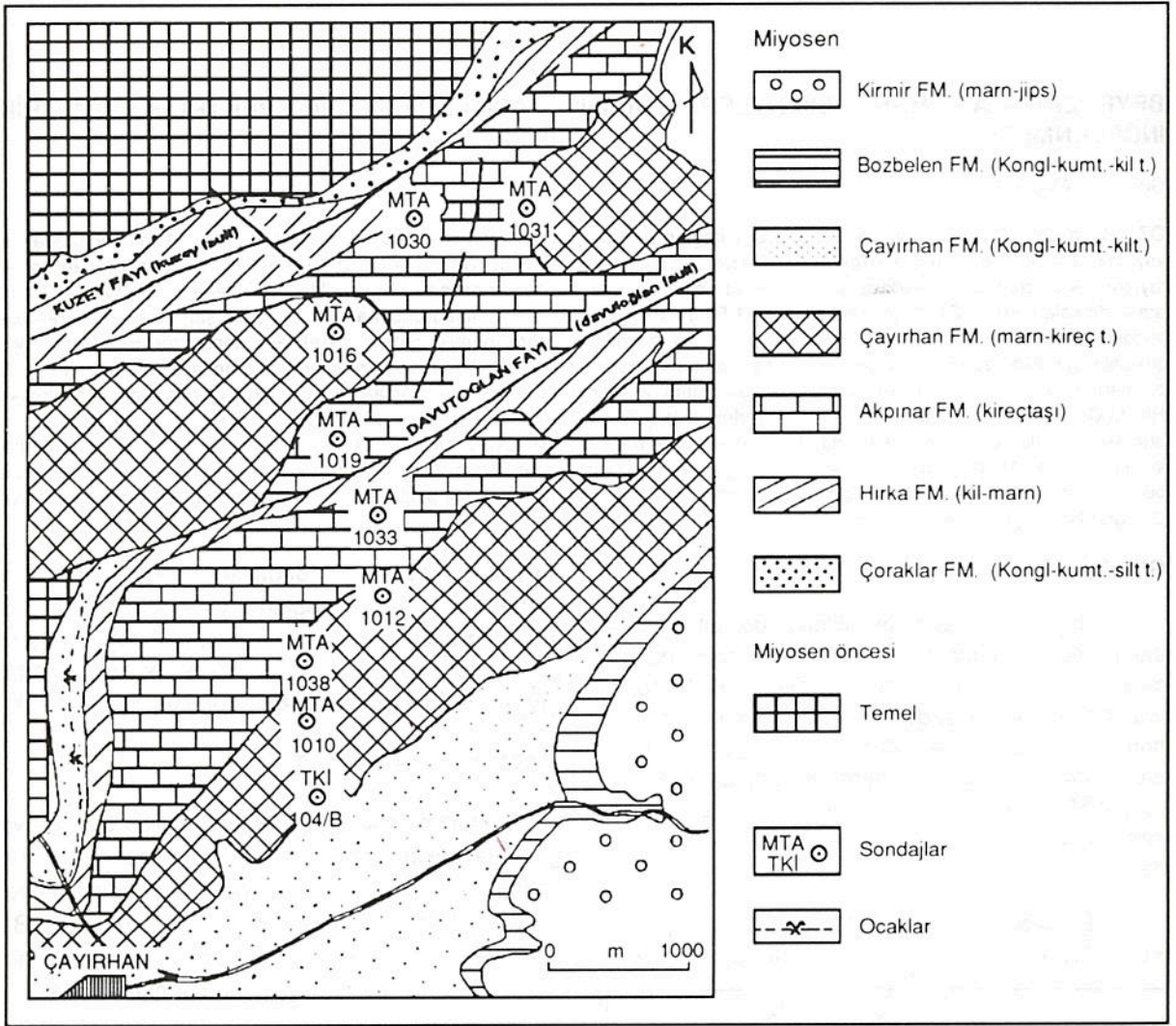
MATERYAL ve METOT

Hüminit maseralı, gerek homojen bileşimi ve gerekse kökeni itibariyle tüm havzadaki kömürün özelliklerini daha iyi bir şekilde ortaya koyabileceği için araştırmanın materyalini oluşturmuştur. Bu özellikleri nedeniyle öncelikle hüminit maserallerinin kazanılması ve bunun üzerinde elementer analizlerin yapılması ve strüktürel yapının araştırılması öngörülmüştür. IR-spektrofotometrik metodun seçilmesinin temel nedeni, numunelerin organik moleküler strüktürlerinin parçalanmadan incelenmesine olanak tanınmasıdır. Zira herhangi bir şekilde farklı metodun, örneğin gaz kromatografisi gibi, seçilmesi halinde, parçalanmış moleküler yapıdaki yan grupların farklılaşmalarının ortaya konulması zorlaşacaktır. Bu durumda ise, moleküler yapıdaki farklılaşmaların ortaya konulabilmesi ortadan kalkacaktır. Bu nedenle, numunelerden mümkün olduğunca fazla hüminit kazanılması, hümik asitlerin fazla deformasyona uğramadan doğrudan doğruya IR-spektrofotometresinde incelenerek moleküler gruplardaki dağılımlarının gözlenmesine çalışılmıştır.



Şek. 1a- Lokasyon haritası.

* Ankara Üniversitesi, Fen Fakültesi, Jeoloji Mühendisliği Bölümü, Ankara.



Şek. 1b- Jeoloji ve Sondaj lokasyon haritası.

NUMUNELERİN HAZIRLANMALARI

Bölgede yapılmış olan sondajlardan alınan kömür karotları laboratuvarda kırıldıktan sonra elenmişlerdir. Kırma ve eleme işlemlerinde hüminitlerin en fazla serbestlendikleri tane boyu aralığı araştırılmış ve 0.25-0.71 mm arasında ortalama olarak en fazla serbestlenmenin gerçekleştiği saptanmıştır. Bu tane boyutu aralığındaki kömür örneklerinden hüminit maserallerinin diğer maserallerden ayrılması ve kazanılabilmesi için yoğunluk esasına göre ayrımı yapılması amacıyla, bu maserallerin en fazla zenginleştikleri yoğunluk aralığı denemelerle araştırılmıştır. En fazla hüminit maserali zenginleşmesi $1.44 < d < 1.50 \text{ gr/cm}^3$ olarak sap-

tanmıştır. Yoğunluk ayrımı için ZnCl_2 çözeltisi kullanılmıştır. Bu sonuçlardan sonra, yüzdürme-batırma esasına göre çalışan bir ön zenginleştirme ünitesi hazırlanmış ve tüm sondajlardan alınan kömür örnekleri bu sistemden geçirilmiştir.

Bu şekilde kazanılmış olan ve hüminit maserallerince zengin numunelerin C, H, N, S analizleri yapılmış ve oksijen içerikleri $O=100-(C+H+N+S)$ formülüyle hesaplanmıştır. Analiz sonuçları kuru külsüz kömür bazında Çizelge 1 de gösterilmiştir.

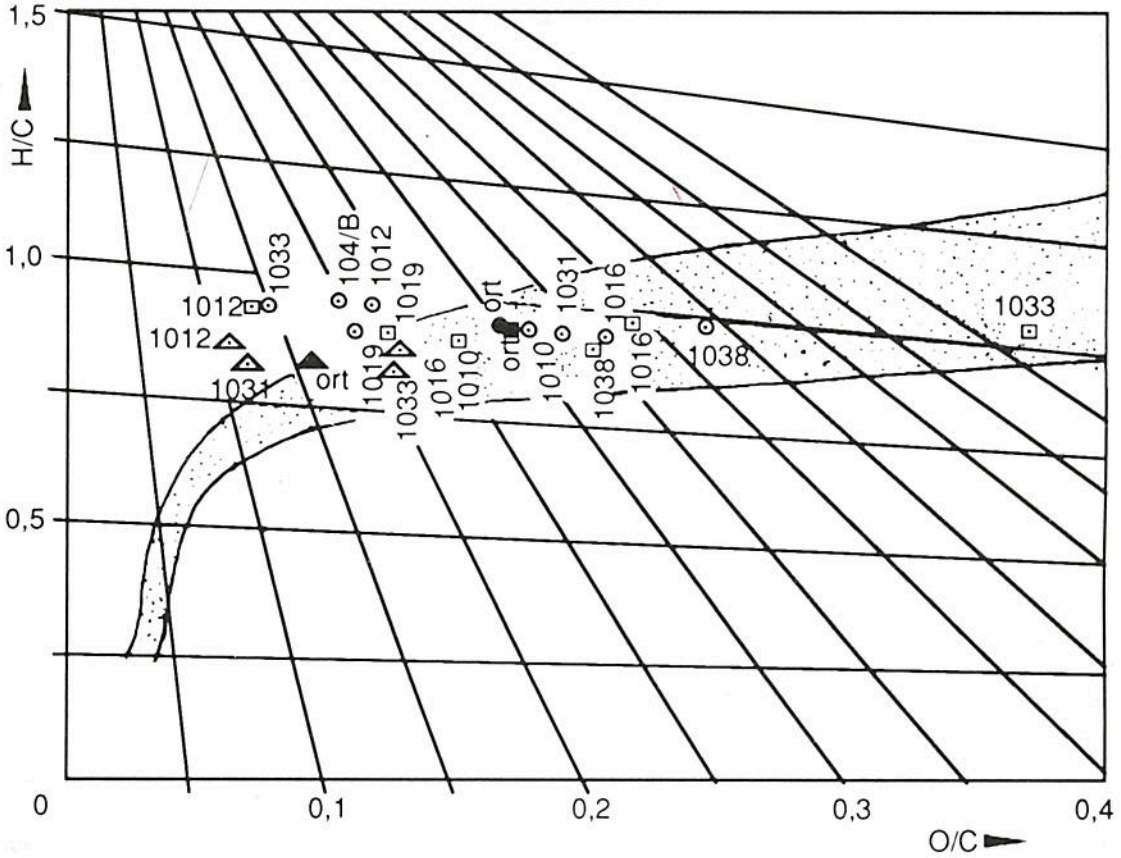
Kazanılan bu zenginleştirilmiş numuneler 100 mikron boyutuna kadar öğütülmüşler ve daha sonra her numuneden 1 gr alınarak % 10 luk (v/v)

potasyum hidroksit (KOH) ile muamele edilmişlerdir. 12 saat süre bekletildikten sonra porselen filtreden geçirilmiştir. Filtreden geçen hümik asit tuzları, % 5 lik (v/v) hidroklorik asit (HCl) ile asitlendirilmiştir. Asitleme işleminden sonra bu ortamda koloidal halde çöken hümik asit ve türevlerince zengin olan kısım 5 dakika boyunca 2000 d/d santrifüjasyona tabi tutularak hümik asitler kazanılmıştır. Hümik asit kazanılması işlemi santrifüjasyon sonunda berrak çözelti kalıncaya kadar uygulanmıştır. Elde edilen hümik asitli tortu 50°C de 4 saat süreyle etüvde bekletilerek kurutulmuştur. Daha sonra spektrofotometrik saflıktaki potasyum bromür (KBr) ile preslenerek IR-tabletleri elde edil-

miştir. IR-spektrumları, Perkins-Elmer/Unicam marka infrared spektrofotometresinde alınmıştır.

HÜMİNİTLERİN C, H, O, N, S İÇERİKLERİ VE DAĞILIMLARI

Hümitiçe zenginleştirilmiş olan örneklerin tespit edilen C, H, N, S içerikleri değerlerinden yararlanılarak oksijen içerikleri $O=100-(C+H+N+S)$ formülüyle hesaplanmıştır. Bu değerlerden yola çıkılarak, O/C, H/C, N/C atomik oranları hesaplanıp alt ve üst horizonun her bir seviyesi için H/C-N/C oranları diyagramları çizilmiştir (Şek. 3). Ayrıca O/C ve H/C değerleri van Krevelen diyagramlarına aktarılmıştır (Şek. 2).



▲ Alt damar horizonu

○ Üst horizon-Alt kömür damarı

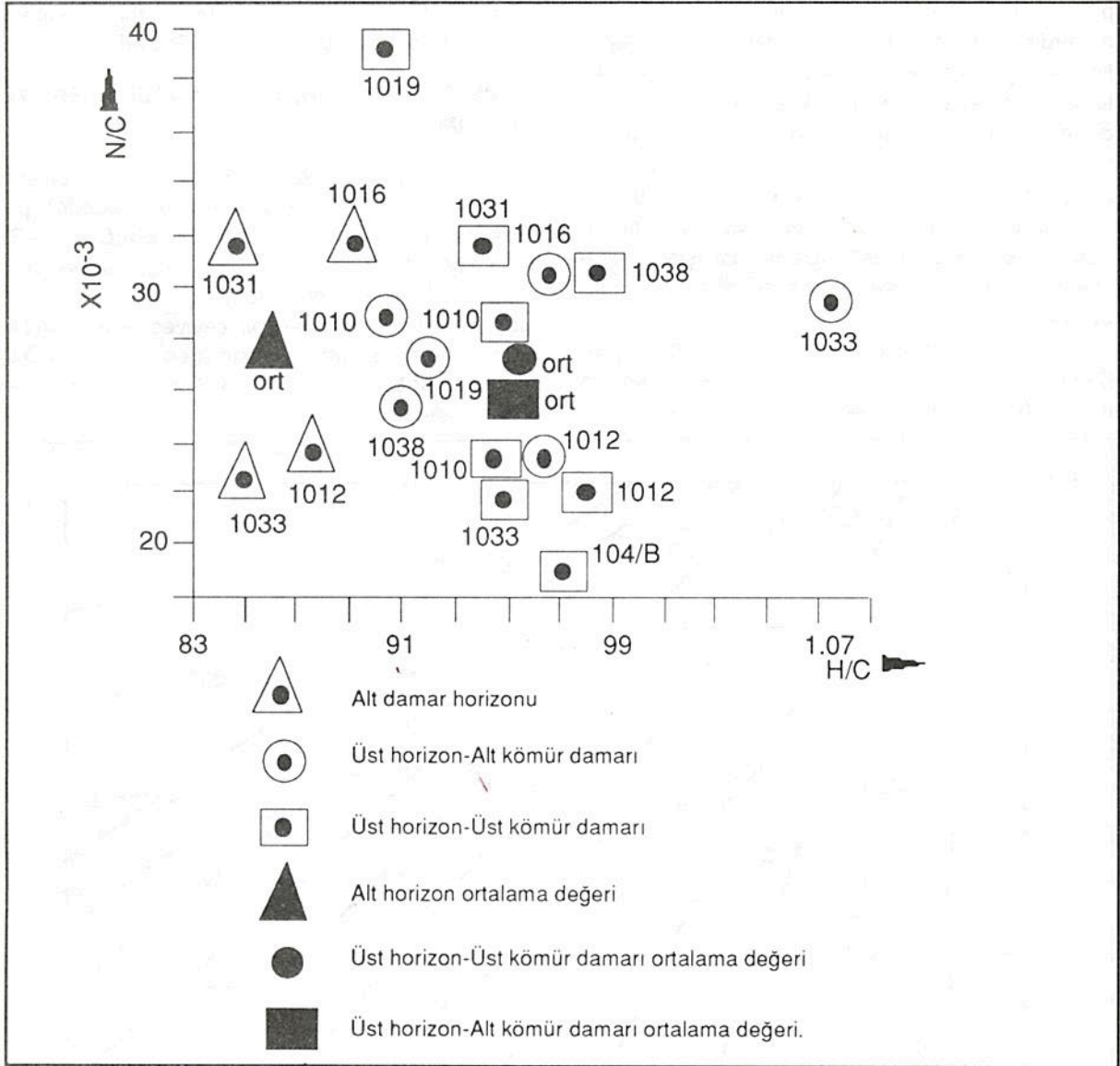
□ Üst horizon-Üst kömür damarı

▲ Alt horizon ortalama değeri

● Üst horizon-Üst kömür damarı ortalama değeri

■ Üst horizon-Alt kömür damarı ortalama değeri

Şek. 2- van Krevelen diyagramı.



Şek. 3- Kömür damarları atomik N/C ve H/C diyagramı.

Bölgedeki linyit damarlarından alt damarın kuru külsüz kömür bazında karbon oranı ortalama olarak % 72.56; hidrojen oranı % 5.21 ve toplam kükürt oranı ise % 4.32 tür. Alt damar horizonu havza bazında üst damara nazaran dar bir alanda yayılmıştır (Yağmurlu, 1988; Kavuşan, 1991, 1993). Alt damar horizonu tüm havzada tipik bir akarsu kanallarınca zengin flüvyatil bataklık ortamında oluşmuş olması nedeniyle, kül oranındaki değişimleri daha fazladır (Siyako, 1983; Yağmurlu, 1988; Kavuşan, 1991, 1993). Üst damar horizonu

damarları çok geniş bir alana yayılmışlardır. Daha düzenli ve homojen bir bataklık ortamında gelişmişlerdir (Arslan, 1975; Siyako, 1983; Yağmurlu, 1988; Kavuşan, 1991, 1993). Bu düzenli ve homojen yayılımdan dolayı analizlerde sık sık değişimler gözlenmemesine rağmen bazen sapmalara rastlanabilmektedir. Bununda muhtemelen paleoturbierinin ana dağıtım kanallarının yakınına tesadüf eden sondajlarda olduğu düşünülebilir. Üst damar horizonunun kuru külsüz bazda karbon oranı ortalama olarak % 63.34, hidrojen oranı ise % 5.02 ve kükürt oranı ise % 4.96 tir (Çizelge 1).

Alt damar horizonunun kuru külsüz bazda karbon oranı üst damar horizonundan daha yüksektir. Fakat hidrojen, kükürt ve azot oranlarının her iki horizonta da birbirine yakın değerlere sahip oldukları görülür (Çizelge 1).

Çizelge 1_ Ortalama analiz değerleri (Kuru külsüz bazda)

SONDAJ NO	C, %	H, %	N, %	S, %
ALT DAMAR HORIZONU				
MTA 1012	79.23	5.73	2.12	1.55
MTA 1033	69.23	4.91	1.81	4.23
MTA 1016	67.00	4.98	2.45	6.27
MTA 1031	74.78	5.24	2.67	5.21
ORTALAMA	72.56	5.21	2.26	4.32

ÜST HORIZON-ALT LİNYİT DAMARI

TKI 104/B	69.10	5.57	1.50	5.50
MTA 1010	63.97	5.02	1.69	3.16
MTA 1038	55.96	4.58	1.97	5.04
MTA 1012	66.70	5.45	1.70	6.70
MTA 1033	70.55	5.58	1.79	7.66
MTA 1019	67.75	5.10	3.08	6.41
MTA 1016	58.02	4.56	1.89	7.82
MTA 1031	60.38	4.74	2.17	1.88
ORTALAMA	64.05	5.08	1.97	5.52

ÜST HORIZON-ÜST LİNYİT DAMARI

MTA 1010	66.59	4.98	2.24	2.67
MTA 1038	61.79	4.70	1.81	3.17
MTA 1012	70.25	5.59	1.90	8.78
MTA 1033	48.23	4.30	1.64	6.85
MTA 1019	68.92	5.26	2.16	3.07
MTA 1016	59.95	4.89	2.07	1.88
ORTALAMA	62.62	4.95	1.97	4.40
ORT. ÜST HORIZ.	63.34	5.02	1.97	4.96

van KREVELEN DİYAGRAMLARININ DEĞERLENDİRİLMESİ

Bölgedeki linyit damarlarında yapılmış olan vitrinit refleksiyon ölçümlerinde alt damarın 0.44 R_{moil}; üst damarın ise 0.39-0.41 R_{moil} arasında değişen değerler gösterdiklerinden alt damarın daha ileri bir derecede kömürleşme aşamasına ulaştıkları saptanmıştır (Kavuşan, 1993). Her iki horizon arasında ortalama 150 m kalınlığında bir sedimanter birimin bulunması; diğer bir ifadeyle alt horizonun üst horizonta 150 m daha derine gömülmüş olması, refleksiyon değerlerinde bariz bir artma olarak saptanmıştır (Kavuşan, 1991, 1993).

Bu sedimanter istifin doğurduğu litostatik basıncın artışı yanında, bölgedeki tektonik kuvvetlerin etkisinde katkıları vardır. Fiziksel parametrelere bağlı olarak saptanan bu refleksiyon değerleri artışlarının nedeni, hüminit maserallerinde kimyasal yapının değişimiyle ve buna bağlı olarak göreceli karbonca bir zenginleşmeyle doğrudan bağlantılı olması gerekir. Bu nedenle huminit refleksiyonlarının ölçüldüğü aynı örneklerden yapılan analizlere dayanılarak van Krevelen diyagramları hazırlanmıştır.

Alt damar horizonu örneklerinin sayılarının az oluşundan dolayı kesin bir yorum yapılamamasına rağmen, faylara yakın olan MTA-1033 ve MTA-1012 örneklerinin diğer örneklerden ve ortalama damar değerinden yüksek bir değere ulaştıkları gözlenir. Bu da göreceli olarak karbonca zenginleşmeyi işaret etmektedir (Şek. 2).

van Krevelen diyagramında, üst horizonunun alt damarında MTA-1033, MTA-1012 ve MTA-1019 sondaj örneklerinde bariz bir sıçrama gözlenmektedir (Şek. 2). MTA-1038 örneğinin karbonca fakir olmasından dolayı, bu örneğin değerlendirme dışı tutulması gereklidir. Davutoğlan fayının kuzey ve güneyinde yer alan ve faya en yakın olan MTA-1019 ve MTA-1033 örneklerinde göreceli olarak bir karbonca zenginleşmeden bahsetmek mümkündür. MTA-1012 ve TKI 104/B örneklerinde gözlenen göreceli zenginleşme ise Davutoğlan fayının güneyinde bulunan fakat yüzeye ulaşmamış olan kırıklanmanın ürünüdür. Bu kırıklanmadan başka, ayrıca buradaki galerilerde üst kömür damarlarında sürüklenmeler de gözlenmiştir.

Üst horizonun üst seviyesinde ise, MTA-1033 ve MTA-1016 örneklerinin karbonca fakir olmalarından dolayı sapma göstermektedir. MTA-1012 ve MTA-1019 örnekleri burada bir sıçrama olarak ortaya çıkmakta olup bununda Davutoğlan fayı ile bunun güneyinde uzanan, kırığı yeryüzüne ulaşmamış olan faylara bağlı olduğu anlaşılmaktadır.

Her damarın ortalama değerlerine bakıldığında alt damar horizonunun, üst damar horizonunun ortalama değerlerinden bariz bir sıçrama yaptıkları gözlenir. Bununda nedeni daha önce belirtilmiş olan 150 m kalınlığındaki sedimanter birime karşılık gelen gömülme derinliğidir.

Genel olarak ele alındığında, Davutoğlu ve güneydeki kırıklanma sonucunda ortaya çıkan enerjinin daha etkin olduğu alanlardaki örneklerin, göreceli olarak daha karbonca zenginleştiklerini göstermektedir.

INFRARED ANALİZLERİNİN DEĞERLENDİRİLMESİ

Beypazarı-Çayırhan linyitlerinden hazırlanan hüminit maseralince zenginleştirilmiş numunelerden elde edilen hümik asitlerin infrared spektrum-

larının göze çarpan piklerinin dalga sayıları Çizelge 2 de verilmiştir. Gerek alt damar horizonunun gerekse üst damar horizonunun örneklerinde hümik asitlerin 1600-1620 cm^{-1} , 2840-2850 cm^{-1} , 2920 cm^{-1} ve 3380-3430 cm^{-1} de pikler verdikleri görülmüştür. 1600-1620 cm^{-1} bantındaki absorpsiyon diğer bantlardaki absorpsiyonlardan daha belirgin olup hümik asitlerin yoğun bir aromatik yapıda olduklarını ortaya koymaktadır. Bu aromatik yapıdaki $>\text{C}=\text{C}<$ bağlarının, bu bölgede pikler verdikleri bilinmektedir.

Çizelge 2- Infrared spektrum dalga sayıları tablosu (cm^{-1})

ALT DAMAR							
			SJ 1012	SJ 1033		SJ 1016	SJ 1031
						1430	1445
			1620	1610		1625	1605
			2850	2840		2840	2840
			2920	2920		2910	2920
			3400	3400		3420	3420
ÜST HORIZON-ALT LINYİT DAMARI							
SJ 104 B	SJ 1010	SJ 1038	SJ 1012	SJ 1033	SJ 1019	SJ 1016	SJ 1031
	1290						
1450	1420	1430	1450	1450	1440	1460	1440
1610	1620	1610	1610	1620	1610	1600	1610
2840	2850	2850	2840	2840	2845	2850	2845
2920	2910	2910	2920	2920	2920	2920	2920
3400	3380	3380	3380	3420	3360	3390	3400
ÜST HORIZON-ÜST LINYİT DAMARI							
	SJ 1010	SJ 1038	SJ 1012	SJ 1033		SJ1016	
	1290						
	1430	1440	1420	1430		1420	
	1620	1610	1630	1620		1610	
	2850	2840	2840	2850		2840	
	2930	2920	2920	2920		2920	
	3380	3400	3380	3430		3430	

2800-3000 cm^{-1} bandı simetrik ve asimetric CH_2 ve CH_3 gerilme titreşimleriyle ilişkilidir. Bu bantlardaki vibrasyonlar aromatik strüktüre bağlı olarak bulunan CH_2 ve CH_3 gruplarının varlığını ortaya koymaktadır. 3400 cm^{-1} vibrasyonu aromatik strüktüre bağlı olan OH gruplarından kaynaklanmaktadır.

1440-1460 cm^{-1} vibrasyonu bazı örneklerde ortaya çıkmaktadır. Bu pik bazı hümitik asitlerin aromatik yapılarında sübstitite aromatik halkaların bulduklarına işaret sayılabilir.

SONUÇLAR

Bey pazarı-Çayırhan havzasında bulunan iki kömür horizonunda gömülme derinliklerine bağlı olarak alt horizonun daha ileri derecede bir kömürleşme evresine ulaştıkları van Krevelen diyagramında gözlenmektedir. Gömülme derinlikleriyle damarların ortalama O/C-H/C değerleri arasında doğru orantılı ilişki vardır.

Bey pazarı-Çayırhan havzasında Davutoğlan bindirme fayının kompresyon enerjisinin serbestlenmesi sonucunda, özellikle üst damar horizonunun kömür damarlarının faya yakın olan örneklerinde, göreceli olarak karbonca bir zenginleşmenin sözkonusu olduğu anlaşılmaktadır.

Hüminitlerin IR-spektrumlarından 1600-1620 cm^{-1} bandındaki absorpsiyon belirgin olup, hüminitlerin yoğun bir aromatik strüktüre sahip oldukları anlaşılmaktadır. Bu band aromatik strüktürde mevcut $>\text{C}=\text{C}<$ bağlarının gerilme titreşimlerine bağlıdır. 2800-3000 cm^{-1} bandının varlığı ise, yapıda CH_2 ve CH_3 gruplarının bulduklarını göstermektedir. Bölgede tektonizmaya bağlı olarak göreceli bir farklılaşmanın tespit edilebilmesine karşılık, aynı örneklerin IR-spektrumlarında elde edilen piklerde bariz bir farklılaşma saptanamamıştır. Oldukça karmaşık ve büyük molekül ağırlıklı olan hümitik asitlerin yan gruplarında çok belirgin bir moleküler transformasyon saptanamamıştır. van Krevelen diyagramlarıyla birlikte ele alındıklarında, kömürleşme sürecindeki basınç artışının, aromatisasyonun artmasını sağlayabildiği ifade edilebilir.

KATKI BELİRTME

Bu çalışmada MTA Genel Müdürlüğü Enerji Hammaddeleri Dairesi kömür servisinin, TKİ Orta Anadolu linyit işletmesinin numunelerin temin edilmesinde gösterdikleri ilgiye teşekkür ederim. Bu çalışma Ankara Üniversitesi araştırma fonu tarafından 85-01-01 kodlu proje olarak desteklenmiştir.

Yayına verildiği tarih, 29 Mayıs 1992

DEĞİNİLEN BELGELER

- Arslan, Y., 1975, Nallıhan-Çayırhan linyit sahasının jeolojisi. 85 s. Yüksek Müh. Tezi. A.Ü.FenFak. (Yayımlanmamış), Ankara.
- Bellamy, L.J., 1954, The Infra-red Spectra of Complex Molecules. 323 s. Methuen&Co. Ltd. Newyork.
- Degens, E.T., 1968, Geochemie der Sedimente. 282 s. Ferdinand-Enke Verlag. Berlin.
- Francis, W., 1961, Coal, its formation and composition. 806 s. Edward Arnold Publ. Comp. London.
- Hummel, O.D., 1966, Infrared Spectra of Polymers. 207 s. Interscience Publishers. Newyork.
- Kavuşan, G., 1991, Bey pazarı-Çayırhan linyitlerindeki C, H, N, S, O dağılımları ve IR-spektrofotometrik araştırılması, tektonik ile değişimleri. A.Ü. Araştırma fonu raporu. 60 s. (Yayımlanmamış), Ankara.
- , 1993, Bey pazarı-Çayırhan linyitlerinin vitrinit refleksiyonları ile tektonizma ilişkileri. Suat Erk Jeol. Simp. Tebliği. A.Ü. Fen Fak.357-363. Ankara.
- Kortüm, G., 1962, Kolorimetrie Photometrie und Spektrometrie. 464 s. Springer Verlag. Berlin.
- Siyako, F., 1983, Bey pazarı kömür havzasının jeolojisi MTA Gen. Müd. Derleme raporu. (Yayımlanmamış), Ankara.
- Sharkey, E.G. ve Mc Cartney, J.T., 1981, Physical Properties of Coal and Its Products. 159-281.in: Chemistry of Coal Utilisation. Ed: Elliot. M.A. John Wiley Inc. Newyork.

Stevenson, F.J. ve Butler, J.H.A., 1969, Chemistry of Humic Acids and Related Pigments. 534-556 in: Organic Geochemistry. Editors: Eglinton, G & Murphy, M.T.J. Springer Verlag. Berlin.

van Krevelen, D.W., 1961, Coal, typology, chemistry, physics, constitution. 495 s. Elsevier Publ. Comp. Newyork.

Yağmurlu, F.; Helvacı, C. ve İnci, U., 1988, Depositional setting and geometric structure of the Beypazarı lignite deposits, Central Anatolia, Turkey. 337-360 s. Int. Journ. of Coal Geology. Vol: 10. Elsevier Publ. Comp. Newyork.

AN EXAMPLE TO SEPIOLITE FORMATION IN VOLCANIC BELTS BY HYDROTHERMAL ALTERATION: KIBRISCIK (BOLU) SEPIOLITE OCCURRENCE

Taner İRKEC* and Taner ÜNLÜ**

ABSTRACT— Geological, mineralogical and chemical properties of a sepiolite occurrence, located in the south of Kibriscik township of Bolu Province, northcentral Turkey, have been investigated in detail, and new mineralogical data have been obtained. Differing from the sedimentary sepiolite deposits, mostly associated with the carbonate/evaporite sequences, Kibriscik sepiolite occurs in the Köroğlu (Gallatian) Volcanic Belt, and has formed by the hydrothermal alteration of the vitric tuff unit of Middle Miocene aged Deveören Volcanites. The mineral, which shows a similar XRD pattern to sepiolite, gives DTA and IR patterns with close resemblance to those of palygorskite, in addition to its chemical composition with rather high alumina content. There are indications of monoclinical symmetry, determined by XRD, and it is thought to be possible that the material represents a new mineral phase.

INTRODUCTION

Kibriscik sepiolite occurrence is located at the Uşakgöl yaylası (plain) district, about 25 km south of the Kibriscik town, 70 km southeast of Bolu Province. The mineralization is included within the Bolu H27 b3 topographic map sheet.

The investigated area is located within the Köroğlu Volcanic Belt, formerly recognized as the "Gallatian Massif", on the treshold between Central Anatolia and Western Black Sea regions. Elevation of the area ranges around 1000-1900 m. Kibriscik-Beypazarı road crosses the investigated area approximately in the north-south direction (Fig. 1).

Geological investigations carried out around the study area may be stated in chronological order as; Leonhard (1903), Milch (1903), Chaput (1931), Stchepinsky (1942), Blumenthal (1948), Erol (-1-952, 1954), Rondot (1956) and, more recently Türkecan et. al. (1991). In the study of Türkecan et. al. (1991), stratigraphy of a wide area, bordered by Seben-Gerede (Bolu Province), Güdül-Beypazarı (Ankara province) and Çerkeş-Orta-Kurşunlu (Çankırı province) has been outlined, and geological mapping in 1:25 000 scale has been realized.

The occurrence was discovered during the ceramic raw materials exploration program of MTA in 1988, and reported by İrkeç and Kırkoğlu (1989). In later years, 1:25 000 and 1:5 000 scale geologi

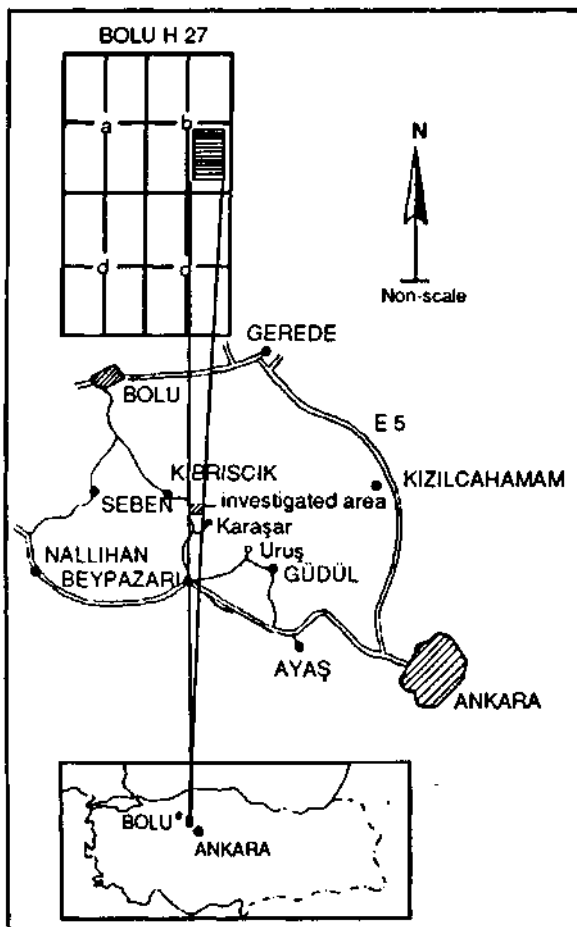


Fig. 1- Location map of the investigated area.


Erathem	System	Series	Stage	Group	Formation Member	Symbol	Thickness (m)	Lithology	Lithological Explanation	FOSSIL CONTENT			
C A I N O Z O I C	Quaternary	PLIOCENE			İlgaz Fm.	Qal	25		Alluvium				
						Tpi	~ 200 m		İLGAZ FM. (Tpi): Thick bedded, gray colored conglomerate, sandstone, siltstone, occasional tuff and claystone	Mimamys sp. Micromys sp.			
	T E R T I A R Y	M I O C E N E	Upper		K Ö R Ö Ğ L Ü G R O U P	Hüyükköy Fm.	Tmkhü		HÜYÜKKÖY FM. (Tmkhü): Tuff, tuffite, limestone, conglomerate, sandstone, siltstone, marl	Planorbarius sp.			
						İlıcadere Volcanites	Deveören Volcanites	Bakacaktepe Volcanites	Tmkb	~ 700 m	⑤	BAKACAKTEPE VOL. (Tmkb): Gray beige-black colored andesite-dacite, lava, tuff, agglomerate	Eumyanion sp. Mirabella sp. Sayimys sp. Desmanodan sp.
											④	DEVEÖREN VOL. (Tmkd): Gray-green black colored basaltic and andesitic lava, white tuff	
											③	İLİCADERE VOL. (Tmki): Gray-black-brown colored, massive basaltic and andesitic lava, agglomerate	
											②	ULUDERE PYR. (Tmku): Andesitic-dacitic, occasional rhyolitic tuff, agglomerate, volcanic breccia	
											①	HİRKA FM. (Tmkh): Sandstone, claystone, shale, tuffite. Silica bands and coal seams. Occasional trona deposits with economic significance	
						Tmki							

Fig. 2- Generalized stratigraphic columnar section of the investigated area (simplified after Türkecan et. al., 1991).

cal maps have been prepared, and the extension of the mineralization was outlined by trenching, followed by the mineralogical characterization of the ore (Irkeç, 1991,1992).

Various laboratory works in addition to field surveys were carried out around the mineralization area. Thirty five rock specimens were investigated under polarizing microscope for petrographic deter-

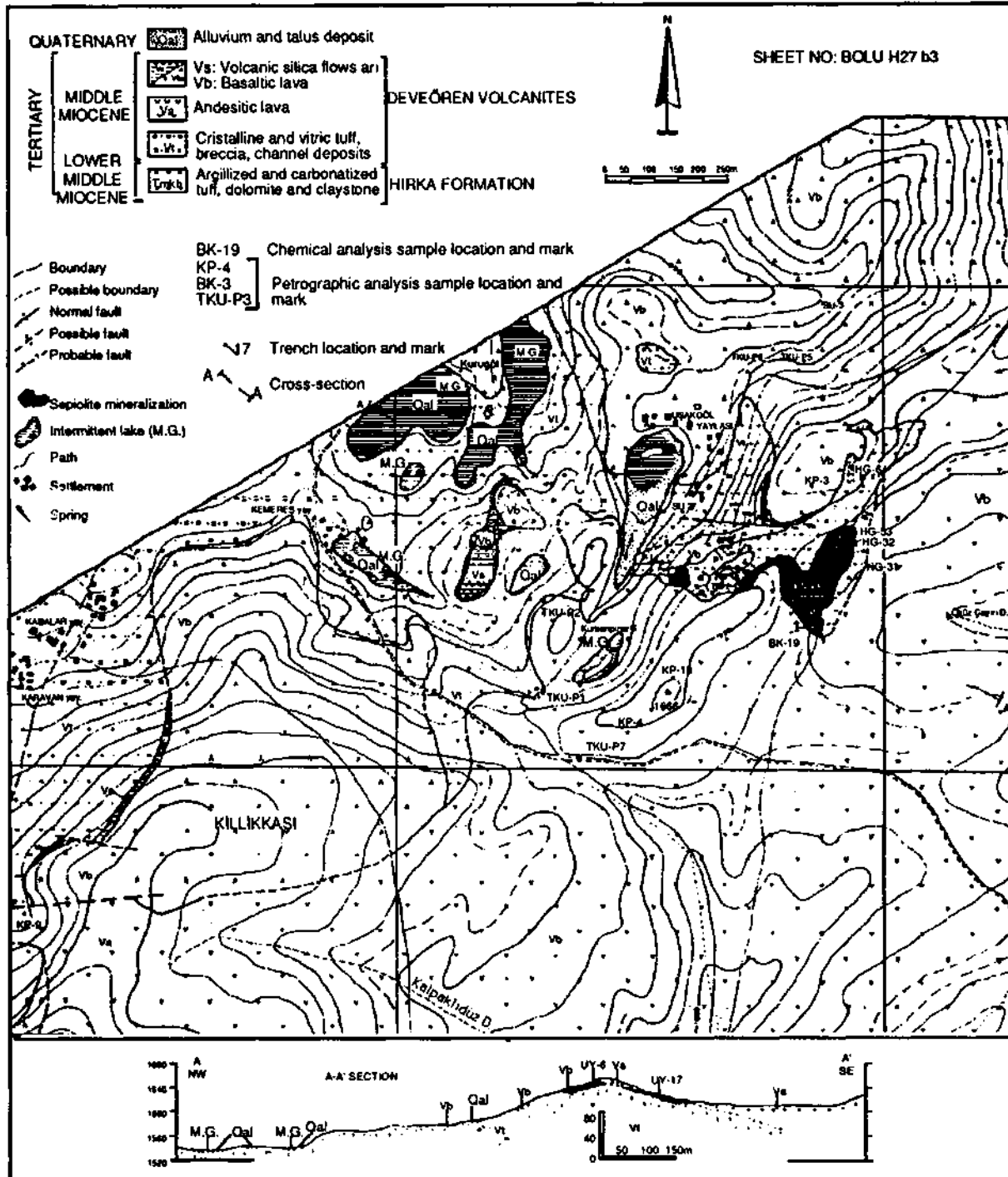


Fig. 3- Geological map of the sepiolite mineralization area around Uşakgöl Yaylası (Plain) and its vicinity (after Irkeç, 1992).

minations. To figure out the crystallographic features and mineral paragenesis of Kibriscık sepiolite, 93 clay and altered rock samples were investigated by X-ray diffraction method. X-ray diffractograms of oriented, ethylene glycole treated and fired KIB-6C sample were obtained, and "step-scanning" applied in a trial to calculate the unit cell parameters. JEOL JDX-8P and RIGAKU-Geigerflex diffractometers were used.

Differential thermal analysis (DTA) and thermal gravimetric (TG) methods were applied on 9 sepiolite and altered tuff specimens to investigate the thermal behaviour, dehydroxilation steps, phase transformations and weight loss of the clay material. RIGAKU-DPS/8151 (Ver. 2.00) instrument was used.

Infrared spectroscopy studies were carried on 6 clay samples by JASCO Super 200 IR instrument, to determine the absorption bands due to the vibration and stretching of chemical bonds.

Scanning electron microscopy (SEM) and transmission electron microscopy (TEM) studies were conducted in GIRIN Laboratories, to investigate the microstructural and micromorphological features. Seven sepiolite, one tuff and diatomite specimen each were investigated by HITACHI S 530 S and JEOL JEM-4000 FX scanning and transmission electron microscopes, respectively.

Chemical analysis performed consist of rock, sepiolite and spring water analysis. Chemical analysis of 20 rock and sepiolite samples for geochemical interpretations were realized in the laboratories of MTA by titration and optic emission spectroscopy. In addition, 25 sepiolite samples were analysed in both GIRIN and MTA Laboratories, by titration, X-ray fluorescence (XRF), energy dispersive X-ray (EDX) and atomic absorption spectrometry (AAS) methods; and 3 present-day spring water specimen by EDTA, flame-photometry, spectrophotometry, AAS, titration and gravimetric methods.

Various technological tests were conducted to determine the specific surface area by BET method, water and oil absorption rates, bleaching capacity, cation exchange capacity, brightness, specific gravity and firing state for ceramic applications, in both GIRIN and MTA Laboratories (İrkeç, 1992).

GEOLOGICAL SETTING

Lithological units, distinguished in the investigated area and its close vicinity consist of the volcanic and sedimentary rocks of the "Köroğlu group"; Pliocene Ilgaz formation and Quaternary alluvium (Türkecan et. al., 1991). The Köroğlu Group, which is exposed in a wide area comprise,

Uruş formation,

Hüyükköy formation,

Bakacaktepe volcanites,

Deveören volcanites,

İlıcadere volcanites,

Kirazdağı volcanites,

Karasivri volcanites,

Uludere pyroclastites, and

Hirka formation, in geochronological order.

Sedimentary and volcanic units except for the Uruş formation, Kirazdağı and Karasivri volcanites are observed in the investigated area. Generalized stratigraphic columnar section of the area is given in Figure 2.

Kibriscık sepiolite occurrence crops out within the Deveören volcanites, which cover the northern half of the study area (Fig. 3), and is named after the Deveören village, around where it is exposed best (Bolu H27 b2 map sheet) (Türkecan et. al., 1991).

Deveören volcanites are composed of basalt, andesite and dacitic lava, tuff and agglomerate. Lavas are gray, black, green and brown in color, and the most typical property is the platy flow structure they show. They generally exhibit cryptocrystalline texture with very fine and random phenocrysts. Tuffs are white to pinkish, and agglomerates reddish in color.

In thin section studies, mineralogical composition of Deveören volcanites range on the boundary between andesite and basalt, and may occasionally be difficult to identify. Andesites (Va) are

generally in hyalopylitic texture, with relicts of plagioclase and opaque mafic mineral phenocrystals. The matrix consists of volcanic glass, plagioclase microliths and crystallites. Basaltic lava (Vb) exhibit fluidal structure and are composed of pyroxene and plagioclase microphenocrysts. These occur in a matrix of parallel aligned microliths and granules of opaque minerals filling the interspaces. Together with the basaltic lava, silica flows (Vs), sometimes reaching a thickness of over 1 m are common. These siliceous rocks may exhibit very different colors (red, white, blue etc.) and texture, and may occur as massive bodies, or oolitic and/or brecciated occurrences of silica replacement. In addition, silica precipitation around hot springs, forming chalcedony, are common (Irkeç,, 1992).

Tuffs of the Deveören volcanites bear significance, considered the occurrence of sepiolite within them. Tuffs are exposed in the Öküzçayırı stream and the mild slopes in northwest. Volcanic breccia crop out at the steep flanks, surrounding the Uşakgöl plain. Thickness of the unit ranges around 40-80 m.

Tuffs show a sequence of crystalline tuff, crystalline+vitric tuff, vitric tuff and resedimented tuff/tuffite transported by small braided streams, in ascending order. Crystalline tuff is dominant at the Uşakgöl plain, while vitric tuff and ash predominate at the northwestern flanks of the Öküzçayırı stream.

Vitric tuff, ash and pumiceous tuff generally exhibit aphanitic texture. They are slightly compacted, and show yellow, dirty white and whitish colors. Argillization is common, and they occasionally carry manganese dendrites and stainings in millirhetric scale along fractures. Zeolitization, recognized by its pale green color is also common. Pumice fragments, less than 1 cm in diameter, and irregular shaped, white silica nodules of variable size, which are thought to have generated from silica-rich intraformational water are occasionally identified. Besides, dark gray-greenish colored, silicified clay veinlets may also be distinguished. Borders of these veinlets with the tuff itself are gradational. These have been interpreted as extremely argillized volcanic intrusions in acidic composition, emplaced as veins or veinlets, cutting the tuffs. Angular chert fragments, which may occasionally reach

coarse block size have been interpreted as intraclasts within the tuff, which was displaced after deposition, probably due to the tectonic activities and the collapse of the crater, during which the fragments of the late-stage silica flows were trapped within them.

Sepiolite occurrences are observed within the vitric tuff. They are irregularly distributed showing gradation into tuff, mostly discontinuous and occasionally silicified, with variable dimensions. Manganese dendrites and staining are also observed within the sepiolite occurrences.

Small scale channel deposits, 1-5 m wide, are found within the tuffs, in the northwestern flanks surrounding the Öküzçayırı stream. These deposits have formed by the alternation of three zones. The system starts with well rounded and spherical volcanic pebbles (mostly augite-andesite), 1-12 cm in diameter, which lie over the tuffs on an erosional surface (Zone A). Pebbles are supported and the imbricate structure is well developed. Groups of pebbles are supported by a matrix in silt and sand size, whose components are again pyroclastic and volcanic originated material. Over Zone A lies a volcanogenic Zone B, comprising clay-silt and sand size material, without any pebbles and internal structure. The uppermost Zone C composes of fine and laminated volcanogenic material which make trough cross-bedding. Paleo-flow direction is thought to extend from north to south and southeast, according to sedimentological findings (Irkeç,, 1992).

Volcanic breccia occurs in two varying characters. The first one comprises volcanic rock fragments, supported by yellow-grayish colored, semi-compacted tuff and pumice. Volcanic fragments, which are angular, having variable dimensions (1-40 cm) are distributed irregularly within the tuff and pumice. They are exposed at the steep flanks in the southeast and east of the Uşakgöl, plain, underlying the basal crystalline tuff, and also exhibiting a complex lateral gradation into the latter. Grains are not supported. Sorting has not developed. In the second type of volcanic breccia, volcanic rock fragments are more abundant, and rather supported, with a well-compacted, red colored, ferrous and welded matrix.

The basement of the tuff and breccia is not observable at the area, due to the overburden. The unit is overlain by basalts in general, and rarely by andesites. It is frequently observed at the same elevations with the andesites.

Fossil content is very poor. Some white colored, porous diatomaceous zones have been distinguished in the upper vitric tuffs. In the marginal zones and close to the channel deposits, locally abundant root-casts and carbonatized root remnants have been identified. Diameters of the root-casts are generally a few mm, and penetrate vertically. Thus, they are thought to be the casts of rushes in a limited swamp.

Structural Units

Very effective volcanic activity, lava flows and pyroclastic material deposition, generally makes the identification of structural units impossible. Generally, NE-SW and NW-SE trending normal faults are recognizable.

The Köroğlu volcanic belt has undergone the influence of NNW-SSE trending compressional regimes, until Late Miocene. Synclines, anticlines and recumbent folds have formed in the Upper Jurassic-Lower Cretaceous formations. Compressional forces, which prevailed until Late Miocene has given rise to the formation of intermountain type basins. North Anatolian Fault has become active in Late Miocene-Early Pliocene. Related tensional stresses have formed normal faults (Türkecan et al., 1991).

Asymmetrical anticlines and synclines may be observed in the Hirka formation in particular, to the south of Bolu H27 b3 map sheet, covering the investigated area. These are discontinuous and small scale tectonic structures.

Direct relation of the investigated sepiolite occurrence with regional tectonism may not be forwarded. It has developed by the effect of small-scale convective systems around the vein-like intrusions close to rhyolite in chemical composition, which filled the local fracture systems formed during volcanic activity.

MINERALOGICAL PROPERTIES

X-Ray Diffraction Results

Sepiolite and palygorskite are clay minerals belonging to in the phyllosiicate group. According to the determination of Brindley and Pedro (1972), they contain two dimensional continuous tetrahedral sheets in T_2O_5 (T=Si, Al, Be...) composition, and discontinuous octahedral sheets, which is the most prominent difference from other clay minerals. Such a feature gives rise to the formation of a channel structure, in rectangular cross section.

The first study on the structural model of sepiolite was carried out by Nagy and Bradley (1955), who suggested the possibility of both orthorhombic and monoclinic symmetries, yet favored the C2/m space group. Later, Brauner and Preisinger (1956) and Preisinger (1959) proposed a new model in the Pnan space group of the orthorhombic system. The main difference between the two models lies in the description of the inversion of tetrahedral sheets, in the centre or edge of the Si-O-Si zig-zag chains.

Number of the octahedral cation positions per unit formula is 8 for sepiolite and 5 for palygorskite. However, all positions need not be occupied. Octahedral vacancy/cation ratio may be tolerated up to 4/1 for palygorskite, and 7/2 for sepiolite. In sepiolite, tetrahedral silicium may be substituted by Al^{3+} and Fe^{3+} in a ratio of 0.2-1.3 per 12 positions. Total octahedral cation number is between 7.0 and 8.0. Octahedral cations are generally Mg^{2+} , however, Al^{3+} , Fe^{3+} , Fe^{2+} , Mn^{2+} and Ni^{2+} substitutions may be possible. By the distribution of occupied octahedral cation positions within the 2:1 chain structure, instead of a regular alternation between the adjacent chains, $A2/a$ (C2/c) space group of monoclinic structure is also theoretically possible.

The Brauner and Preisinger model, thus the Pnan space group of orthorhombic symmetry has been emphasized in numerous studies (Brindley, 1959; Zvyagin, 1967; Gard and Follet, 1968; Rautureau et al., 1972; Rautureau, 1974; Rautureau and Tchoubar, 1974; Yücel et al., 1981). On the other hand, one of the few findings indicating monoclinic

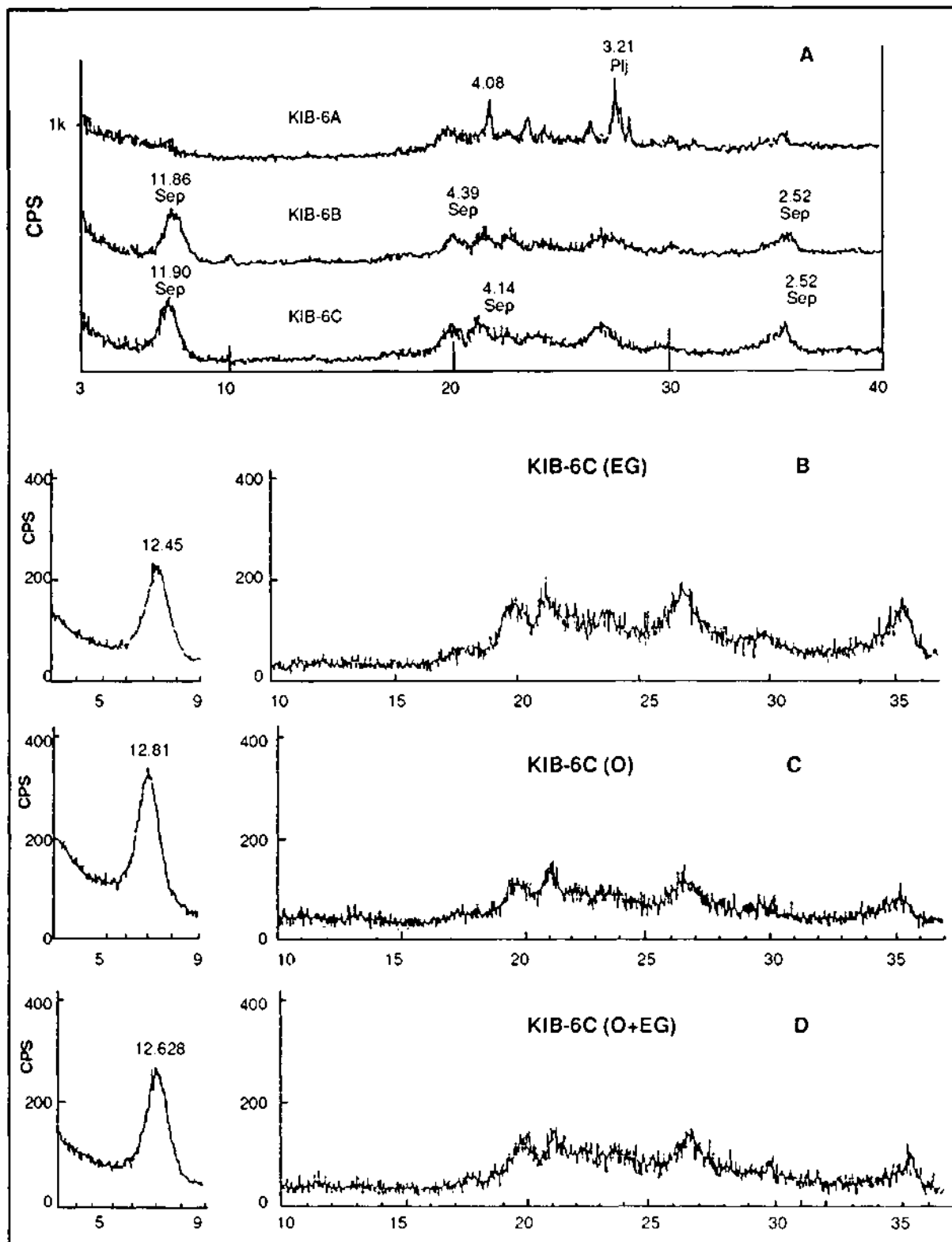


Fig. 4- Original XRD patterns of KIB-6 A, B and C samples (A), ethylene glycolated (B), oriented (C) and EG+O (D) X-ray diffractograms of KIB-6C sample.

Table 1- X-ray diffraction data for the Kıbrısçık sepiolite samples, collected from the trenches in the south of the Uşakgöl plain

Trench No.	Sample No.	Mineral Content									
		Sep	Qtz	CrS	Zeo	Amr	Mnt	Cl	Mcl	Plg	K-Fld
UY-3	UYX-3					●					
	KIB-21	X	○		X	△-○	X			X?	
UY-4	UYX-4	●									
	KIB-20	○		X		○					
	UY-4	●					X				
UY-5	UYX-5					●					
	BX-7a	X		X		●		△ 100° 110° 120°			X
	BX-7b		<X			●		△ 100° 110° 120°			X
	BX-7c		<X			○	○-○		<X		X-△
	KIB-19	X _B [?]	<X	X		○-○	△ B				<X
UY-6	UYX-6	●									
	KIB-6a	X	△	○						○	
	KIB-6b	○									
	KIB-6c	●									
	UY-6	●									
UY-7	BX-8a	X		<X		○		△ 100° 110° 120°			X
	BX-8b	△	<X	X		○					
	BX-8c	△ B		X		○-○	X				X
	KIB-16					●					
UY-8	KIB-17	△ _B [?]		X		○				○	
UY-9	BX-9	X _B [?]		△		△	△-○				△-○
	KIB-18			○			○-○				△
UY-10	BX-10a			X			○-○		X	○	
	BX-10b	X _B [?]				●		X _B [?]			
	UY-10			X		○	X _B [?]	X _B [?]		X	X
UY-13	BX-11a	△		X		△-○		X _B [?]		○	
	BX-11b	○				△					△
	BX-11c	●	X							X	
	UY-13	○	△							X	
UY-14	BX-12a	X _B [?]				●					
	BX-12b	△	<X			○				X	
	UY-14	△ [?]				●					
	UY-14a			<X		●					
	UY-14b	△ [?] B				●					
UY-15	BX-3	△				○-○	○-○				
	BX-13a	○			X					<X	
	BX-13b	○-○			△					○-○	
	BX-13c	△		△		△ [?]					X-△
UY-16	BX-14		<X	△		△		○		△	
UY-17	BX-15	○	<X	X		△					<X
	UY-17	○	△			○					
UY-20	BX-16		<X	X		○	△-○			X	

Sep: Sepiolite, Qtz: Quartz, Crs: α -cristobalite, Zeo: zeolite minerals (mostly heulandite, clinoptilolite and mordenite), Amr: amorphous silica (volcanic glass, opal-CT), Mnt: montmorillonite, Cl: undetermined clay mineral, Mcl: micaceous clay minerals, Plg: plagioclase, K-feld: potassium feldspar

- Dominant mineral
- Abundant mineral
- Medium abundance
- △ Little amount
- X Very little amount
- ↑ Uncertain reflection
- B Broad reflection

sepiolite structure is a sepiolite occurrence in a volcanic sequence, exposed around the Karaşar village of Beypazarı town, Ankara Province. Analytical data from XRD, IR and DTA-TG studies yielded significant variations from those of the sedimentary sepiolite. The most outstanding difference in the

Mineral paragenesis of 42 specimens collected from the trenches marked in Figure 3, determined by XRD analysis, are given in Table 1. Amorphous material predominating in most of the specimens may be vitric tuff, volcanic glass or diatomite originated. Amorphous silica from tuffaceous

Table 2- Comparison of the basal reflections of Kıbrısçık sepiolite with others

<i>hkl</i>	<i>d calc</i>	<i>I</i>	<i>I/I_o</i>	<i>I</i>	<i>I/I_o</i>	<i>I</i>	<i>I/I_o</i>	<i>I</i>	<i>I/I_o</i>
110	12.07	11.90	100	12.03	100	12.20	100	12.10	100
130	7.482	-	-	7.493	8	7.40	10	7.50	7
060	4.495	4.453	80	4.498	19	4.52	80	4.49	25
131	4.301	4.145	90	4.303	30	4.31	60	4.29	35
260	3.741	3.714	69	3.735	20	3.76	20	3.74	25
080	3.370	3.306	81	3.341	24	3.34	20	3.34	45
331	3.195	-	-	3.188	18	3.16	20	3.18	15B
370	2.928	-	-	-	-	-	-	2.95	5
0.10.0	2.697	-	-	-	-	-	-	2.66	8NR
441	2.618	-	-	2.609	20	2.58	70	2.59	45NR
281	2.617	-	-	2.588	23	-	-	-	-
371	2.557	2.521	71	2.557	26	-	-	-	-
550	2.414	-	-	2.436	14	2.44	30	-	-
222	2.409	-	-	-	-	-	-	2.39	20NR
321	2.261	-	-	2.253	15	2.25	30	2.26	20
082	2.072	-	-	-	-	-	-	2.06	10

hkl: reflection surface I/I_o: intensity NR: not resolved B: broad

1. Kıbrısçık sepiolite; Irkeç, 1991, 1992; 2. Eskişehir-Sivrihisar-Ahiler sepiolite (VN-3); Irkeç., 1991, 1992; 3. Tintinara (South Australia) Al-sepiolite; Rogers et. al., 1956; 4. Vallecas (Spain) sepiolite; Brindley, 1959

comparison of the XRD patterns is the splitting of 131 and 331 reflections. 3 angle was determined to be 96,80, suggesting the monoclinical symmetry (Irkeç, 1992).

material and volcanic glass dominates in UY-3,5.7 and 10 trenches, while tuff+diatomite dominate in UY-14 trench. Tuff originated amorphous material is generally accompanied by feldspar, quartz and cris-

tobalite. Occurrence of clay minerals such as sepiolite and montmorillonite have been identified locally in certain trenches and horizons. These are generally accompanied by zeolite minerals.

UY-6 trench is the one where sepiolite formation is most intensive. The uppermost 30 cm section of the 1,5 m deep profile consists of weakly altered, medium to fine particled, abundant feldspar bearing crystalline tuff. In the XRD pattern of the KIB-6A specimen characterizing this section (Fig 4A), reflections of feldspar [plagioclase (An:38 %)] have been determined (3.211 Å, 4080Å, 3.766Å, 2.527Å). (110) reflection of sepiolite at 12.21 Å and (060) reflection at 4.479Å reflect a weak alteration. (421) reflection of heulandite at 3.931 Å is typical. The rising up of the background starting from $2\theta = 18^\circ$ shows the inclusion of amorphous material.

Down the tuff horizon, alteration becomes more effective. KIB-6B specimen has been taken from this horizon, which is fine grained, light brown to beige colored when wet with a dotted texture. The most prominent feature in the XRD pattern is the increase in the distinction and intensities of the sepiolite reflections (Fig. 4A). 8.84 Å and 3.93 Å zeolite reflections (possibly heulandite) are determined.

At the basement of the second tuff horizon, 80 cm deep, massive sepiolite horizon lies, from which the KIB-6C sample has been taken (Fig. 4A). The sample is beige colored and has a soapy appearance when wet. It has a very low density ($\sim 0.66 \text{ gr/cm}^3$). XRD recording of ethylene glycolated, oriented and EG+oriented sample has been taken. Step-scanning XRD has been conducted on the centrifugated sample, in a trial to calculate the unit cell parameters. Basal reflections determined and comparison with other sepiolites are presented in Table 2.

No significant shift has been determined in the positions of the reflections, for the EG treated sample (Fig. 4B), as sepiolite and palygorskite do not have the property of swelling by the absorption of organic compounds into their channels. Only some slight shifts in the positions of the reflections with the c-parameter may occur by 0.2-0.3 Å. In the KIB-6C sample, 11.904 Å peak has shifted to 12.45 Å position after glycolation. As the absorption cen-

teris are mostly structural channels and there occur no exchangeable cations (CEC=5-40 meq/100 g) in the interlayer space, swelling does not occur.

On the other hand, the intensity of (110) reflection increases considerably and shifts to 12.81 Å position in oriented samples. (Fig. 4C). By the glycolation of oriented sample, (110) reflection shifts to 12.628 Å position (Fig. 4D).

Heating at 200°C causes no significant change in the position of the (110) reflection. At 400°C, this reflection shifts to lower 2θ angle (6-7 Å) position.

Data obtained by step-scanning XRD have been refined by computer program, to calculate the unit cell parameters. These are, $a=13.73 \text{ Å}$, $b=26.52 \text{ Å}$, $c=5.00 \text{ Å}$, and $B=90^\circ$ (orthorhombic).

Aluminum is an element that can make substitution in the tetrahedral and octahedral sheets of the sepiolite crystal lattice. High alumina content of the Kibriscik sepiolite is comparable to the Tintinara Al-sepiolite in southern Australia (Table 2). Tintinara sepiolite is a pedogenic occurrence and consists of montmorillonite, illite, kaolinite and fine grained dolomite, as a mixture with sepiolite (Rogers et. al., 1956). Basal reflections determined from the XRD pattern of the acid treated clay fraction of the Tintinara sepiolite yielded the values given in Table 2, which accord well with those of several others. Tintinara sepiolite contains 52.43 % SiO_2 , 7.05 Al_2O_3 , and 15.08 MgO . Chemical composition of Kibriscik sepiolite resembles that of palygorskite, however, XRD data do not support it.

At the basal part of the UY-6 trench, fractures and fissures cutting the massive sepiolite occurrence from bottom to top contain a black colored mineral, stuccoed and impregnated. XRD pattern of the black colored material yielded 2.401 Å, 2.186 Å, 3.47 Å and 1.423 Å reflections, which are characteristic to manganese oxide minerals. These reflections possibly characterize manjiroite $[(\text{NaK})(\text{Mn}^{2+}\text{Mn}^{4+})_2\text{O}_{16}\cdot 2\text{H}_2\text{O}]$ and hollandite $[\text{BaK}_2(\text{Mn}^{4+}\text{Mn}^{2+})_2\text{O}_{16}\cdot 2\text{H}_2\text{O}]$. These veinlets and disseminations of manganese oxide minerals show that the hydrothermal activities in the region continued after the hydrothermal stage that produced the sepiolite-

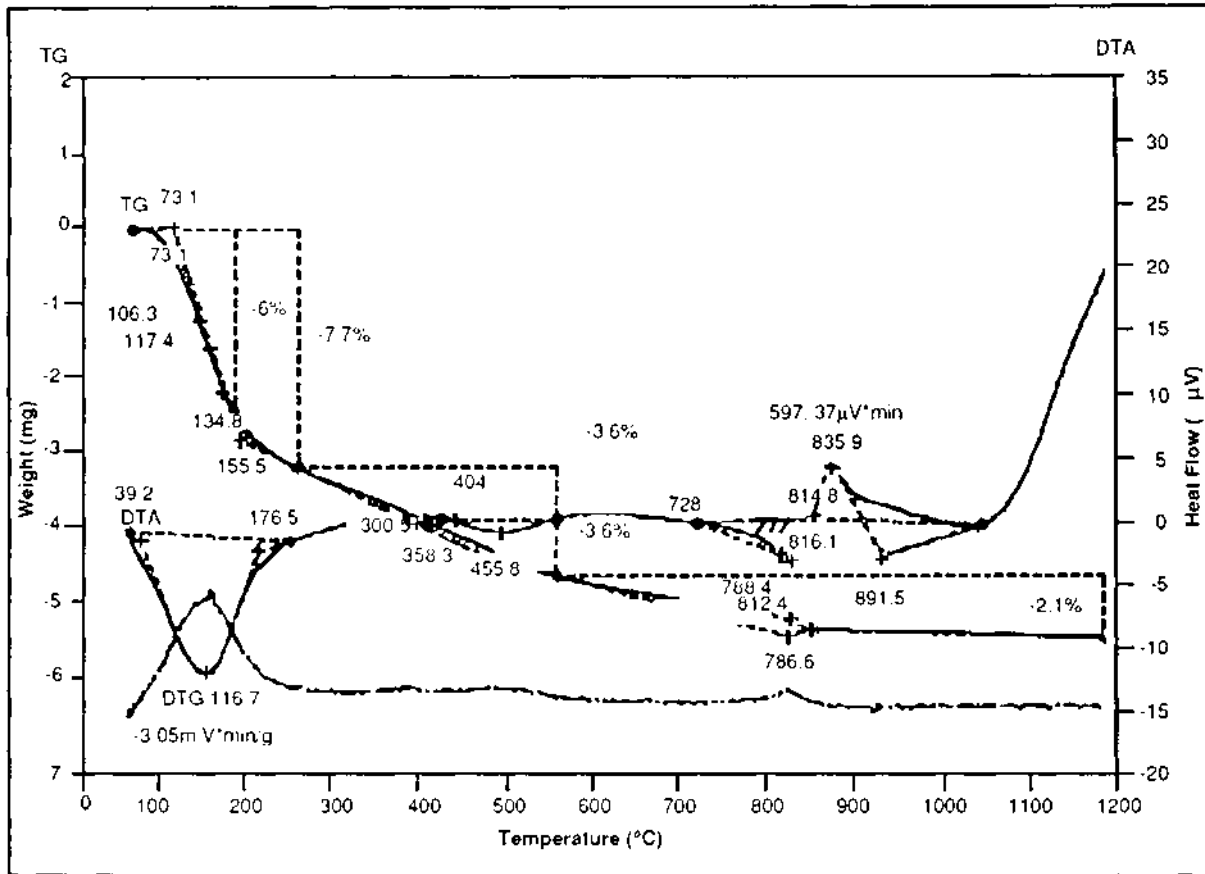


Fig. 5. DTA and TG pattern of KIB-6C sample.

zation. Temperature of the solutions should be less than 100°C, considered the paragenetic relationship. Sepiolite and manganese oxide occurrences are overlain by andesitic and basaltic lava flows around the hill with 1666 m. elevation.

At the UY-14 trench, located about 50 m. SSW of the UY-6 trench, some important features have been determined. Crystalline tuff that proceed into vitric tuff toward the upper portion dominate at the basal parts. Nodular chalcedony occurrences, 5-7 cm. in diameter, are common together with angular silica blocks. Vitric tuff contains diatomite mats, and siliceous and altered volcanic veins. In this trench, gradation from vitric tuff into sepiolite may be observed by barren eye. A completely altered, pinkish-beige colored volcanic structure yielded a chemical composition close to. rhyolite (Table 3). A sample from the west wall of the trench, on the vitric tuff-sepiolite gradation has

yielded sepiolite reflections with low intensity, in addition to opal-CT. Splitting of the (131) reflection reminds monoclin symmetry. Lithological and paragenetic relations in this trench point to a hydrothermal effect.

Mineral paragenesis for the Kibriscik sepiolite may be summarized as follows:

sepiolite + feldspar (mostly plagioclase);

sepiolite + plagioclase + quartz + a-cristobalite;

sepiolite + zeolite (heulandite, clinoptilolite) + feldspar,

montmorillonite + sepiolite + heulandite + plagioclase + quartz;

montmorillonite+ plagioclase+ quartz (+ a-cristobalite) + mica;

Table 3- Chemical analysis results of the rock and clay samples collected around the sepiolite mineralization at Uşakgöl plain, and its vicinity

	KTÜ-1	KTÜ-2	KTÜ-3	KTÜ-4	KTÜ-5	KTÜ-6	KTÜ-7	KTÜ-8	KTÜ-9	KTÜ-10	KTÜ-11	KTÜ-12	KTÜ-13	KTÜ-14	KTÜ-15	KTÜ-16	KTÜ-17	KTÜ-18	KTÜ-19	KTÜ-20	
SiO ₂ (%)	62.10	62.00	60.40	62.00	63.70	65.40	63.90	71.60	70.00	65.20	96.00	94.20	92.80	90.80	94.20	79.00	81.80	61.20	68.00	60.00	
TiO ₂	0.60	0.60	1.00	0.70	0.50	0.60	0.60	0.40	0.50	0.60	<0.10	<0.10	<0.10	<0.10	<0.10	0.10	0.20	0.30	0.30	0.70	
Al ₂ O ₃	16.00	17.00	17.10	17.60	18.00	16.30	17.50	14.50	14.70	17.10	<1.00	<1.00	<1.00	1.50	1.00	5.00	6.30	9.20	9.10	7.20	
Fe ₂ O ₃	6.30	5.50	6.10	5.50	4.70	5.30	4.50	1.80	3.00	4.00	3.60	3.00	4.00	1.40	1.60	1.80	1.60	4.00	2.70	2.40	
MnO	0.10	0.10	<0.10	0.10	<0.10	>0.10	0.20	<0.10	0.10	<0.10	<0.10	0.10	<0.10	<0.10	<0.10	<0.10	<0.10	0.10	0.10	0.10	4.20
MgO	2.32	2.05	1.59	1.95	0.72	0.92	1.21	0.88	0.60	1.43	0.01	0.06	0.44	1.88	0.66	6.98	2.43	12.60	8.45	11.60	
CaO	4.50	5.20	5.20	5.30	4.80	3.00	3.40	2.80	2.80	3.00	<0.20	0.80	0.20	<0.20	0.70	0.70	1.20	1.20	1.10	1.00	
Na ₂ O	4.09	4.25	4.55	3.77	4.31	3.23	2.69	1.34	2.02	2.87	0.40	0.01	0.12	0.01	0.08	0.15	0.81	0.40	0.41	0.17	
K ₂ O	2.30	1.80	2.00	1.70	1.80	2.70	2.00	1.40	2.20	2.20	<0.10	<0.10	0.10	0.10	0.10	0.30	0.30	1.10	0.70	1.00	
P ₂ O ₅	0.20	0.30	0.40	0.50	0.20	0.20	0.10	0.10	0.10	0.10	0.10	0.40	0.10	>0.10	<0.10	<0.10	0.10	0.10	0.10	0.10	
SO ₃	<0.01	<0.01	<0.01	<0.01	<0.01	<0.01	<0.01	<0.01	<0.01	<0.01	<0.01	<0.01	0.22	<0.01	<0.01	<0.01	<0.01	<0.01	<0.01	<0.01	
LOI	1.30	1.17	1.16	0.75	1.28	2.15	3.61	4.72	3.11	3.21	0.48	0.97	1.34	3.38	2.47	6.42	5.25	9.89	8.47	9.76	
TOTAL	99.81	99.97	99.50	99.87	100.01	99.80	99.71	99.54	99.13	99.71	100.59	99.54	99.32	99.07	100.11	99.85	99.99	100.09	99.43	98.13	
REI(ppm)	130	90	100	100	80	120	90	90	120	120	20	30	80	40	20	50	60	80	100	100	
Cu	100	70	70	70	100	30	30	40	30	30	100	100	150	20	30	30	20	15	15	70	
Cr	200	100	300	<30	30	100	300	70	70	100	40	<20	<20	<20	20	20	20	20	<20	<20	
V	<40	200	200	200	150	<40	<40	100	<40	150	<40	<40	<40	<40	150	<40	<40	<40	<40	<40	
Sr	<300	700	400	400	400	300	400	400	400	400	<300	<300	<300	<300	>300	<300	400	400	<300	<300	
Ba	400	700	400	400	400	700	700	200	300	300	<200	<200	300	<200	<200	200	200	300	200	30000	
Zr	300	400	300	300	300	200	400	150	200	200	<100	<100	<100	<100	<100	100	100	200	200	<100	
Au(ppb)	<100	<100	<100	<100	<100	<100	<100	<100	<100	<100	<100	<100	<100	<100	<100	<100	<100	<100	<100	<100	
FeO(%)	3.40	2.44	0.77	0.38	0.38	0.51	0.19	0.19	0.25	0.38	2.57	1.49	2.31	0.38	0.51	0.13	0.19	0.13	0.13	trace	

Note: 1. SiO₂, TiO₂, Al₂O₃, Fe₂O₃, CaO, MnO, K₂O, P₂O₅ & Rb analysis by XRF (Kevex XRF) 2. DL of the trace elements by OES (%) are: Ag: 0.0002, Cu: 0.001, Rb, Cr, Sn, Pb, Bi, Ni: 0.002, MgO, Na₂O analysis by AAS (Perkin-Elmer 270); SO₃ analysis by Leco; F₂O analysis by aira- contents below these DL could not be determined for the samples.

Basalt
Pillow-basalt
Basalt
Red-colored brecciated
basaltic andesite
Andesite
Channel deposits (andesite)
Channel deposits (tuff/sandstone)
Crystalline tuff
Litic tuff
Crystalline-litic tuff
Volcanic glass
Volcanic glass
Volcanic glass
Volcanic glass
Volcanic glass
Volcanic glass
Volcanic glass
Volcanic glass
Volcanic glass
Rhyolite
Diatomaceous tuff
Mantle breccia
Sepiolite
Mn-bearing sepiolite

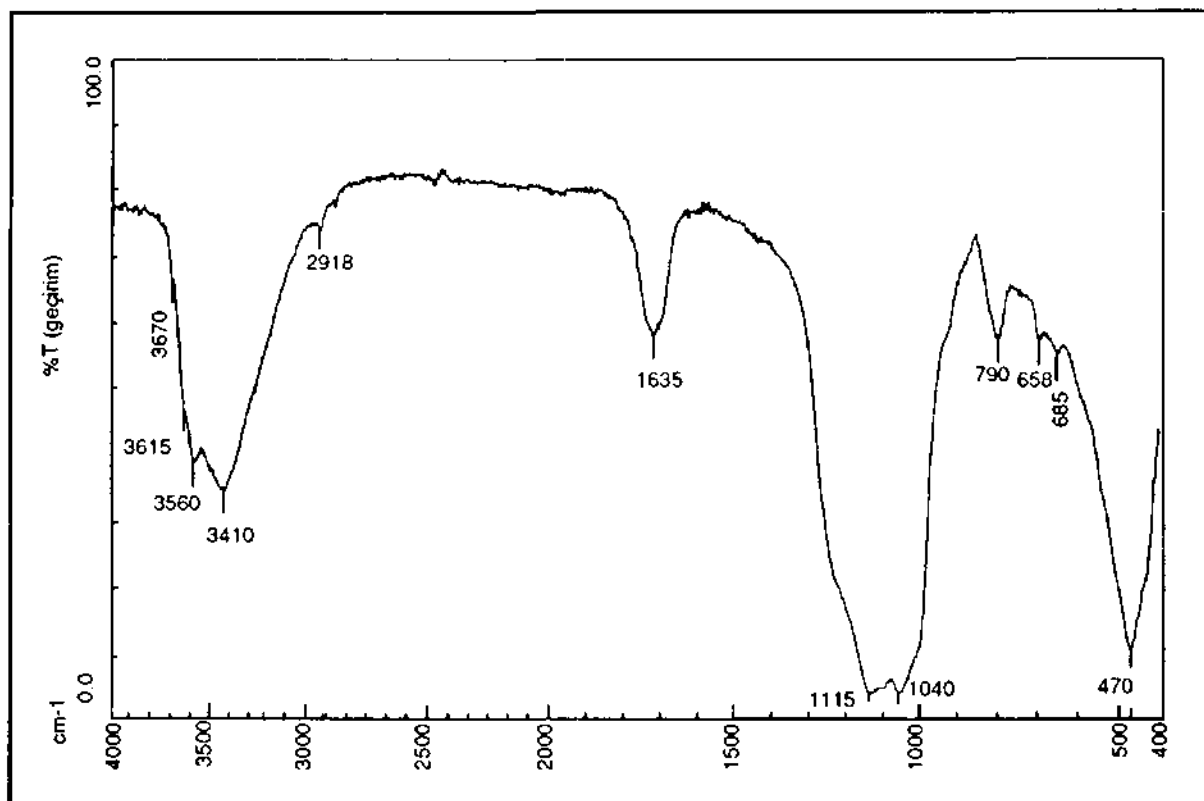


Fig. 6- IR spectrum of KIB-6C sample.

opal-CT + quartz+ α -cristobalite.

Paragenetic relations reflect a hydrothermal origin. No carbonate sequence has been determined around the hill with 1666 m. elevation. The presence of heulandite, which is a Ca-zeolite, show a silica saturated or oversaturated environment. This mineral is not stable over 400°C, and is synthesized at 200-360°C, under 15.000-37.000 psi pressure.

Sepiolitization is concentrated around the fissures and fractures, which have served as conduits for the uprisal of the hydrothermal fluids. Probably the same fluids, which have produced the alteration into sepiolite, has continued to be effective after the formation, and given rise to the occurrence of manganese oxide veinlets. Some of these fissures have later been filled by silica forming veins.

DTA and TG investigations

Palygorskite and sepiolite generally exhibit

similar thermal behaviour (Caillere and Henin, 1957; Hayashi et. al., 1969; Imai et. al., 1969; Martin Vivaldi and Fenoll, 1970; Nagata et. al., 1974; Serna et. al., 1975; Mifsud et. al., 1978). DTA patterns of these minerals may be examined in three temperature ranges: (1) low temperature region (<300°C), (2) central region (300-600°C), and (3) high temperature region (>600°C).

Due to the extraordinary chemical composition with rather low magnesia and high alumina content, which is related to the mode of occurrence by hydrothermal alteration, DTA pattern of Kibriscik sepiolite varies significantly from that of a sedimentary one (Fig. 5). The endothermic peak related to the loss of absorbed and zeolitic water below 300°C appears around 110-120°C, being broader and lower in intensity. In the central region, instead of two characteristic endothermic peaks at 350°C and 500-550°C in sedimentary sepiolite, due to the loss of coordination water, Kibriscik sepiolite generally yields a single and weak endotherm at 460-

480°C, reflecting the pattern of palygorskite. In the high temperature region over 600°C, the sharp endothermic peak at 800°C due to the complete dehydroxylation of the structure is not observed for the Kibriscik sample; and enstatite formation is more gradual. Some weak endotherms at around 780-820°C, which may be due to the feldspar content, are observable, a-cristobalite conversion probably starts at around 1000°C for the investigated sample, which should normally be expected around 1200°C.

Infrared (IR) investigations

IR pattern of the Kibriscik sepiolite shows different peculiarities from the other sepiolites (Fig. 6). In the IR pattern of KIB-6C sample, 3685-3625 cm⁻¹ bands due to the Mg-OH vibration (Otsuka et. al., 1968) have not developed well. Instead of a single band at 1200 cm⁻¹ due to Si-O-Si p bonding, a broad band appears combined to the 1100-1000 cm⁻¹ bands. Intensity of the 470 cm⁻¹ band is increased probably due to a chemical composition rich in silica. Possible substitution of Al³⁺ in the tetrahedral layer for Si⁴⁺, and that of Al³⁺ and Fe³⁺ for Mg²⁺ in the octahedral layer have affected the IR spectrum considerably. The absence of the 3685 cm⁻¹ and 1200 cm⁻¹ bands resembles the IR spectrum of palygorskite.

SEM and TEM investigations

Three sepiolite, one tuff and one diatomite specimen from the Uşakgöl area have been investigated under SEM. Instead of the characteristic fibrous structure (fibres generally being longer than 5 μm) observed under SEM for sedimentary sepiolite, Kibriscik sepiolite composes of laths, whose length ranges in nanometer scale. In the SEM micrograph of KIB-6B specimen (Plate 1, Photo 1), glass-shard structure is seen to be preserved, while alteration becomes more effective and total crystallization trend increases locally (Plate 1, Photo 2).

In the TEM micrograph of KIB-6C specimen (Plate 1, Photo 3), sepiolite laths growing on the margins of volcanic glass particles are typical. Length of these laths, which have not obtained a fibrous form yet, ranges around 50-200 nm.

GEOCHEMICAL INVESTIGATIONS

Chemical analysis of rock samples

To make an approach to the mode of occurrence of Kibriscik sepiolite by geochemical methods, 20 rock and clay samples have been collected and analysed under 8 groups (Table 3). Results of the rock chemistry studies are summarized below:

1- Almost similar elemental composition determined in all the samples shows that the sepiolite-bearing area has continuously been effected by hydrothermal alteration, which produced homogenization among the elements.

2- The oldest hydrothermal alteration stage that could be determined in the field is the spilittization of basic rocks, and points to an aqueous environment, which is thought to compose of shallow and intermittent lakes.

3- The next hydrothermal alteration stage is that caused by the intrusion of veins, in rhyolitic composition, around which hydrothermal convective cells with meteoric and occasionally magmatic water interference have produced local alterations in the host rocks. Sepiolite formation is possibly in close connection with this system.

4- Aluminum source for the Kibriscik sepiolite, which is a Mg-Al silicate, is the vitric tuff itself. Values given in Table 3 clearly reveal it. On the other hand, these tuffs are almost sterile, considered Mg. Thus, an external source of Mg needs to be looked for. This source is thought to be essentially basalts, and to a minor extent, the andesites.

5- Occurrence of sepiolite at the contacts between the tuff and the veins in rhyolitic composition and the high SiO₂ and MgO contents versus other components in these veins, are results arising from the effective role of these veins in the leaching of the neighbouring rocks. As supported by field evidence, local temperature changes produced by these veins and the percolating solutions have dissolved Mg from the basalts and andesites, and migrated into tuffs, where Al was also supplied, thus producing the unusual Mg-Al silicate mineral.

6- Final ring of this effective hydrothermal al-

Table 4- Chemical analysis results of several sepiolite samples from the Kibriscik area

Oxides	KIB-6C (UY-6)	KIB-6B (UY-6)	KIB-6A (UY-6)	BK-13A (UY-15)	BK-13B (UY-15)	BK-16 (UY-17)
SiO ₂	71.26	68.80	70.20	57.00	60.50	71.00
Al ₂ O ₃	4.40	10.75	6.20	8.50	8.00	8.60
MgO	11.10	7.18	9.60	10.10	9.70	7.07
Fe ₂ O ₃	3.01	2.60	2.40	2.50	2.00	3.00
FeO	-	0.10	0.20	-	-	0.20
MnO	0.05	<0.10	-	0.20	0.30	<0.10
TiO ₂	0.25	0.50	-	0.30	0.30	0.30
CaO	0.44	0.45	0.55	2.00	2.50	0.39
Na ₂ O	trace	0.01	0.20	3.70	3.90	0.11
K ₂ O	0.74	1.00	0.95	1.20	0.70	1.00
P ₂ O ₅	0.04	0.10	-	0.30	0.20	0.10
L.O.I	8.72	7.25	8.65	13.35	10.60	6.80
TOTAL	100.01	98.79	98.95	99.15	98.70	98.62

(-) not analysed; DL: % 0.01

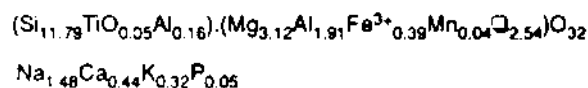
teration chain is represented probably by the veinlet systems, rich in Mn and Ba, cutting all the former products, Mg content of these veinlets are again considerably high, in accordance with its mobile character. This geochemical cycle has been tried to be schematised in Figure 7.

7- Assuming that the final weathering process had effected all the samples under the same conditions, final alteration effects have not been taken into account.

Chemical composition of the sepiolite

One of the most prominent properties of Kibriscik sepiolite is the unusual chemical composition of the material. It resembles that of palygorskite, and is thought to be in close connection with the composition of the host rock and mode of formation. Chemical analysis results of sepiolite samples collected around the Uşakgöl Plain are given in Table 4.

An approach has been made to calculate the structural formula of the BK-13A sample, whose XRD pattern contains only the reflections specific to sepiolite. Assumed that there is no other crystalline phase intercalated in the sample, the structural formula has been calculated as;



and the mineral described as Al-Fe Sepiolite.

By plotting of $(\text{Al}+\text{Fe})^{\text{VI}}$ and Mg^{VI} values, calculated according to 6+charge in octahedral layer, on the Weaver and Pollard (1973) and Foster (1960) diagrams, Kibriscik sepiolite is located at the compositional gap region, and seems to be close to palygorskite; but trivalent cation number is lower.

These data suggest that the Kibriscik sepiolite may be a new clay mineral with its own characteristics, but detailed crystallographic investigations still remain to be carried out.

Chemical analysis of some present-day spring water were carried out, and the activity coefficients calculated according to the Debye-Hückel equation were plotted on the MgO-SiO₂-H₂O activity diagram of Wollast et. al. (1968). It was seen that the values plotted lie on the border between the sepiolite precipitation and amorphous silica saturation areas. pH of the water specimens range around 9-9.5 and concentration of silica is very high. Thus, it was decided that direct chemical precipitation of sepiolite from present-day spring water is not possible.

MODE OF OCCURRENCE

Contrary to the sedimentary type sepiolite occurrences, which are generally associated with the carbonate/evaporite sequences, Kibriscik sepiolite has formed in a volcanic sequence, by the alteration of pyroclastic material. The source rock proved to be vitric tuff, according to field observations and mineralogical evidence.

Alteration and recrystallization processes of natural glasses under hydrothermal conditions have been investigated by many researchers (White, 1983; Crovisier et. al., 1983; Thomassin, 1983; Touray and Thomassin, 1984; Thomassin et. al., 1989). Wirsching (1976), Holler and Wirsching (1978), and Barth-Wirsching and Holler (1989) have simulated the formation of natural zeolites using various glasses in open and closed systems. Different zeolites have been synthesized depending on the chemical composition of the starting material, pH and concentration of the solution, temperature and pressure conditions.

One of the most recent and detailed investigation on the alteration of natural glasses under various physicochemical conditions is that of Larsen et. al. (1991). Basalt wool, diabase wool, glass wool and glass fiber have been used as the starting materials. Samples that were ground to 100 mm. were treated with deionized water at 100°, 125°, 150° and 200°C under autogenous pressure and at 200°C under 2000 bar pressure, without stirring the solution. The tests were carried out under closed system conditions and in 2-30 days period. Glass wool has produced analcime and sepiolite, at 125°C and 30 days of reaction period. Formation of analcime accords well with the findings of Abe and Aoki (1976), for closed systems. According to these researchers, analcime easily forms around 100°C and at pH values over 10. According to the published data of Bowen and Tuttle (1962), Echle (1974) and Hast (1956), sepiolite starts to form at 125°C and pH>10, and the process continues up to 200°C.

Under experimental conditions, hydrothermal alteration is controlled by the solubility of the glass,

and formation of the amorphous and crystalline reaction products. Glass solubility is controlled by the removal of modifying ions from the crystal structure producing a hydrated glass tayer, followed by the dissolution of the components of structure (Holland, 1966; Scholze, 1988). This process also prevails for the hydrothermal alteration. High content of Na and K in the starting material increases the reactivity of the material and alteration proceeds faster.

Experimental conditions and findings seem to suit well with those of the natural associations. Mineral paragenesis of Kibriscik sepiolite is considerably different from the Sivrihisar sedimentary sepiolites, with zeolites (mainly heulandite and clinoptilolite, to a lesser extent phillipsite and mordenite) mostly accompanying sepiolite, in addition to feldspar, quartz and montmorillonite. High Na and K content of the Kibriscik sepiolite is another important criterion indicating the different mode of occurrence. Observations and findings indicating the hydrothermal alteration for the formation of Kibriscik sepiolite may be summarized as follows:

1- Kibriscik sepiolite occurrence is completely located in a volcanic sequence of the Koroğlu volcanic belt, without any neighbouring carbonate or evaporite sequence.

2- As revealed clearly in UY-14 trench, alteration increases gradually from the vitric tuff towards the veins in rhyolitic composition, and sepiolite formation is accelerated. Silica veins and nodules in the same trench also show the hydrothermal activity.

3- Manganese oxide minerals determined within sepiolite in UY-6 trench (manjiroite and hollandite) contain high amount of alkalis. Especially the high content of Ba in hollandite reveal the effect of hydrothermal activity. In the KTU-20 sample given in Table 3, Ba content as high as 3000 ppm has been determined.

4- As stated in Coombs et. al. (1959), heulandite is a zeolite mineral characterizing the environments saturated or oversaturated by silica. Formation by the hydrothermal alteration of acidic

volcanic rocks or volcanic glass is very common. It forms at a temperature range of 200-360°C, and the structure is deformed over 400°C. Thus, temperature of the hydrothermal solutions may be estimated to be between 125°C and 360°C.

5- X-ray diffraction data reveal a sepiolite structure; however, other mineralogical analysis, such as DTA, IR and the chemical analysis results yield data more closer to those characteristic for palygorskite. It seems quite possible that the material described as Al-Fe sepiolite in this study may be a new mineral species, with an intermediary composition between sepiolite and palygorskite.

6- Microtextural interpretations, especially the "mineral growth with total crystallization trend" accompanying "solution breccia" like structures, specified by SEM and TEM studies, point to a stat-

ic-inhomogenous environment.

7- Sr content of Kibriscik sepiolite is lower than Sivrihisar sedimentary sepiolite, while it is characterized by higher contents of Cu, Mn, Ti, V, Zr and Ba (Irkeç, 1992). These elements have a genetic meaning in the identification of hydrothermal activities, and their relationship with each other yield important hint points in the establishment of genetic models.

8- As mentioned earlier, source of Mg^{2+} ions is thought to be the neighbouring widespread basic volcanic rocks, from which it is mobilized by percolating hydrothermal solutions. Due to the very limited extension of the veins in rhyolitic composition, which realized heat transfer to the convection, alteration and mass transfer in the host rocks were limited. Possibly a weakly developed connection be-

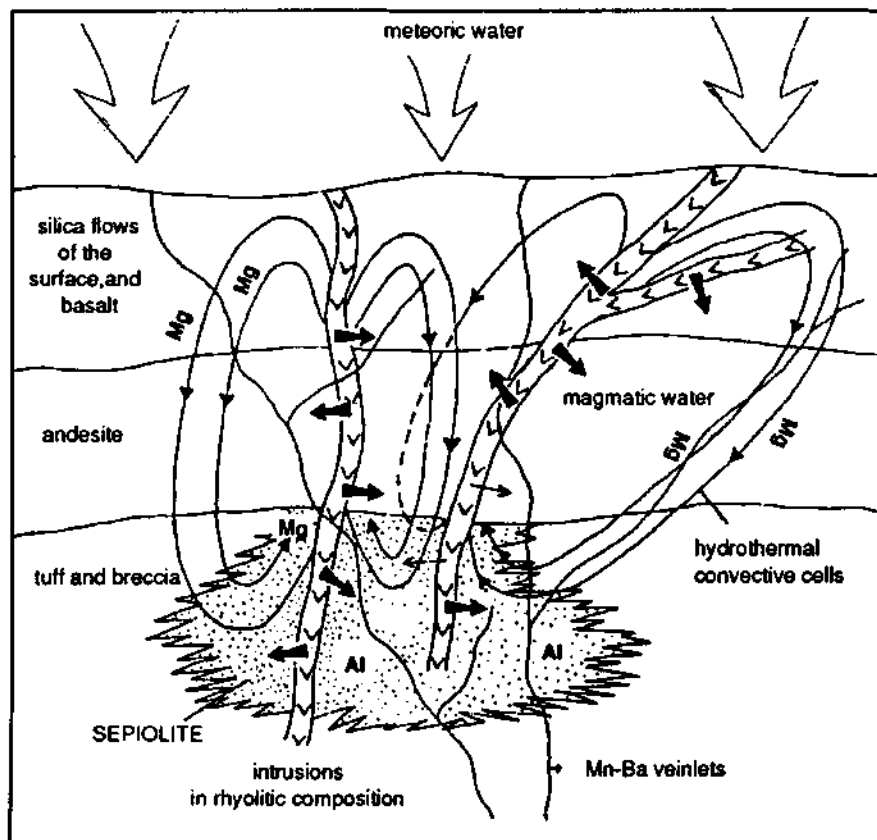


Fig. 7- Schematized mode of occurrence of Kibriscik sepiolite.

tween the fissures that served as the conduits for hydrothermal fluids, and free discharge to the surface limited the system as small convective cell, and did not permit the formation of a widespread mineralization.

ACKNOWLEDGEMENT

This paper is a brief summary of the M. Sc. thesis of the first author, under the supervision of the second author, and submitted to the Geological Engineering Dept., Faculty of Science, Ankara University.

The authors are deeply indebted to Assoc. Prof. Drs. Baki Varol and Sönmez Sayılı of the same Department, Messrs. Hakan Gençoğlu, Ahmet Türkecan, Halim Mutlu and Mustafa Kırkoğlu, geological engineers and Dr. Noriyuki Fujii, Japanese expert of MTA, for their kind suggestions in various stages of the study. Special thanks are due Dr. Shinji Tomura and Dr. Ritsuro Miyawaki of GIRIN (Japan), for providing opportunity to carry out several mineralogical investigations in their laboratories.

Manuscript received January 18, 1993

REFERENCES

- Abe, H. and Aoki, H., 1976, Experiments on the interaction between Na_2CO_3 - NaHCO_3 solution and clinoptilolite, with reference to anatization around Kuroko-type mineral deposits: *Chem. Geol.*, 17, 89-100.
- Barth-Würsching, U. and Höller, H., 1989, Experimental studies on zeolite formation conditions: *Eur. J. Mineral.*, 1, 489-506.
- Blumenthal, M., 1948, Bolu civari ile Aşağı Kızılırmak mecrası arasında Kuzey Anadolu silsilelerinin jeolojisi: *MTA Pub., Serie B, No. 13*, 265 s.
- Bowen, N.L. and Tuttle, O.F., 1962, The system MgO - SiO_2 - H_2O : *Bull. Geol. Soc. Am.*, 60, 439.
- Brauner, K. and Preisinger, A., 1956, Struktur und Entstehung des Sepioliths: *Tschermaks Miner. Petrog. Mitt.*, 6, 120-140.
- Brindley, G.W., 1959, X-ray and electron diffraction data for sepiolite: *Am. Mineral.*, 44, 495-500.
- Brindley, G.W., and Pedro, G., 1972, Report of the AIPEA Nomenclature Committee: *AIPEA Newsletter*, 4, 3-4.
- Caillere, S. and Henin, S., 1957, The sepiolite and palygorskite minerals [In *The Differential Thermal Investigation of Clays*], R.C. Mackenzie (ed)], *Mineral. Soc., London*, pp 231-247.
- Chaput, E., 1931, Notice explicative de la carte geologique au 1:135 000 de la region d'Angara (Ankara): *Bull. Fac. Sci., Univ. İstanbul*, 7/3, pp 1-46.
- Coombs, D.S.; Ellis, A.D.; Fyle, W.S. and Taylor, A.M., 1959, The zeolite fadses, with comments on the interpretation of hydrothermal synthesis: *Geochim. Cosmochim Acta*, 17, 53-107.
- Crovisier, J.L.; Eberhart, J.P.; Juteau, T. and Ehret, G., 1983, Transmission electron microscopy of basaltic glass alteration in seawater at 80°C: *Fortschr. Mineral.*, 61, 48-49.
- Echle, W., 1974, Zur Mineralogie und Petrogenese jungtertiärer tuffitischer Sedimente im Neogen-Becken nordlich Mihalıççık (Westanatolien, Türkei): *N. Jb. Miner. Abb.*, 121, 43-84.
- Erol, O., 1952, Ankara kuzeyinde Mire ve Aydos Dağları bölgesinin jeolojisi hakkında ön rapor: *MTA Rep.*, 2457 (unpublished), Ankara.
- , 1954, Köroğlu-Işık dağları volkanik kütesinin orta bölümleri ile Beypazarı-Ayaş arasındaki Neojen havzasının jeolojisi hakkında rapor: *MTA Rep.*, 2279, (unpublished), Ankara.
- Foster, M., 1960, Interpretation of the composition of trioctahedral micas: *US Geol. Surv. Prof. Pap.*, 354-B, 11-50.
- Gard, J.A. and Follet, E.A., 1968, A structural scheme for palygorskite: *Clay Minerals*, 7, pp 367-369.
- Hast, N., 1956, A reaction between silica and some magnesium compounds at room temperatures and at +37°C: *Arkiv Kemi* 9, pp 343-360.
- Hayashi, H.; Otsuka, R. and Imai, N., 1969, Infrared study of sepiolite and palygorskite on heating, *Am. Mineral.*, 53, pp 1613-1624.
- Holland, L., 1966, *The Properties of glass surfaces: Chapman and Hall, London*, 546 p.

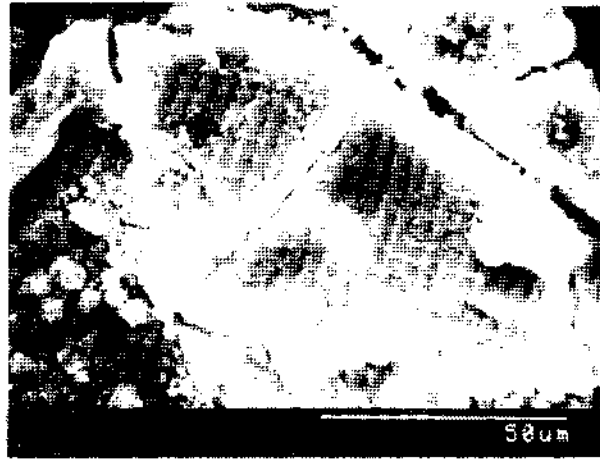
- Holler, H. and Wirsching, U., 1978, Experiments on the formation of zeolites by hydrothermal alteration of volcanic glass: L.B. Sand and F.A. Mumpton, ed., *Natural Zeolites: Occurrence, Properties, Use*, Pergamon Press, Elmsford, New York, 329-336.
- Imai, N.; Otsuka, R.; Kashide, H. and Hayashi, R., 1969, Dehydration of palygorskite and sepiolite from Kuzuu District, Tochigi Pref., Central Japan: *Proc. Int'l Clay Conf.*, Tokyo, 1, pp 99-108.
- İrkeç, T., 1991, Bolu-Kıbrısçık sepiyolitinin mineralojik ve kimyasal özellikleri ve Eskişehir-Sivrihisar sedimanter sepiyoliti ile karşılaştırılması, *Proc. 5th Nat. Clay Symp. (Eskişehir-Turkey)*, (M. Zor, ed.), pp 3-17.
- , 1992, Kıbrısçık (Bolu) sepiyolit oluşumlarının mineralojik-kimyasal özellikleri ve kökenine yaklaşım M. Sc. Thesis, Ankara Univ., Fac. of Sci., Ankara, 200p.
- and Kinkoğlu, M., 1989, 88-22b3 No.lu Bolu-Ankara Kaolin aramaları projesi kapsamında 1988 arazi sezonunda Zonguldak-Bolu-Ankara yollarında yapılan çalışmalara ilişkin ön etüd raporu, MTA Rep., 8536 (unpublished), Ankara.
- Larsen, G.; Plum, K.H. and Förster, H., 1991, Zeolites and other hydrothermal alteration products of synthetic glasses, *Eur. J. Mineral.*, 3, 933-941.
- Leonhard, R., 1903, *Geologische Skizze des Galatischen Andesit-gebietes nördlich von Ankara*, N. Jb. Min. B., 16, pp 99-109.
- Martin Vivaldi, J. L and Fenoll, P., 1970, Palygorskites and sepiolites (Hormites) [In "Differential Thermal Analysis" R.C. Mackenzie (ed)], Academic Press, London, I, pp 553-573.
- Mifsud, A.; Rautureau, M. and Fornes, V., 1978, Etude de l'eau dans la palygorskite a l'aide des analyses thermiques, *CCM*, 13, pp 367-374.
- Milch, L., 1903, Die Ergussgesteine des Galatischen Andesitgebietes, N. Jb. Min. B., 16, pp 110-165.
- Nagata, H., Shimoda, S. and Sudo, T., 1974, On dehydration of bound water of sepiolite, *CCM*, 22, pp 285-293.
- Nagy, B. and Bradley, W.F., 1955, The structural schema of sepiolite, *Am. Mineral.*, 40, pp 885-892.
- Otsuka, R., Hayashi, H. and Shimoda, S., 1968, Infrared absorption spectra of sepiolite and palygorskite: *Memoirs of the School of Sci. & Eng. (Waseda Uni.)*, 32, pp 13-24.
- Preisinger, A., 1959, X-ray study of the structure of sepiolite, *CCM*, 6, pp 61-67.
- Rautureau, M., 1974, Analyse structurale de la sepiolite par microdiffraction electronique, These Universite d'Orleans, 89 p. (unpublished).
- and Tchoubar, C., 1974, Precisions concernant l'analyse structurale de la sepiolite par microdiffraction electronique, *C.R. Acad. Sci. Paris*, 278 B, pp 25-28.
- ; ——— and Mering, J., 1972, Analyse structurale de la sepiolite par microdiffraction electronique, *C.R. Acad. Sci. Paris*, 274 C, pp 269-271.
- Rogers, L.E.; Quirk, J. and Norrish, K., 1956, Occurrence of an aluminum-sepiolite in a soil having unusual water relationships, *J. Soil Sci.*, 7, pp 177-184.
- Rondot, J., 1956, 1/100 000 lık 39/2 (güney kısmı) ve 39/4 no.lu paftaların jeolojisi (Seben-Nallıhan-Beypazarı ilçeleri), MTA Rep., 2517 (unpublished), Ankara.
- Scholze, H., 1988, *Glas-Natur, Struktur, Eigenschaften*: Springer Verlag, Berlin, 407 p.
- Serna, C., Ahlrichs, J.L. and Serratosa, J.M. 1975, Folding in sepiolite crystals, *CCM*, 23, pp 452-457.
- Stchepinsky, V., 1942, Beypazarı-Nallıhan-Bolu-Gerede bölgesi jeolojisi hakkında rapor, MTA Rep., 1363 (unpublished), Ankara.
- Thomassin, J.H., 1983, Early mineralogical evolution at the surface of volcanic glass during seawater alteration, *Experimental data*, *Fortschr. Mineral.*, 61, pp 206-207.
- ; Boutonnat, F.; Touray, J.C. and Baillif, P., 1989, Geochemical role of the water/rock ratio during the experimental alteration of a synthetic basaltic glass at 50°C. An XPS and STEM investigation, *Eur. J. Mineral.*, 1, pp 261-274.
- Touray, J.C. and Thomassin, J.H., 1984, Bilans et mecanismes d'interaction des verres basaltiques et de l'eau de mer en conditions hydrothermales, *Symposium de l'USCV, Bruxelles, Rivista della Stazione sperimentale del Vetro*, 14, pp 111 -116.

- Türkecan, A., Hepşen, N., Papak, I., Akbaş, B., Dinçel, A., Karataş, S., Özgür, İ., Akay, E., Bedi, Y., Sevin, M., Mutlu, G., Sevin, D., Ünay, E. and Saraç, G., 1991, Seben-Gerede (Bolu)-Güdül-Beypazarı (Ankara) ve Çerkeş-Orta-Kurşunlu (Çankırı) yörelerinin (Koroğlu Dağları) jeolojisi ve volkanik kayaların petrolojisi, MTA Rep., 9193 (unpublished), Ankara.
- Weaver, C.E. and Pollard, L., 1973, *The Chemistry of Clay Minerals*, Elsevier, Amsterdam, 213 p.
- White, A.F., 1983, Surface chemistry and dissolution kinetics of glassy rocks at 25°C, *Geochim. Cosmochim. Acta*, 47, pp 805-815.
- Wirsching, U., 1976, Experiments on the hydrothermal alteration processes of rhyolitic glass in dosed and open system, *N. Jb. Miner. Mh.*, 5, pp 203-213.
- Wollast, R.; Mackenzie, F. and Bricker, O., 1968, Experimental precipitation and genesis of sepiolite at earth-surface conditions: *Am. Mineralogist* 53, pp 1645-1661.
- Yücel, A.M., Rauterau, M., Tchoubar, D. and Tchoubar, C., 1981, Calculation of the X-ray powder reflection profiles of very small needle-like crystals, II. Quantitative results on Eskişehir sepiolite fibers: *J. Appl. Clays*, 14, pp 431-454.
- Zvyagin, B.B., -1967, *Electron Diffraction Analysis of Clay Mineral Structures*, Plenum Press, New York, 122 p.

PLATE

PLATE-I

- Photo 1- SEM micrograph of the KIB-6B sample (preserved glass-shard texture).
- Photo 2- SEM micrograph of the KIB-6B sample (effect of alteration and total crystallization trend).
- Photo 3- TEM micrograph of KIB-6C sample (sepiolite fibers and volcanic glass relicts).



1



2



3

ORIGIN AND PETROLOGY OF EKECİKDAĞ GRANITOID IN WESTERN CENTRAL ANATOLIAN CRYSTALLINE MASSIF

T. Kemal TÜRELİ*; M. Cemal GÖNCÜOĞLU" and Orhan AKIMAN"

ABSTRACT— A belt formed by a number of granitoid intrusions is situated at the western part of the Central Anatolian Crystalline Massif. One of the granitoid intrusion at the southwest of the belt crops out between Aksaray and Ortaköy and is called Ekecikdağ. Ekecikdağ granitoid, which is composed of monzogranites and granodiorites, intruded both the metamorphic and ophiolitic host rocks. Ekecikdağ granitoid is differentiated into following subunits with respect to their petrographical and chemical composition: Borucu granodiorite-monzogranite, Sinandı mikrogranite, Hisarkaya porphyritic granite, Kalebalta teucogranite and aplite granite. All these subunits are genetically related to each other. Borucu granodiorite-monzogranite represents the main magmatic phase whereas aplite granite the latest. Ekecikdağ granitoid has a calcalkaline character and show aluminofelitic trend. It has features which favour both I and S types of granite. Enclaves observed in granitoid is thought to be xenoliths derived from pre-existing gabbroic rocks during the emplacement of the granitic magma. The geochemical data suggest a post collisional tectonic setting and a continental crustal source for Ekecikdağ granitoid. In regard to regional data, during Upper Cretaceous, the existence of an ensimatic arc to the north of the Central Anatolian Crystalline Massif is suggested. It is also proposed that collision and obduction of this ensimatic arc on to the Central Anatolian continental crust caused crustal thickening and increase in the geothermal gradient in the region. This gave rise to the partial melting of the continental crust and to the formation of a granitic magma.

STRATIGRAPHY OF THE EASTERN SECTION OF THE PASINLER-HORASAN (ERZURUM) REGION

Cevdet BOZKUŞ***

ABSTRACT— In the eastern part of the Pasinler-Horasan Neogene basin, the lowermost section consists generally of tuffs, andesites and basalts. This association is nomenclated as "Karakurt volcanics". They are underlain by an ophiolitic melange of Lower Cretaceous age which is unconformably overlain by the Oligocene Çayarası formation consisting of clastic rocks. The basin is bounded by sinistral strike-slip faults controlling sedimentation of various continental detritic rocks. These are distinguished as Aras and Horasan formations, both Pliocene in age, representing respectively marls and claystones of deep lagoonal environment, conformably overlain by fine grained sediments. Terrace gravels, alluvial fans and colluvium represent the Quaternary sedimentation.

CLAY SEDIMENTOLOGY OF SEDIMENTARY SEQUENCE BELONG TO ÇAN (ÇANAKKALE). ORHANELİ AND KELEŞ (BURSA) LIGNITE OPEN PIT MINE

Emel BAYHAN***; Abdurrahim ŞAHBAZ*** and Sezai GÖRMÜŞ***

ABSTRACT— In this study clay fraction belonging to the Miocene aged sedimentary coal bearing sequence from Çan, Orhaneli, Keleş districts have been separated and smectite, illite, kaolinite and chlorite paragenesis have been defined. Major element analysis have been made of monomineralic smectites. These are dioctahedral (beidellite) and trioctahedral (saponite) in character, and occurrences of these smectites have been examined. Smectites belonging to the tuffaceous series have been formed from the alteration of volcanic material whereas those from clayey carbonaceous series either as in situ neoformation of detrital materials or as the transformation of detrital smectites, kaolinite have been formed as a result of alteration of rocks with feldspar, while illite and chlorite have been derived from metamorphic rocks.

MAJOR-, MINOR-, AND TRACE-ELEMENT ANALYSES OF REFRACTORY SILICATES USING A SINGLE BORATE DISINTEGRATION METHOD

Bahattin AYRANCI*

ABSTRACT._ Fusion disintegration performed under non-oxidizing conditions using an induction oven is an alternative procedure for the decomposition of samples containing refractory components, so that the oxidation states of iron as well as major-, minor-, and trace-element analyses can be determined from a single sample disintegration.

A NEW TYPE SEDIMENTARY-DIAGENETIC SEPIOLITE IN SIVRIHİSAR (ESKİŞEHİR)

Mefail YENİYOL**

ABSTRACT._ This study describes a meerschaum sepiolite that differs from the conventional meerschaums of lump type with respect to its genesis, mode of occurrence, texture and composition. The present one is found together with layered sepiolite deposits in the upper section of Neogene dolomitic sequence in the south of Sivrihisar. It is layered, lens shaped and consists of dolomite and/or calcite minerals as detritic grains. Sepiolite had been formed during diagenesis, after deposition of reworked carbonate material, and occupied the intergranular space in varying proportions. The best ones are porous, lightweight, white and they can be easily carved when they are immersed in water.

A HUMIC ACID STUDY OF THE BEYPAZARI-ÇAYIRHAN LIGNITES USING IR-SPECTRAPHOTOMETER

Gültekin KAVUŞAN***

ABSTRACT.- Davutoğlan and Kuzey faults are two important tectonic features in Beypazarı-Çayırhan (Türkiye) basin. The basin has 3 seams of coal, one in the lower horizon with narrow extension and two in the upper horizon with an overall thickness of 3 m on the average. The samples were obtained by drilling several boreholes in the perpendicular direction to the faults and ground to 0.25-0.70 mm. Huminite macerals were separated with $ZnCl_2$ solution ($d= 1.44-1.50 \text{ gr/cm}^3$). Maceral-rich samples were then treated with KOH solution (5%) and the alkali-soluble fraction was then precipitated with concentrated HCl. The humic acids so purified were examined by IR-spectroscopy. The H/C ratios of coal seams display an increasing trend in van Krevelen diagrams due to the increasing burial depth and it has been seen that the H/C-O/C values of the seams taken from the drills close to Davutoğlan fault, lower than the average seam values. This behavior indicates that an increase in coalification rate is the consequence of the rise in temperature and tectonic pressure caused by Davutoğlan fault. The strong IR band at $1600-1620 \text{ cm}^{-1}$ indicates the presence of $>C=C<$ bands and remarkable aromatization in the structure. On the other hand, characteristic C-H stretching bands at $2800-3000 \text{ cm}^{-1}$ is an indication for the presence of $-CH_2$ and $-CH_3$ groups.

NOTES TO THE AUTHORS

Papers to be published in the MTA Bulletin must meet the MTA publication requirements. The booklet of publication standards could be obtained from the MTA Publications Department. (MTA Genel Müdürlüğü Bilimsel Dokümantasyon ve Tanıtma Dairesi Başkanlığı, Ankara-Turkey).

The following sections explain briefly the rules for the preparation of the manuscripts. LANGUAGE - Each issue of the Bulletin has Turkish and English editions.

Authors wishing to publish in Turkish and in English are to supply the text and the figures in both languages.

Abstracts written in Turkish and English should be supplied with the papers to appear in Turkish edition. English abstracts of the papers appearing only in the Turkish edition are also published in the English edition of the same issue.

Authors are asked to supply the translations of the text, figures, tables, plates etc. of their papers to be published in the English edition of the Bulletin.

Turkish authors submitting papers to appear in the English edition are to supply the Turkish translations of their papers.

MANUSCRIPT - A manuscript should include title, name of the authors and the address, abstract, introduction, main body of the text, conclusion, discussion (if necessary), references and additional explanations (if necessary).

ABSTRACT - Abstract should be brief not exceeding 200 words, should give enough information about the paper without having to consult to the other sections of the text. It should be publishable separately in an abstract bulletin. The abstract should include the purpose, new contributions in the light of the additional data and their interpretations. No references to be made to the other sections of the text, figures and to other publications. Footnotes must be avoided.

Persons who bear some degree of responsibility for the results of the paper should be acknowledged. Those contributions that are part of normal functions are not to be acknowledged.

References to be made only to those papers cited in the text. The style of the references are given below;

Pamir, H.N., 1953, Türkiye'de kurulacak hidrojeoloji enstitüsü hakkında rapor: Türkiye Jeol. Kur. Butt., 4, 63-68.

Baykal, F. and Kaya, O., 1963, İstanbul bölgesinde bulunan Karboniferin genel stratigrafisi: Maden Tetkik ve Arama Enst. Derg., 61, 1-9.

Ketin, İ., 1977, Genel Jeoloji: İst. Tek. Üniv., İstanbul, 308p.

Anderson, D.L, 1967, Latest information from seismic observations: Gaskell, T.F., ed., in The Earth's Mantle: Academic Press, London, 355-420.

Citings should be made in the following ways; «.....according to Altınlı (1972)» «.....(Sirel and Gündüz, 1976). If the authors of the given reference are more than two «..... et al.» abbreviation for «and others should follow the name of the senior author; for instance «Ünalın et al. (1976) described the Kartal formation.....». To refer to an article which is published in another publication, firstly the original and secondly the publication in which the article has appeared should be mentioned; for instance «it is known that Lebling talks about Lias around Çakraz (Lebling, 1932; in Charles, 1933)». Personal communications or correspondence should be similar to the following examples: «O. Eroskay, 1978, personal communication-, "according to N. Toksöz 1976, written communications.

LENGTH OF THE MANUSCRIPT - The manuscript submitted for publication with all illustrations, should not exceed 30 typed pages. The size of the pages and the space used should be in accordance with the regulations given under the preparation of the text heading.

Selection of the size of the illustrations and their accommodation in the text should be carefully studied to avoid loss of detail and space.

Fold-outs are not allowed, thus the figures must have suitable dimensions for a reduction in 16x21 cm as the maximum publication size.

PREPARATION OF THE TEXT - The manuscript submitted for publication should be typed on an A 4 (29.7x21 cm) size paper with double spacing, leaving a margin 2.5 cm on the sides. Special lettering and formulae must be hand written with indian ink on a tracing paper. Illustrations and tables where to be located should be indicated with a pencil by the author on the manuscript. Words should have a double and a single underlining for bold lettering and italics, respectively.

Footnotes should be avoided unless necessary, it should not exceed ten lines, and should be numbered consecutively throughout the manuscript.

ILLUSTRATIONS - Figures, tables, plates, maps should be carefully selected with regards to their necessity, suitability and quality.

The drawings should be prepared in black and white. They should be drawn carefully and clearly. Lines and letters should be such that, when reduced, details won't be lost and the size of the letters will not become smaller than 2 mm. Unstandardized symbols and letters, utilized for the drawings should be explained either in the drawing or within the explanations section of the text. Bar scale must be included in the drawings. Photographs must be of high quality, glossy prints with sharp details and good contrast.

Figures, tables, and plates should be numbered independently from each other. Numberings should be in such an order which must be in accordance with the citing in the text. Figures and tables must be numbered by using arabic numerals and plates with roman numerals. Single photographs to be classified as figures and numbered accordingly.

The numbers of the illustrations and the name of the authors must be written with a pencil behind each illustration.

Figure captions must not be written on the illustrations. Captions for figures and tables should be collected on separate lists. Captions for each plate should be given alone.

SENDING THE MANUSCRIPT - Three sets of the manuscripts are required as one set should be the original, and two others be copies. Copies of the illustrations could be given in blue prints or photocopies.

Copies of the manuscript of an unaccepted paper is not returned to the authors.

Photographs which are designed to be printed as plates should be arranged on a white cardboard in the required order. This arrangement is not necessary for the second set. Dimensions of the cardboard should be the same size as the page of the Bulletin or reducible to that size. Respective numbers should be written on each photograph in the plates.

If the manuscript does not meet the requirements of MTA publication standards, it would be returned to the authors for correction. The revised manuscript is reconsidered by the Editorial Board of MTA for publication.

SHORT COMMUNICATIONS - Within the short communications section of MTA Bulletin scientific researches and applications in earth sciences and data obtained from such studies are published in short, well defined and outlined texts. Such texts are published in the forthcoming issues without delay to establish rapid scientific communication among the earth scientists.

The text to be published in the short communications section should not exceed four typed pages including the illustrations, meeting the requirements outlined in the proceeding sections. Short communications should not include abstract.

REPRINTS - For each article published, authors will receive 25 reprints free of charge, extra copies are subject charge.